

1-1-2012

Disrupting cxcr2 macromolecular complex pdz-domain interactions during inflammatory chemotaxis

Marcello Castelvete
Wayne State University,

Follow this and additional works at: http://digitalcommons.wayne.edu/oa_theses

Recommended Citation

Castelvete, Marcello, "Disrupting cxcr2 macromolecular complex pdz-domain interactions during inflammatory chemotaxis" (2012). *Wayne State University Theses*. Paper 172.

This Open Access Thesis is brought to you for free and open access by DigitalCommons@WayneState. It has been accepted for inclusion in Wayne State University Theses by an authorized administrator of DigitalCommons@WayneState.

**DISRUPTING CXCR2 MACROMOLECULAR COMPLEX PDZ-DOMAIN
INTERACTIONS DURING INFLAMMATORY CHEMOTAXIS**

by

MARCELLO P. CASTELVETERE

THESIS

Submitted to the Graduate School

of Wayne State University,

Detroit, Michigan

in partial fulfillment of the requirements

for the degree of

MASTER OF SCIENCE

2012

MAJOR: BIOCHEMISTRY AND MOLECULAR
BIOLOGY

Approved by:

Advisor

Date

© COPYRIGHT BY
MARCELLO P. CASTELVETERE
2012
All Rights Reserved

DEDICATION

*I dedicate this work to my family and Natasha,
for all their support.*

ACKNOWLEDGMENTS

I would like to thank the following people who, through collaboration, thoughtful advice, instruction, or patience, have helped me along the way:

Advisor: Dr. Chunying Li

Thesis committee members: Dr. David Evans and Dr. Ladislau Kovari

Laboratory colleagues: Yanning Wu, Shuo Wang, Yuning Hou and Xiaoqing Guan

The Biochemistry Department at Wayne State Universities School of Medicine

TABLE OF CONTENTS

Dedication	ii
Acknowledgements	iii
List of Tables	vii
List of Figures	viii
Chapter 1 Introduction	1
1.1 Neutrophils	1
1.2 Chemokines, IL-8	2
1.3 CXCR2, an IL-8 Receptor	4
1.4 G-protein Signaling	5
1.5 CXCR2 Contains a PDZ-motif	8
1.6 NHERF1 Binds CXCR2	10
1.7 PLC β 2, CXCR2's Downstream Effector	13
1.8 Chemokine Signaling Triggers Chemotaxis	15
1.9 CXCR2 Modulators	19
1.10 Formation of the Uropod	20
1.11 A Means to an End	21
1.12 Summary of IL-8 Migration	22
Chapter 2 Materials & Methods	25
2.1 Antibodies and Reagents	25
2.2 Plasmids, Cloning, and Mutagenesis	25
2.3 Cell Culture and Transfection	26
2.4 Human Neutrophil Isolation from Buffy Coats	26

2.5 Murine Neutrophil Isolation from Mouse Bone Marrow	27
2.6 Western Blots	27
2.7 Pulldown Assay	28
2.8 Pairwise Binding	29
2.9 Macromolecular Complex Assembly	29
2.10 Co-immunoprecipitation	29
2.11 CXCR2 Peptide in Vitro Competitive Binding	30
2.12 CXCR2 Degradation	30
2.13 Zigmond Migration Chamber	31
2.14 Statistical Analysis	32
Chapter 3 Results	33
3.1 HL-60 Differentiation	33
3.2 Human Neutrophils and dHL-60 Cells	34
3.3 Biochemical Assay Results	36
3.4 CXCR2 C-terminal Synthetic Peptide	42
3.5 CXCR2 Degradation	43
3.6 Migration Introduction	46
3.7 Distance Traveled	48
3.8 Directness	53
3.9 Forward Migration Index	56
3.10 FMI Through Time	59
3.11 Sector Maximum	61
3.12 Rose Diagram	64

3.13 Center of Mass	66
3.14 Rayleigh Test	68
Chapter 4 Discussion	70
4.1 Conclusion of Biochemical Data	70
4.2 Conclusion of Migrational Data	72
4.3 Thoughts	74
4.4 Future Directions	75
References	77
Abstract	100
Autobiographical Statement	101

LIST OF TABLES

Table 3.1 Distances Traveled	50
Table 3.2 Distances Traveled Vs. Controls	52
Table 3.3 Directness	53
Table 3.4 Average Directness	56
Table 3.5 Endpoint FMI's	58
Table 3.6 COM Distance from Origin	67
Table 3.7 Rayleigh Test	69

LIST OF FIGURES

Figure 1.1 CXCR2 is a GPCR	7
Figure 1.2 NHERF1 PDZ Domain-motif Interactions	12
Figure 1.3 Activation of PLC β 2	14
Figure 1.4 PIP3 Dictates Cellular Polarization	24
Figure 2.1 Zigmond Chamber	32
Figure 3.1 dHL-60 Expression of NHERF and PLC Isoforms	35
Figure 3.2 CXCR2 Interacts with NHERF	37
Figure 3.3 PLC β Isoforms Interact with NHERF	39
Figure 3.4 Macromolecular Complex Formation	41
Figure 3.5 CXCR2 C-tail Peptide	42
Figure 3.6 NHERF1 Nucleates CXCR2 and PLC β 2	43
Figure 3.7 CXCR2 Degradation	45
Figure 3.8 Distances Defined	48
Figure 3.9 Directness Vs. Time	54
Figure 3.10 Forward Migration Indexes Defined	57
Figure 3.11 Average FMI's	58
Figure 3.12 X-FMI Vs. Time	60
Figure 3.13 Y-FMI Vs. Time	61
Figure 3.14 Sector Maximum	63
Figure 3.15 Rose Diagrams	65
Figure 3.16 Center of Mass Vs. Time	66

CHAPTER 1

INTRODUCTION

1.1 Neutrophils

The human body is prone to attacks from a host of pathogens and underlying all bodily defense is a strong immune response. As a result, immune systems are under a constant state of surveillance and pathogen elimination. Immune cells must act fast and efficiently to combat illness and circulating neutrophils represent the body's first line of defense. Neutrophils are the most abundant inflammatory cell type and account for 60-70% of white blood cells in circulation (5×10^9 cells per liter) [3]. In the early stages of acute inflammation neutrophils are recruited in great numbers to initiate an immune response. They are short lived, averaging a 4-5 day lifespan and once they complete their immunological duties are recycled by host macrophages [4].

Neutrophils play a vital role in host defense, and once stimulated, change from a relatively unanimated circulatory state to an aggressively invading immune cell. As neutrophils circulate through blood vessels they may encounter inflammatory signals attached to endothelial cells by heparin sulfates [5]. These signals activate receptors on the neutrophils which cause them to immediately arrest themselves on endothelial cells, alter their shape becoming polarized, activate migratory enzymes, perform extravasation of the blood vessel, demonstrate directed movement toward inflammation, and carry out a respiratory burst [6]. These changes in behavior are ultimately due to inflammatory signals, such as chemokines, binding to their cognate cellular receptors, thus beginning an intracellular signaling cascade [7, 8]. Infiltration of inflamed tissue is imperative to host defense, yet the uncontrolled invasion of leukocytes is responsible for

a variety of pathological conditions, including rheumatoid arthritis, ischemia-reperfusion injury, arteriosclerosis, virus-induced myocarditis, psoriasis, and allergic reactions [9].

Neutrophils migrate through the body's extracellular matrix to sites of inflammation, where they establish an important source of cytokines or other immune factors and have a defining role in the outcome of the inflammatory state [10]. As leukocytes migrate they express the necessary proteins to adhere to a variety of extracellular matrix macromolecules, such as laminins, collagens and fibronectin [11]. Chemoattractants, produced from microorganisms, necrotic, stromal, epithelial, and other cells present during inflammation, also bind to extracellular matrix elements due to their negative charges. The chemoattractants diffuse away from their source of origin, forming a gradient, causing neutrophils to respond by migrating up the gradient towards the inflamed tissue [12]. Neutrophils can sense shallow gradients of chemoattractant, while remaining stationary, which is essential for navigation through crowded areas [13]. Interleukin-8 (IL-8), a strong activator of neutrophils, is one such chemoattractant involved in inflammation and requisition of neutrophils to sites of injury or infection [14].

1.2 Chemokines, IL-8

Chemokines are a class of small chemotactic cytokines, roughly ten kilo-Dalton globular proteins, that signal to cells through seven-transmembrane G-protein coupled receptors (GPCRs) located in the cellular membrane. Chemokines have four characteristic cysteines, and are classified based on the arrangement of the first two cysteines, they are C, CC, CXC, and CX₃C (X being any amino acid) [15]. The

chemokine receptors are named by the chemokine class they bind, for example CCR1 through CCR9 bind CC chemokines and CXCR1 through CXCR7 bind CXC chemokines. Chemokines are involved in numerous biological processes such as inflammation, cell recruitment, wound healing, tumor growth, metastasis, angiogenesis or angiostasis, and lymphoid development. For a review of chemokines and their functions see [16].

One subtype of CXC chemokines, which possess the ELR (glutamic acid – leucine - arginine) amino acid motif, increase angiogenic effects in endothelial cells and are important in regulation of chronic inflammatory diseases [17]. ELR-CXC chemokines are also involved in neutrophil signaling by binding to their cognate receptors, CXCR1 and CXCR2 (CXC chemokine receptor 1 and 2), which stimulates an inflammatory response through intracellular G-protein signaling cascades and signal amplification [18]. Evidence of ELR's importance in chemotactic signaling has been verified, as the ELR motif is required for IL-8 to mount a proper inflammatory response, and mutation of the ELR's arginine residue abolishes binding to CXCR2 [19]. It is also worthy to mention the ELR motif is present on seven of the 17 total CXC chemokines, and all seven are neutrophil activating chemokines, having a high affinity for CXCR2 [20].

All ELR CXC chemokines are neutrophil chemoattractants and induce chemotaxis, cellular polarization, intracellular $[Ca^{2+}]$ release, bioactive lipid production, activation of adhesion proteins, granule exocytosis, and the respiratory burst associated with neutrophils' antimicrobial effects. These ELR-CXC chemokines play a direct role in chronic inflammatory diseases and inflammatory responses [21]. Of the ELR containing CXC chemokines IL-8 (CXCL8) has been firmly established as a pro-inflammatory

chemokine. Biologically active IL-8 is released by a variety of cell types, such as epithelial cells, endothelial cells, fibroblasts, keratinocytes, synovial cells, chondrocytes, macrophages, cells surrounding a necrotic focus, as well as many tumor cells, and it mediates a potent response in neutrophils by binding to CXCR2 [7, 22, 23]. IL-8 is generated as a 99-amino acid precursor protein, and after a cleavage of a 20 residue leader sequence it is released extracellularly. In its mature form IL-8 consists of 72 amino acids and a heparin-binding domain. Processing of IL-8 greatly increases its biological activity, making this peptide one of the most potent chemoattractants for neutrophils [20, 24-26].

1.3 CXCR2, an IL-8 Receptor

Two different ELR chemokine receptors on neutrophils, CXCR1 and CXCR2, both bind to IL-8 [23, 27]. These two receptors share a 77% sequence identity, with two blocks containing a particularly high rate of conservation, and both genes are co-localized on chromosome 2q35 [28, 29]. CXCR2 has a high affinity for IL-8 as well as other members of the ELR-CXC chemokine family (e.g., CXCL1 or MGSA/GRO α , CXCL5 or ENA-78, and CXCL7 or NAP-2), whereas CXCR1 has a high affinity for IL-8 only [22, 30]. Stimulation of either receptor triggers an increase in cytosolic [Ca $^{2+}$], chemotaxis, and granule exocytosis [31, 32].

Despite their similarities, CXCR1 and CXCR2 differ in how they transduce the IL-8 signal, ultimately creating different functional outcomes and behaviors. One example, is phospholipase D (PLD) activation and the respiratory burst are only triggered by CXCR1 activation, which indicates CXCR1 and CXCR2 function independently of each

other. Studies have also confirmed CXCR2, and not CXCR1, is the primary chemokine receptor required in mediating cellular chemotaxis in endothelial cells and neutrophils [33-35]. Furthermore, CXCR2 is able to actively respond to IL-8 at much lower concentrations. This evidence points to CXCR2 being used as a long-range chemoattractant receptor when IL-8 concentration is low, and as chemokine levels increase near the site of inflammation, CXCR1 will begin PLD activation and respiratory burst, causing tissue damage [36, 37].

Many unique proteins have been identified that associate with CXCR2, either in its unstimulated state (11 proteins), stimulated (7 proteins), or both (6 proteins) [38]. These proteins are thought to act as part of a CXCR2 chemosynapse, regulating the function of CXCR2 and mediating signal transduction by activating and repressing certain downstream signaling molecules. Many *in vivo* studies demonstrate the detrimental effects of excessive leukocyte cytokine signaling and show CXCR2 plays an important role in inflammatory diseases, such as atherosclerosis [39], chronic obstructive pulmonary disease [40], rheumatoid arthritis [41], multiple sclerosis [42], oligodendrocyte derived neuroimmunological diseases [43, 44], inflammatory bowel disease [45, 46], psoriatic epidermis [47], and in bronchial biopsies of chronic obstructive pulmonary disease patients [48].

1.4 G-protein Signaling

CXCR2 is a seven-trans-membrane (7TM) spanning signaling receptor, which is a distinct group of related proteins within the heterotrimeric G-protein coupled receptor superfamily. G-proteins associate with the cytoplasmic side of 7TM receptors and

mediate signal transduction by linking the receptor to one or many downstream effector proteins [22, 49]. All GPCRs possess seven trans-membrane domains, having three extracellular loops, and three cytosolic loops. The C-terminus is found in the cytosol along with the 2nd and 3rd cytosolic loops, which are important for G-protein signaling [50]. When stimulated by IL-8, CXCR2 initiates a series of G-protein mediated downstream events, such as the mobilization of intracellular [Ca²⁺] and phosphatidylinositide hydrolysis, which generates inositol 1,4,5-trisphosphate (IP₃) and diacylglycerol (DAG), and initiates cellular responses [51].

CXCR2 interacts with a complex of heterotrimeric G-proteins, named G α , G β , and G γ in order of decreasing mass. The α -subunits differ greatly from the other family members, defining the nomenclature of individual complexes, and associate with DRY motif (aspartate-arginine-tyrosine) on the 2nd cytosolic loop of CXCR2 [52]. G β and G γ tightly bind in a heterodimer (G $\beta\gamma$), and associate with lipid membranes, where 7TM receptors are imbedded [53]. In the resting state G α binds GDP, forming G α GDP. G α GDP associates with G $\beta\gamma$, forming a G α GDP-G $\beta\gamma$ complex that contacts CXCR2 intracellularly, see **Figure 1.1**. Upon CXCR2 stimulation the GDP bound to G α is exchanged for GTP, resulting in a G α subunit structural change, G α GTP then dissociates from G $\beta\gamma$ and is free to diffuse from the membrane. Both dissociated G α GTP and G $\beta\gamma$ are active forms of G-proteins and can modulate the function of various downstream effectors. The GTP bound to G α is hydrolyzed by an intrinsic GTPase-function of G α , forming G α GDP and inorganic phosphate. Once GTP is hydrolyzed, G α GDP returns to the resting state by associating with G $\beta\gamma$, completing the signaling cycle [54] [55, 56].

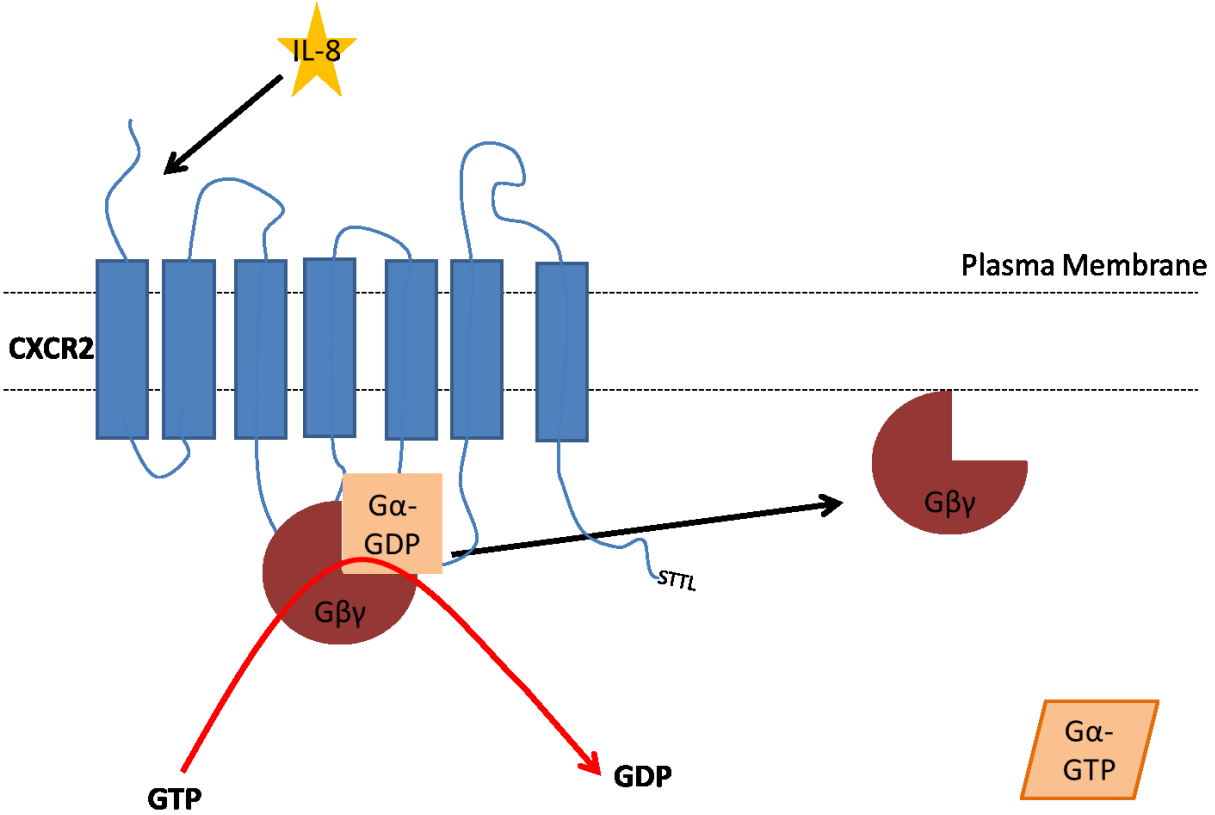


Figure 1.1 CXCR2 is a GPCR

CXCR2 is a seven transmembrane chemokine receptor. IL-8 binds to CXCR2 inducing the associated G α subunit to exchange GTP for GDP. The bound G $\alpha\beta\gamma$ heterotrimer then dissociates into separate G α and G $\beta\gamma$ subunits, and activate downstream effectors. STTL refers to CXCR2's carboxy-terminal PDZ motif (serine-threonine-threonine-leucine).

GPCRs can function catalytically, amplifying the original signal, by activating roughly 10 molecules of G α over a few seconds [57, 58]. Furthermore, discriminatory signaling by G-proteins produces a variety of low molecular weight second messengers, including cyclic adenosine monophosphate (cAMP) or inositol triphosphate, further amplifying the original signal. These small messengers selectively generate dramatic intracellular changes, such as selective protein phosphorylation, gene transcription, cytoskeleton reorganization and membrane depolarization [56]. There are multiple

subtypes of each G-protein, although only certain combinations will form associable heterotrimers. $G\alpha$ subunits are divided into four different subtypes ($G\alpha_i$, $G\alpha_s$, $G\alpha_q$ and $G\alpha_{12/13}$) the $G\beta$ subunit has five distinct subtypes (β_1 - β_5), and $G\gamma$ subunits have ten different subtypes, making up hundreds of combinations [59]. On top of all the possible combinations of G-protein complexes that can associate with a single GPCR, multiple receptors can activate a single effector, and a single receptor can activate multiple effectors, forming complicated signaling networks [54, 60-63].

The time active $G\alpha$ and $G\beta\gamma$ subunits remain separated for signaling is crucial, and usually very short, depending entirely on how fast GTP is hydrolyzed by $G\alpha$. But the intrinsic $G\alpha$ GTPase-activity is usually long and insufficient, taking on the order of minutes to complete. The GTPase-activity of $G\alpha$ can be expedited by other proteins, named GTPase-activating proteins (GAP). These GAPs can be the target protein of $G\alpha$ for downstream signaling, or a specific modulator known as a regulator of G-protein signaling (RGS). For a review see [64]. In neutrophils, IL-8 stimulation of CXCR2 leads to $G\beta\gamma$ activation of its downstream effector, phospholipase C β_2 (PLC β_2), which creates second messengers as well as stimulates calcium influx [25, 51, 65-67].

1.5 CXCR2 Contains a PDZ-motif

Regulation of CXCR2 signaling can be accomplished through receptor desensitization, which uncouples G-proteins and internalizes the receptor, so the cell is not as sensitive to ligand stimulation [68-71]. After chemokine stimulation G-protein-coupled receptor kinases (GRKs) phosphorylate CXCR2's cytosolic tail and alter the binding sites of CXCR2 modulators. The phosphorylation of CXCR2 is required for

some processes, such as chemotaxis and internalization, but not others, like PLC β 2 activation and [Ca $^{2+}$] mobilization [36, 72-75]. In neutrophils, IL-8 preferentially binds CXCR2, inducing high levels of C-terminal tail phosphorylation and instigating rapid CXCR2 internalization [76, 77].

CXCR2 sequestration is reliant on the endocytotic functions of clathrin-coated pits and dynamin [78-80]. Receptor internalization is mediated by a peptide motif recognized on the C-terminal tail of CXCR2, LLKIL (leucine-leucine-lysine-isoleucine-leucine), and an aspartate residue in the second extracellular loop [52, 81]. The LLKIL motif is necessary for internalization by adaptin-2 (AP-2) [82]. After ligand stimulation, phosphorylation of CXCR2's C-terminus by GRK2 encourages binding of AP-2 as well as β Arrestin which form the clathrin coated vesicles necessary for internalization [83, 84]. Like other types of GPCRs, CXCR2 undergoes trafficking between intracellular compartments and the membrane.

Once internalized CXCR2 has been de-phosphorylated it can be transferred to late endosomes for degradation or recycled to the plasma membrane for another round of signaling [77]. A domain was found in the C-terminus of CXCR2 that regulates post-endocytotic sorting back to the cellular membrane [85]. Originally CXCR2 degradation was thought to occur via the ubiquitination pathway, but is instead modulated by the type I PDZ ligand on CXCR2's C-terminus. CXCR2 lacking the PDZ ligand will be shuttled to the late endosome, and degraded, at a much higher rate than the wild-type (WT) CXCR2, ultimately affecting chemotaxis towards CXCR2 ligands [85].

1.6 NHERF1 Binds CXCR2

The NHERF protein family consists of four members: NHERF1 (EBP50), NHERF2 (E3KARP), NHERF3 (PDZK1) and NHERF4 (IKEPP). NHERF1 and NHERF2 contain two PDZ domains while NHERF3 and NHERF4 possess four PDZ domains [86]. The human NHERF1 gene, *SLC9A3R1*, encodes a 358 amino acid protein (38.6kD) with two tandem PDZ domains that share 74% homology [87]. High homology in PDZ domains probably arose through evolutionary gene duplication as PDZ domains are highly conserved modular structures which occur frequently throughout the genome and are present in an overwhelming number of phyla [88-90].

The two NHERF1 PDZ domains, PDZ I and PDZ II, have similar secondary structures, and collectively make up nearly 70% of NHERF1. They are followed by a 30 amino acid C-terminal region that associates with members of the merlin-ezrin-radixin-moesin family (MERM), a group of membrane-cytoskeleton adaptor proteins [91]. Both PDZ domains of NHERF1 are type I PDZ domains, preferentially binding to short C-terminal peptide sequences of target proteins, X-(S/T)-X-(V/L) [92, 93]. NHERF1 binds to cytoskeletal adaptor proteins through its MERM-binding domain, and links them to integral membrane proteins through the PDZ motif on their C-terminal tail, such as the one found in CXCR2 [94, 95]. Experiments show PDZ I and PDZ II domains bind to their C-terminal PDZ-ligands at nanomolar affinity, to which crystal structures have illuminated much of their specificity [96].

A crystal structure of NHERF1 binding to the C-terminal region of Cystic Fibrosis Transmembrane Conductance Regulator (CFTR) was reported along with NHERF1

binding to the $\beta 2$ Adrenergic Receptor and Platelet-derived Growth Factor Receptor (PDGFR) [96, 97]. These experiments demonstrate the NHERF1-PDZ I core domain consists of six β strands ($\beta 1$ - $\beta 6$) and two α helices ($\alpha 1$ and $\alpha 2$), and the PDZ-motif inserts into the binding pocket in a β strand addition [98], see **Figure 1.2**. A slightly larger hydrophobic binding pocket is found in NHERF1 compared to other type I PDZ proteins, as NHERF1 prefers binding leucine at P_0 instead of valine (P_0 refers to the ligands carboxy-terminal amino acid, the previous being P_{-1} , P_{-2} , etc.). Leucine was shown to enter a deep cavity formed by Tyr24, Gly25, Phe26, Leu28, Val76, and Ile79 [2]. These residues form a tight hydrophobic pocket for the isobutyl side chain of P_0 leucine and mediates the hydrogen bonding and coordination of H₂O atoms, which accounts for the strict stereochemical requirement of a C-terminal leucine [99-101].

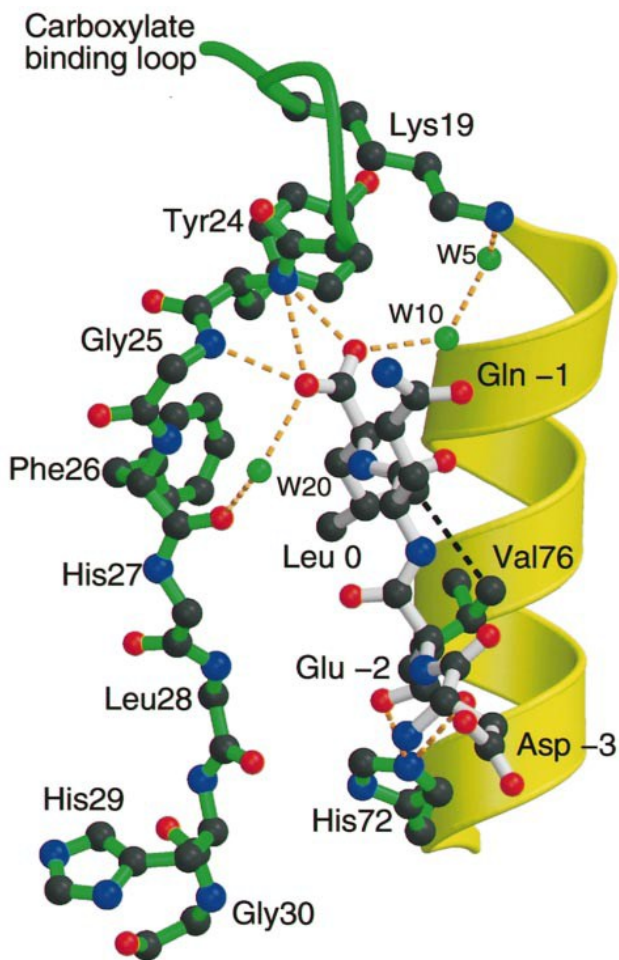


Figure 1.2 NHERF1 PDZ Domain-motif Interactions

The NHERF1 PDZ1 peptide-binding pocket (green) bound to the C-terminal PDZ-motif (gray). Binding occurs in an antiparallel β strand addition, as the ligand fits into a pocket between the $\alpha 2$ helix and the $\beta 2$ strand. The PDZ-motif is a consensus type I PDZ ligand, X-S/T-X-V/L (aspartic acid-glutamic acid-glutamine-leucine). Water molecules are represented as green dots, hydrogen bonds are orange dashed lines, and hydrophobic interactions are black dashed lines. Image was obtained from [2].

A separate pocket for the P_{-2} side chain is also important for binding, as studies showed NHERF1 preferentially binds to X-(S/T)-X-L, and changes resembling P_{-2} phosphorylation lost all PDZ domain-motif interaction [97, 99]. The P_{-2} amide nitrogen and carbonyl oxygen both bind conserved residues in the PDZ domain binding pocket, and the hydroxylated side chain oxygen atom of (S/T) at P_{-2} specifically interacts with

the N3 nitrogen of a histidine residue in class I PDZ domains [2, 96]. The possibility of 7TM receptors C-terminus being phosphorylated, thus determining PDZ domain interactions, has made a great impact in understanding regulatory functions of PDZ-containing GPCRs now that the specifics have been worked out. In vitro studies show that phosphorylation of serine residues and binding of adaptor proteins to CXCR2's C-terminus facilitate internalization and intracellular movement, which attests to the importance of these C-terminal residues in CXCR2 cycling [102].

Another role of NHERF1 involves the regulation of small signaling molecules. CXCR2 can stimulate activation of PLC β 2, which increases intracellular calcium levels from [CA $^{2+}$] stores, this in turn initiates an extracellular [CA $^{2+}$] influx through store-operated calcium channels (SOCs). It was shown that NHERF1 interacts with SOCs and PLC β 2 through PDZ domains, suggesting NHERF1 can nucleate them into a complex on the plasma membrane [103]. NHERF1 can also dimerize or oligomerize through its two PDZ domains which could nucleate many receptors, ion channels, effector molecules and actin-interacting proteins, using NHERF1 as a scaffold to stably anchor these complexes to the actin cytoskeleton [104-106]. Recently we found NHERF1 interacts with CXCR2 and PLC β 2 through PDZ-dependent interactions [1].

1.7 PLC β 2, CXCR2's Downstream Effector

Mammalian phospholipase C- β 2 (PLC β 2) is a multi-domain signaling enzyme whose primary role is to generate low-molecular weight signaling molecules and propagate signal transduction from 7TM receptors [107, 108]. During stimulation PLC hydrolyzes the lipid phosphatidylinositol 4,5-bisphosphate (PIP $_2$), generating two

secondary messengers: inositol 1,4,5- trisphosphate (IP3), a potent calcium mobilizing second messenger, and diacylglycerol (DAG), which activates the downstream effector protein kinase C (PKC) [107], **Figure 1.3**. PLC β 2 is one of many Phosphatidylinositide-specific PLC enzymes, which can ultimately be divided into six families: β , γ , δ , ϵ , η , ζ , and range between 85 to 150 kDa [109].

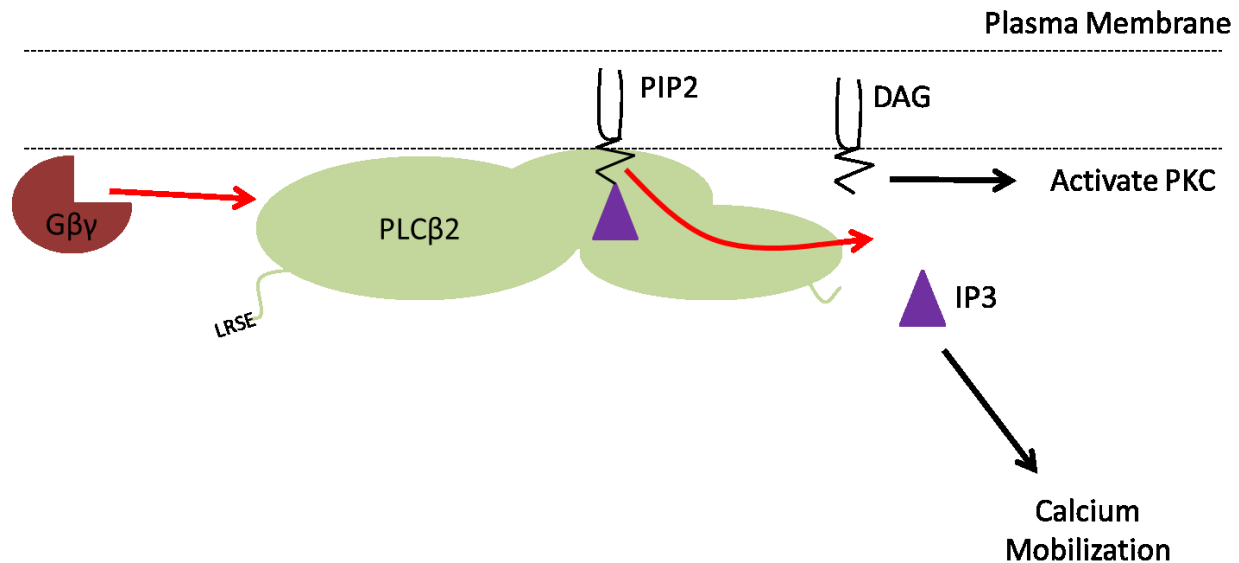


Figure 1.3 Activation of PLC β 2

PLC β 2 associates with the plasma membrane, as does G $\beta\gamma$. Active G $\beta\gamma$ stimulates PIP2 cleavage by PLC β 2, resulting in DAG and IP3 formation. Downstream effects of DAG and IP3 formation include PKC activation and calcium influx. ESRL corresponds to PLC β 2's PDZ-motif (glutamic acid – serine – arginine – leucine).

The β family consists of 4 isozymes, PLC β 1 through PLC β 4, which are regulated by G-proteins and contain a consensus PDZ motif at their carboxyl termini (PLC β 2's PDZ-motif is glutamic acid – serine – arginine - leucine) [110]. PLC β 2 is primarily expressed in hematopoietic cells, PLC β 3 and PLC β 1 are found in a wide variety of cells and tissue types, and PLC β 4 is expressed predominantly in neuronal cells [111-113].

Eukaryotic PLC β enzymes contain a sequence of modular domains which are organized around a catalytic α/β barrel formed from its conserved X and Y-box regions [114]. These modular domains include a pleckstrin homology (PH) domain, EF-hand motifs, a C2 domain, and additional regulatory units present on the PLC β and PLC γ subtypes [107].

The PH domain is a highly conserved motif around 120 amino acids in length that confers specificity to different lipids or proteins and is located in the N-terminal region of PLC [115]. PH domains are prominently found in proteins associated with cellular membranes and can bind specific phosphoinositides (e.g. PIP₂, PIP₃), although PLC β 2's PH domain is not phosphoinositide specific [116-119]. They also have the ability to bind G $\beta\gamma$ subunits, especially in PLC β 2, where G $\beta\gamma$ binding to the PH domain is sufficient for enzymatic activation, and increases product release [119-121]. Furthermore, CXCR2 activity is able to recruit a variety of proteins through inositide-specific PH domains to the leading edge of migrating cells [122].

Regulation of G $\beta\gamma$ subunit specific activation of PLC β 2 is through phosphorylation by cAMP-dependent protein kinase A (PKA) [123]. In response to CXCR2-PLC β 2 mediated calcium influx, some forms of adenylyl cyclase will activate a downstream protein kinase, thereby phosphorylating and deactivating PLC β 2, repressing calcium influx [124]. Phosphorylation by PKA also uncouples receptors that signal through G α_i proteins, such as CXCR2 which alludes to a greater on-off switch of PLC β signaling [125].

1.8 Chemokine Signaling Triggers Chemotaxis

When the neutrophil cell surface receptor CXCR2 is stimulated from the inflammatory chemokine IL-8, the G-protein heterotrimer becomes activated. CXCR2 coupled G-protein signaling triggers a variety of downstream effects which ultimately dictate cellular behavior and spur the cell to polarize its cytoskeleton, form actin derived pseudopodia, and begin chemotaxis [126-128]. The asymmetric manner in which cells polarize involve a slew of feedback mechanisms that modulate actin extension at the leading edge (frontness pathway) and promote contractile cytoskeletal forces at the rear (backness pathway) [129, 130]. The first level of response in chemotaxing cells is the separation of uniformly distributed transmembrane chemoattractant receptors into the asymmetric localization of phosphatidylinositol 3,4,5-trisphosphate (PIP3) [131]. Proteins that interact with, synthesize, or degrade PIP3 are the first effectors in the signaling process and they utilize PIP2, the same precursor molecule used by PLC β 2.

When PLC β 2 cleaves PIP2, IP3 and DAG are formed, and PIP2 is enzymatically removed from that region of local membrane. IP3 dissociates from the membrane and binds to its receptor on the surface of the endoplasmic reticulum (ER) which stimulates an increase of intracellular [Ca $^{2+}$]. The spike in intracellular [Ca $^{2+}$] initiates an influx of extracellular [Ca $^{2+}$] through SOCs to replenish the depleted internal stores, and also activates [Ca $^{2+}$] dependent enzymes. DAG, the cleaved lipid portion of PIP2, in conjunction with an influx of [Ca $^{2+}$] from IP3, activates Protein Kinase C (PKC) which helps propagate the original signal by phosphorylating target proteins. A few different isoforms of PKC are expressed in human neutrophils, and PKC activity is crucial for neutrophil chemotaxis, but not actin mobilization [132-135].

Instead of cleaving the inositol head-group off the glycerol-lipid side chains, like PLC β 2, some proteins phosphorylate or de-phosphorylate the head-group. One of these proteins is the class I phosphatidylinositol-3-kinase γ enzyme (PI3K), which is expressed mainly in hematopoietic cells [136]. PI3K phosphorylates the 3' position on inositol phospholipids in the cytosolic plasma membrane, namely PIP2 (phosphorylated on inositol carbons 4 and 5) is converted to PIP3 (phosphorylated on inositol carbons 3, 4 and 5) [137]. PI3K is stimulated by free G $\beta\gamma$ subunits from activated CXCR2, or another small G-protein Rac-1, which are both localized to the leading edge of polarized neutrophils [138-140].

As PI3K is localized to portions of the plasma membrane, other proteins such as PTEN (phosphatase and tensin homology deleted on chromosome ten protein), are delocalized from the front of the cell and become restricted to the rear and lateral sides. PTEN is a phosphatase that removes the 3-position phosphate from the inositol ring, thereby converting PIP3 back into PIP2 [122, 141, 142]. Re-localization of PTEN occurs through a PIP2 binding domain on its N-terminus, which associates with areas of PIP2 accumulation [143]. PTEN also contains a PDZ-motif and forms a ternary complex with NHERF2, PTEN and PDGFR, which has been implicated in chemotaxis and tumor growth [144].

Like PTEN, SHIP-1 co-localizes with PIP2 and is responsible for removing the 5-position phosphate from inositol rings in human neutrophils [145]. Thus, CXCR2 downstream effectors will remove PIP2 from the leading edge, thereby removing PTEN/SHIP-1 from the leading edge leaving PI3K to phosphorylate PIP2 into PIP3 [146-148]. A reciprocal accumulation of PIP3 is formed at the leading edge and a

surplus of PIP2 is dispersed throughout the cells lateral and posterior areas essentially forming a phosphatidylinositol gradient, which reflects the extracellular chemokine signal [149].

Evidence suggests that localization of PIP3 results in the polymerization of F-actin at the leading edge, which leads to pseudopod formation and extension by the Rho-family-GTPases Rac-1 and Cdc42 [150-154]. *In vitro* studies have linked PIP3 activity with Rac-1 and Cdc42, which are protein moderators involved in actin dynamics and possesses GTPase activity (active only when bound to GTP) [155, 156]. A disruption of a Rac-1 GAP, DdRacGAP1, leads to increased levels of actin polymerization and pseudopod formation, and a dominant negative form of Rac-1 prevents pseudopod formation and cell migration [157]. PRex-1 exchanges GDP for GTP on Rac-1 and is synergistically activated by the PI3K product PIP3 and active G $\beta\gamma$ subunits, suggesting GPCR stimulation and subsequent PI3K activity is sufficient for Rac-1 to be activated [154, 158, 159]. Active Rac-1 is necessary for pseudopod formation and actin mobilization at the leading edge and together with active G $\beta\gamma$ can stimulate PI3K activity. This facilitates a feedback loop by creating more PIP3, activating PRex-1, which promotes Rac-1 activity [160, 161].

In a similar fashion to Rac-1, Cdc42 is important for cellular chemotaxis and cellular polarity. A dominant negative expression of Cdc42 causes cells to move randomly in chemokine gradients and disrupts polarization [162-165]. G $\beta\gamma$ subunits cause Cdc42 to activate PAK1, a serine/threonine protein kinase [166]. PIX α , a small GEF that contains a PH domain, is constitutively associated with PAK1, and mediates the activation of Cdc42 by G $\beta\gamma$ *in vivo* [167-169]. PIX α activity is also required for PTEN

localization to the trailing edge of cells, probably through activation of Cdc42 [167]. This suggests Cdc42 is required for intracellular gradient formation of a chemoattractant signal and Rac-1 is required to promote movement by stimulating actin mobilization.

The induction of leading edge actin polymerization is mediated by the Arp2/3 protein complex. A huge variety of GEFs can promote Rac-1/Cdc42 activation, and downstream effectors of Rac-1 and Cdc42, such as WAVE (SCAR) and WASP (Wiskott-Aldrich Syndrome protein) promote Arp2/3 actin polymerization [170, 171]. SCAR and WASP contain actin binding domains, selective phospholipid binding domains similar to PH domains, and both are activated by PIP3 [172, 173]. Furthermore, they only interact with the activated (GTP-bound) forms of Rac-1 and Cdc4, thus localizing actin, active Cdc42/Rac-1, PAK1 and the ARP2/3 complex together near sites of PIP3 accumulation and G β γ subunits [174].

1.9 CXCR2 Modulators

LASP-1 is a cytoskeletal scaffold protein implicated in actin bundling and stabilization, and binds to CXCR2 in both basal and activated forms on the LLKIL motif necessary for AP-2 sequestration [175-177]. Furthermore, LASP-1's SH3 domain interacts with proteins that localize to the leading edge of migratory cells and plays an important role in cytoskeletal organization and migration in neutrophil like HL-60 cells [178, 179]. Another CXCR2 binding protein, Vasodilator-stimulated phosphoprotein (VASP), promotes actin filament elongation and pseudopod formation by regulating actin networks, attracting profiling-actin complexes, and destabilizing actin-capping proteins [180-184]. Both VASP and LASP-1 can be controlled by regulatory kinases

PKA and PKG. VASP can also be phosphorylated by PKC, which contributes to their regulation once IL-8 signaling is initiated [185-188].

IQGAP1 is postulated to bind CXCR2 in its inactive form and, once Cdc42 is activated, IQGAP1 will associate with activated Cdc42, enabling IQGAP1 to release CXCR2. IQGAP1 then is free to dimerize and bind F-actin, cross-link actin filaments, and mediate chemotaxis [38]. Furthermore, IQGAP1 binds and inhibits the GTPase activity of Cdc42/Rac-1, stabilizing them in active-signaling forms [189, 190]. Two other proteins that affect GTPase activity of CXCR2's G-proteins are 14-3-3 γ and RGS12. 14-3-3 γ inhibits RGS proteins, allowing G α subunits to remain active for a longer period of time [191, 192]. The GAP protein RGS12 associates with CXCR2 through its PDZ domain, and stimulates G α to hydrolyze GTP and return to its resting state. The interplay between RGS12, 14-3-3 γ and CXCR2 is thought to control CXCR2 G-protein signaling after IL8 initiation, but their regulation is still unknown [64, 193, 194].

1.10 Formation of the Uropod

Uropod contraction (backness pathway) at the rear of the cell is necessary to allow the cell to move forward towards the leading edge. In neutrophils backness signals, which include PTEN/SHIP-1 localization, activation of a second GTPase (Rho), a Rho-dependent kinase (p160-ROCK), and Myosin II activation, results in actomyosin contraction at the rear of the cell [195-198]. Activated GTPase Rho is responsible for activation of p160-ROCK, which enhances phosphorylation of myosin light chain (MLC), inhibits MLC phosphatase, and stimulates actin-myosin contraction [199]. MLC contraction is also dependent on [Ca²⁺] /Calmodulin for proper function, as a PLC β 2

mediated $[Ca^{2+}]$ influx is required for proper tail retraction and detachment from certain substrates [200].

Despite a requirement for migrational frontness, Cdc42 also plays an essential role in Rho activation in the uropod [169, 201, 202]. These small G-proteins act as another layer of signaling on top of the PIP2/PIP3 separation in cells, as Rho inhibits Rac-1 frontness activity, actin assembly, polarity, and motility, and active Rac-1 represses Rho activity in the uropod [195, 203]. This all implies a Rac-1 dependent frontness and a Rho-dependent backness that regulate cellular polarity, initiated through CXCR2/G-protein activation of Cdc42.

1.11 A Means to an End

Neutrophils respond to stimulating signals in a hierarchical manner. “End target” signals, such as bacterial products like *N*-formyl-methionine-leucine-phenylalanine (fMLP), are preferred targets over “intermediate” signals, such as chemokines like IL-8 [204]. fMLP is a potent chemoattractant and has been implicated in directing cell movement, phagocytosis, release of proteolytic enzymes, cytokine production and generation of reactive oxygen intermediates [205]. The human formyl-peptide receptor (FPR), belongs to the seven transmembrane GPCR superfamily, like CXCR2, and is expressed on neutrophils as well as many other inflammatory cells. Since bacteria and mitochondria are the only two sources of formylated peptides, FPR can direct inflammatory cells to sites of either bacterial invasion or host tissue damage [206].

Neutrophils can distinguish between the intermediary and end target signals through their different intracellular signaling pathways. Proof of this was established as

treatment of neutrophils with PI3K inhibitors represses IL-8 migration, but not fMLP migration. Even though both IL-8 and fMLP can activate the same isoform of PI3K and mediate responses in a PIP3 dependent manner, fMLP, but not IL-8, activates p38 mitogen activated protein kinase (MAPK) [207, 208]. fMLP signaling also activates a different phospholipase than IL-8, phospholipase A2 (PLA2), which converts phosphatidylcholine to arachidonic acid, and along with MAPK activity permits the cells to further respond to bacterial products [209]. What is more interesting it that PI3K activity is abolished when both intermediate and end target signals are present, so that intermediary signals are disregarded. This is thought to occur through a MAPK-dependent activation and/or re-localization of PTEN to the plasma membrane, which reverts PIP3 back into PIP2.

1.12 Summary of IL-8 Migration

In summary, localized areas of inflammation will produce chemokines to attract immune cells to repair damage. The highly potent IL-8 is received by CXCR2 on neutrophil membranes and spurs chemotaxis towards the signal. IL-8 stimulated CXCR2 will activate $G\alpha$ and subsequently free $G\beta\gamma$, which in turn activates local $PLC\beta2$ and PI3K. $PLC\beta2$ converts PIP2 into IP3 and DAG, which act synergistically to begin a signaling cascade through PKC and calcium affected proteins. PI3K phosphorylates PIP2 creating PIP3, and together with $PLC\beta2$ remove PIP2 from the area of CXCR2/IL-8 stimulation, forming a PIP3 gradient near active CXCR2. PTEN/SHIP-1 colocalizes with PIP2 and is sequestered to the posterior and lateral sides of the cell. The re-

localization away from the front of the cell allows all PIP3 that diffuses away from the leading edge to be converted back to PIP2, isolating the PIP3 to the leading edge.

At the leading edge PIP3 and G $\beta\gamma$ synergistically promote GTP exchange of Rac-1. Active Rac-1 recruits WASP and SCAR through its CRIB domain, which both increase Arp2/3 complex-mediated actin polymerization. Rac-1 also stimulates PI3K activity increasing PIP3 formation, creating a positive feedback loop that is localized at the leading edge of the cell. Cdc42 is also activated by G $\beta\gamma$ and PI3K action on the GEF PIX α . These active proteins are recruited to sites of PIP3 and actin polymerization by Arp2/3 effectors similar to Rac-1, where they stimulate actin-derived pseudopod formation and create a leading edge. Furthermore active Cdc42 triggers Rho activity, and through p160-ROCK, Myosin II, and PLC β 2-derived calcium influxes, actomyosin fibers begin to contract in the uropod [210]. Thus, sites of CXCR2 stimulation ultimately lead to areas of actin polymerization and forward movement. See **Figure 1.4**.

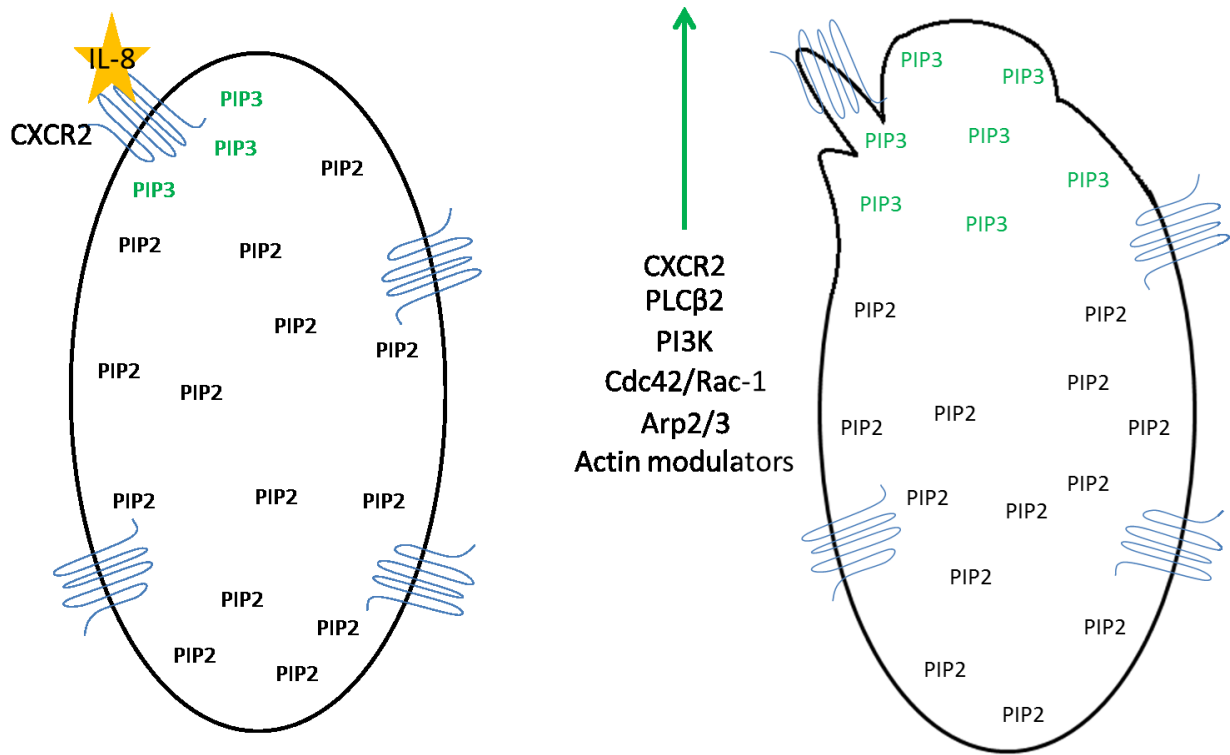


Figure 1.4 PIP3 Dictates Cellular Polarization

After ligand binding to CXCR2 a local population of PIP3 is produced, forming an intracellular gradient. PIP2 is removed from the leading edge through PLC2 and PI3K, and accumulates in the posterior. PIP3 recruits proteins involved in migrational frontness including Cdc42, Rac-1, the Arp2/3 complex, and actin modulating proteins.

CHAPTER 2

MATERIALS & METHODS

2.1 Antibodies and Reagents

Anti-human and murine CXCR2, PLC β 1, β 2, and β 3 antibodies were purchased from Santa Cruz Biotechnology (Santa Cruz, CA). Rabbit anti-NHERF1 polyclonal antibody was from Sigma, and mouse anti-NHERF1 monoclonal antibody was from Santa Cruz. Anti-HA HRP and anti-FLAG HRP were obtained from Sigma. Lipofectamine 2000, Hanks' buffered salt solution (HBSS), Fura-2, and the cell culture media and fetal bovine serum (FBS) were procured from Invitrogen. ChariotTM peptide/protein delivery reagent was purchased from Active Motif (Carlsbad, CA). Chemokines IL-8/CXCL8, growth-related oncogene α (GRO α /CXCL1), and *N*-formyl-methionine-leucine-phenylalanine (fMLP) were obtained from ProSpec (East Brunswick, NJ). The human and murine CXCR2 C-tail peptides (biotin-conjugate at N terminus): WT (biotin-FVGSSSGHTSTTL for human CXCR2 C-tail; and Biotin-FVSSSSANTSTTL for mouse CXCR2 C-tail), PDZ motif deletion, Δ TTL, or PDZ motif mutant, AAA, were synthesized by Genemed Synthesis, Inc. (San Antonio, TX).

2.2 Plasmids, Cloning, and Mutagenesis

The His-S-tagged fusion proteins for the full-length of CXCR2 or PLC β 2, or the C-terminal tail fragments of CXCR2 (last 45 amino acids; *i.e.* amino acids 316–360 for human CXCR2, and amino acids 315–359 for murine CXCR2) or human PLC β 2 (last 100 amino acids, *i.e.* amino acids 1086–1185) were generated by PCR cloning into pTriEx-4 or pET30 vectors (Novagen). The fusion proteins were purified using Talon

beads (binding to His tag), and eluted with 200 mM imidazole. The imidazole-eluted affinity-purified His-S-tagged CXCR2 or PLC β 2 fusion proteins (full-length and/or C-terminal tail fragments) were used in subsequent biochemical assays.

2.3 Cell Culture and Transfection

The HL-60 cells were obtained from American Type Culture Collection (ATCC) (Manassas, VA) and maintained in Iscove's modified Dulbecco's medium (Invitrogen) supplemented with 10% FBS, and penicillin/streptomycin at 37 °C with 5% CO₂. HL-60 cells were differentiated into the granulocyte lineage with 1.2% Me₂SO in Iscove's modified Dulbecco's medium with 10% FBS for 5–7 days. The HEK293 cells and HT-29 human colonic epithelial cells were purchased from ATCC and cultured in Dulbecco's modified Eagle's medium (DMEM) (Invitrogen) supplemented with 10% FBS as described before [211]. HEK293 cells were transfected using Lipofectamine 2000 with HA-tagged human CXCR2, murine CXCR2, and FLAG-tagged PLC β 1, β 2, β 3, and β 4, respectively, for various biochemical assays.

2.4 Human Neutrophil Isolation from Buffy Coats

Briefly, neutrophils from buffy coats (purchased from LifeBlood Inc.) of citrated human peripheral blood collected from healthy donors were isolated by dextran sedimentation followed by density gradient centrifugation in Histopaque (Sigma), as described in [212]. Contaminating red blood cells were lysed by hypotonic shock with 0.2% NaCl. The purity and viability of isolated neutrophils was assessed by trypan blue

dye exclusion, and the viability of isolated neutrophils was routinely found to be >98%. Neutrophils were used immediately after isolation for all assays.

2.5 Murine Neutrophil Isolation from Mouse Bone Marrow

Isolation of murine neutrophils from bone marrow was carried out as reported previously [213]. Briefly, the femurs and tibias were removed from euthanized mice and the bone marrow cells were flushed out of the bones with ice-cold Ca^{2+} - and Mg^{2+} -free HBSS (HBSS⁻). Bone marrow cells were collected by centrifugation at $800 \times g$ for 5 min, and then resuspended in 3 ml of HBSS⁻. The cells were layered over a discontinuous 3-layer Percoll (Amersham Biosciences) gradient (75, 67, and 52%) and subjected to centrifugation at $1,060 \times g$ for 30 min at 22–24 °C. The lowest band between 75 and 67% (the 75/67% interface) was then collected as the neutrophil fraction and washed twice with HBSS⁻. Any remaining red blood cells were eliminated by hypotonic lysis, and the purity of the neutrophils was typically $\geq 90\%$ as assessed by crystal violet staining.

2.6 Western Blots

Cells were washed twice in PBS, then lysed in lysis buffer (PBS, 0.2% Triton) supplemented with protease inhibitors (1 mm phenylmethylsulfonyl fluoride, 1 $\mu\text{g}/\text{ml}$ of aprotinin, 1 $\mu\text{g}/\text{ml}$ of leupeptin, and 1 $\mu\text{g}/\text{ml}$ of pepstatin) and HALT phosphatase inhibitor cocktail (Thermo Scientific), and the clear supernatant ($16,000 \times g$, 15 min) was assayed for protein concentration using Quick Start Bradford Dye Reagent (BIO RAD). Samples were mixed with NuPAGE LDS Sample Buffer 4x (Invitrogen) containing 10%

2-mercaptoethanol (BIO RAD) and heated to 70°C for 10min and separated by SDS-PAGE on Mini-PROTEAN precast TGX-Gels (BIO RAD) 7.5%, any-KD, or Express PAGE gels 10% (GeneScript). The membranes were immunoblotted with NHERF1, NHERF2, or PLC β 1, β 2, β 3 antibodies and visualized using a BioSpectrum 500 Imaging system (UVP).

2.7 Pulldown Assay

Freshly isolated human or murine neutrophils, dHL60 cells, or HEK293 cells overexpressing various constructs (3HA-tagged human CXCR2, murine CXCR2, or FLAG-tagged PLC β 1, β 2, β 3, β 4) were used for the GST pulldown assays, as reported in [211, 214]. In brief, the cells were lysed in lysis buffer (PBS, 0.2% Triton) supplemented with a mixture of protease inhibitors (containing 1 mM phenylmethylsulfonyl fluoride, 1 μ g/ml of aprotinin, 1 μ g/ml of leupeptin, and 1 μ g/ml of pepstatin) and phosphatase inhibitor mixture (Sigma), and the clear supernatant (16,000 \times g, 15 min) was mixed with various GST-PDZ fusion proteins (GST-NHERF1, GST-NHERF2, or GST-PDZK1) or GST alone at 4 °C for 3 h. The complex was pulled down by glutathione-agarose beads (BD Biosciences) at 4 °C for 1 h, washed three times with lysis buffer, and eluted in Laemmli sample buffer containing β -mercaptoethanol. The eluents were separated by SDS-PAGE and immunoblotted with anti-HA, CXCR2, or PLC β 1, β 2, β 3, or anti-FLAG (for PLC β 4) antibodies, and the blots were visualized using a BioSpectrum 500 Imaging system (UVP).

2.8 Pairwise Binding

Purified GST-NHERF1 was mixed with purified His-S-CXCR2 C-tail fragments in binding buffer (PBS, 0.2% Triton) supplemented with a mixture of protease inhibitors at 22–24 °C for 1 h. Next the mixtures were incubated with S-agarose beads (Novagen) for 2 h. The beads were washed three times with binding buffer and eluted with Laemmli sample buffer. The eluents were separated by SDS-PAGE and immunoblotted with anti-NHERF1 antibody.

2.9 Macromolecular Complex Assembly

Purified His-S-tagged PLC β 2 C-tail (last 100 amino acids at C terminus containing the PDZ motif) or His-S-murine CXCR2 C-tail (last 45 amino acids at the C-terminus containing the PDZ motif) was mixed with GST-PDZ scaffold proteins (or GST alone) in 200 μ l of binding buffer (PBS, 0.2% Triton, supplemented with protease inhibitors), and the complex was pulled down with S-protein-agarose. This step is also referred to as pairwise binding as described above. The dimeric complex was then mixed with HEK293 cell lysates overexpressing 3HA-CXCR2 or full-length PLC β 2 for 3 h at 4 °C, and washed extensively with lysis buffer. The bound proteins were then eluted and immunoblotted using anti-HA (for CXCR2) or PLC β 2 antibodies.

2.10 Co-immunoprecipitation

Fresh cells (dHL-60 or murine bone marrow neutrophils) were cross-linked with 1 mM dithiobis (succinimidyl propionate), [215]. Thereafter, the cells were solubilized in PBS, 0.2% Triton, and cleared lysates (16,000 \times g, 15 min) were processed for co-

immunoprecipitation and immunoblotting, as described before [211, 214]. A Co-immunoprecipitation Kit (Pierce) was used to immobilize the anti-CXCR2 IgG to the resin and the co-precipitated protein complex was eluted with Laemmli sample buffer before being subjected to immunoblotting and probed for PLC β 2 and NHERF1. The same membrane was stripped using RestoreTM Plus Western blot Stripping Buffer (Thermo Scientific) and reprobed for CXCR2.

2.11 CXCR2 Peptide in Vitro Competitive Binding

In brief, affinity-purified HA-tagged human CXCR2 (37.5, 75, and 150ng) was immobilized on the nitrocellulose membrane by spotting, and the membrane was blocked with TBS, 0.1% Tween supplemented with 1 μ g/ml of BSA (TBST-BSA) for 1 h at 22 °C. During this time, 10 μ g of His-S-tagged NHERF1 was mixed with TBST-BSA in the presence or absence of 25 μ g of human CXCR2 C-tail WT peptide for 1 h at 22–24 °C, and then the mixture was added to the membrane and incubated for 12 h at 4 °C. The membrane was washed extensively and immunoblotted with S-HRP (Novagen), which detects the S-tag within the His-S-NHERF1 fusion proteins on Western blot.

2.12 CXCR2 Degradation

HL-60 cells were differentiated into the granulocyte lineage (dHL-60) as previously described. 1x10⁶ cells dHL-60 cells were delivered 3.33 μ g of peptide (WT or DEL) through the ChariotTM peptide/protein delivery system, per the Chariot protocol (www.activemotif.com/documents/5.pdf) [214]. Cells were incubated for 0min, 3hours, or 6hours, in IMDM supplemented with 0.5% FBS and IL-8 (100ng/ml). Samples were

then rinsed, pelleted, and lysed in lysis buffer as described above. Protein estimations were taken and a Western blot was performed on the samples to determine total CXCR2 amount [80]. Processing of the Western blot data was completed as described previously.

2.13 Zigmond Migration Chamber

HL-60 cells were differentiated into the granulocyte lineage (dHL-60), with 1.2% DMSO in IMDM medium with 10% FBS for 5-7 days as described above [83, 216]. CXCR2 C-tail peptide (0.333ug of WT or Δ TTL) was delivered to 3×10^5 dhL60 cells through the ChariotTM peptide/protein delivery system [214]. 22x40-1.5 mm glass cover slips (Fisher Scientific) were coated in fibronectin, and dHL-60 cells were allowed to adhere to the slips for 30min. Cells were rinsed in IMDM and the coverslip was inverted onto the top of the Zigmond chamber. Clamps were applied to secure the coverslip in place and 90ul of IMDM was added to each chamber well [217, 218]. See **Figure 2.1**.

The Zigmond chamber was placed in a TC1-100 microscopic temperature controller (37°C, Bioscience Tools), and mounted onto a VWR (Randor, PA) microscope with a Vista Vision mounted camera. Chemoattractants, 50ng/ml IL-8 or 0.5uM fMLP, were added to the appropriate wells [83]. Images were captured on uIMAGE micro image analysis software, every 30 seconds for a total of two hours (240 images) [219]. The images were processed using ImageJ software (<http://rsbweb.nih.gov/ij/>), migratory paths were tracked using the Manual Tracking plug-in (<http://rsbweb.nih.gov/ij/plugins/track/track.html>), and any additional data processing was obtained using the Chemotaxis Tool (<http://www.ibidi.com/>) and through Microsoft

Excel. dHL-60 cells that migrated were randomly selected for tracking from each experiment.

2.14 Statistical Analysis

Error is expressed as the standard deviation of at least three independent experiments. Statistical significance of the migration experimental data was determined by the Rayleigh test, a value of $p < 0.05$ is considered to be significant.

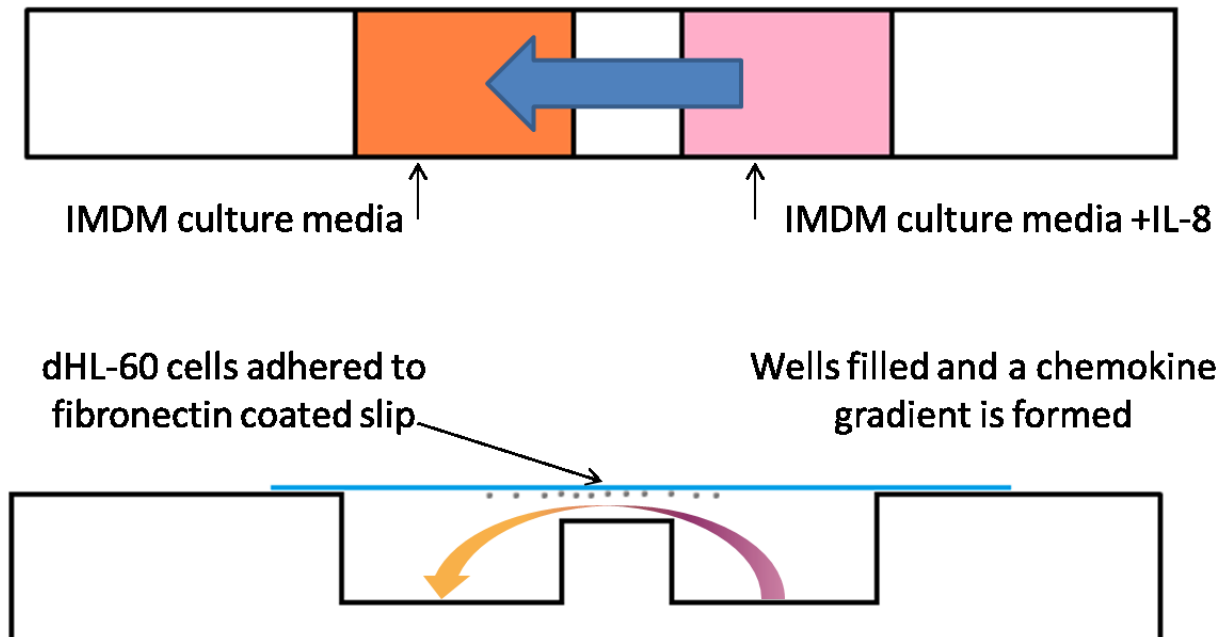


Figure 2.1 Zigmond Chamber

An illustration of the Zigmond chemotaxis chamber, the only difference between the wells (colored pink and orange) is the presence of a chemokine, which will diffuse through the gap created between the chamber bridge and a glass coverslip. As chemokine diffuses across the gap a gradient is formed (see curved arrow). Chemotaxing cells will respond to the gradient and migrate along the fibronectin coated coverslip towards the well containing IL-8.

CHAPTER 3

RESULTS

3.1 HL-60 Differentiation

Due to differences in expression of components used for receptor signal transduction, it was important to choose a cell line which closely resembles naturally occurring human neutrophils. It is beneficial to study CXCR2 in cells that naturally express the receptor and its complementary components, opposed to an overexpression system which can take the signaling mechanism out of context. HL-60 cells differentiated along the granulocytic pathway closely resemble neutrophils in many facets and, most importantly, express endogenous CXCR2 [220]. These cells are hematopoietic in origin, derived from a patient with acute promyelocytic leukemia, and represent a pluripotent leukemic cell line used extensively in laboratory research [221]. HL-60 cells are an immense contribution to the study of leukocytes and represent a reliable cell line for inflammatory research [222].

The HL-60 promyelocytes can be differentiated towards neutrophils (the granulocyte lineage) with exposure to Me₂SO (DMSO) [220]. Once HL-60 cells begin differentiation there is an increased expression of various chemokine receptors and their G-protein regulators, equating them towards naturally produced neutrophils [223-226]. These differentiated cells have been used extensively to study G-protein signaling and various other neutrophilic and monocytic activities. Differentiated HL-60 cells polarize, migrate towards chemoattractants, and detect chemokine gradients comparable to human neutrophils isolated from peripheral blood [13, 151].

3.2 Human Neutrophils and dHL-60 Cells

The NHERF proteins, like many other PDZ proteins, play a role in organization of plasma membrane domains, through clustering and anchoring specifically recognized motifs of target proteins [90]. PDZ mediated binding of NHERF1 is important at both ends of chemotaxing cells and provides multiple points of interaction for PDZ-motif containing proteins. CXCR2 possesses a PDZ-motif, suggesting CXCR2 becomes anchored to the scaffolding protein similar to SOCs, PLC β 2, or PTEN and PDGFR [227].

Like CXCR2, the PLC β family contains a type I PDZ-motif at their carboxy terminus. The small signaling molecule generators PLC β 1, PLC β 2 and PLC β 3 were investigated to determine their expression in dHL-60 cells. PLC β 2 and PLC β 3 are important in HL-60 differentiation along the granulocytic pathway, as their nuclear localization coincides with differentiation [228]. PLC β 2 is the prominent isoform expressed in human neutrophils, and is by and large the major isoform functioning during neutrophil chemotaxis, bearing responsibility for IP3 production and [Ca²⁺] influx, while PLC β 3 plays only a small role and PLC β 1 is non-existent [229-231]. If dHL-60 cells express proteins similar to human neutrophils, the data would be more relevant in *in vivo* models of human inflammation.

I used a Western blot to assay expression of proteins in dHL-60 cells, **Figure 3.1**. The data shows dHL-60 cells express NHERF1 (**A**), however NHERF2 (**B**) is undetectable in dHL-60 cells and seems to have a very low level of expression in undifferentiated HL-60 cells. PLC β 1 (**C**) was undetected in dHL-60 cells, which is congruent with other findings, and coincides with expression in neutrophils, which only

express PLC β 2 and PLC β 3 [232]. Differentiated HL-60 cells express high levels of PLC β 2 (**D**) and low levels of PLC β 3 (**E**) which also coincide with human neutrophils. As expected, dHL-60 cells produce proteins necessary for chemokine signal transduction, similar to other leukocytes.

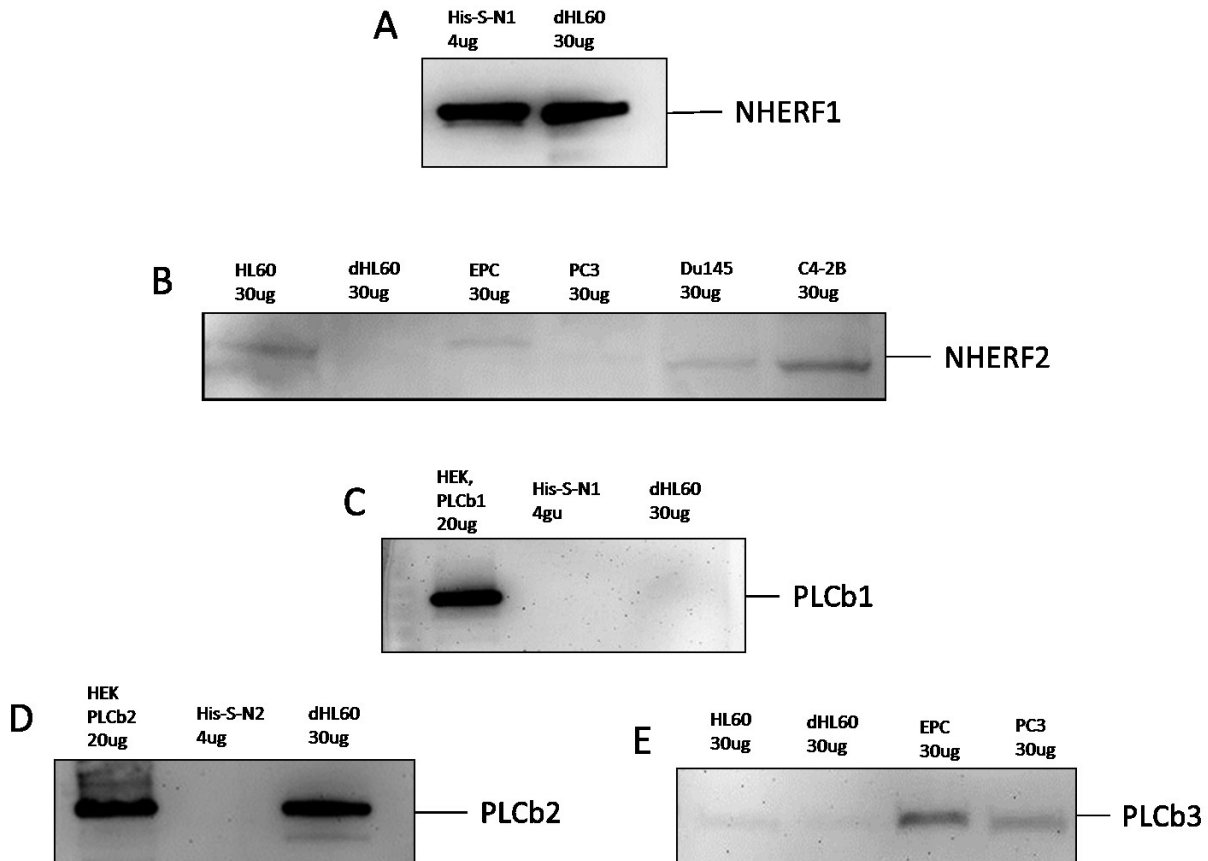


Figure 3.1 dHL-60 Expression of NHERF and PLC Isoforms

All dHL-60 samples contain 30ug of protein lysate, each membrane is immunoblotted with the appropriate antibody. (**A**) NHERF1 expression is detected and the purified His-S-tagged NHERF1 (N1) protein is used as a control. (**B**) NHERF2 expression is undetected compared to various cancer and HL-60 samples, known to express NHERF2, (His-S-tagged NHERF2 was undetectable). (**C**) PLC β 1 expression, undetected, compared to HEK cells overexpressing PLCB1. (**D**) PLC β 2 expression in dHL-60 cells compared to HEK cells overexpressing PLC β 2, expression is consistent with expectations. (**E**) PLC β 3 expressed at low levels, compared to control sample cells known to express PLC β 3.

3.3 Biochemical Assay Results

Due to PDZ-motif presence on CXCR2, initial studies linking CXCR2 and the NHERF proteins were carried out, [1] refers to our published article. Through a GST-tagged pulldown assay we found human CXCR2 overexpressed in HEK293 cells binds the scaffolding proteins NHERF1, NHERF2 and slightly to PDZK1 (NHERF3), see **Figure 3.2 (A)**. Murine CXCR2 from HEK overexpression (**B**) and, isolated from bone marrow neutrophils can also be pulled down by NHERF1, but not NHERF2 or NHERF3 (**D**). Furthermore, CXCR2 derived from human neutrophil cells preferentially interact with NHERF1, and can also bind NHERF2 (**C**), and this is also observed in CXCR2 from dHL-60 cells (**E**).

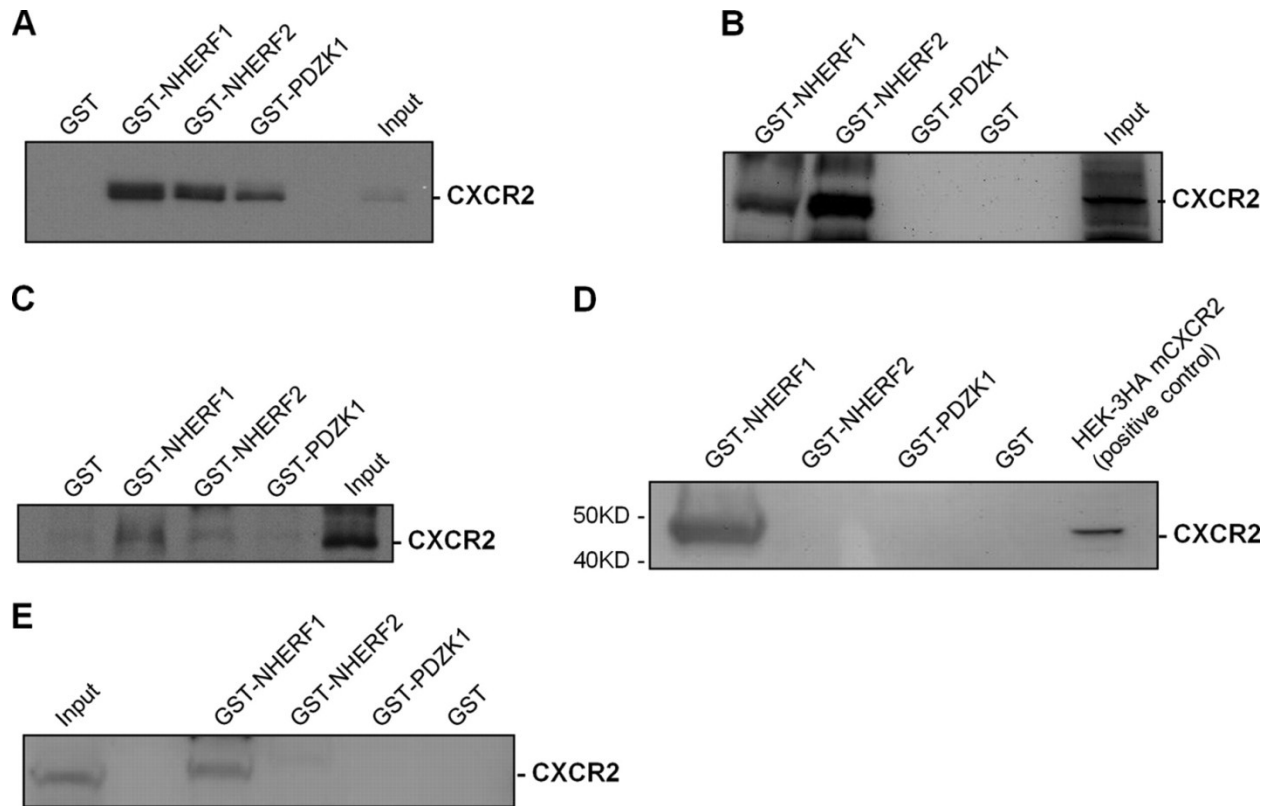


Figure 3.2 CXCR2 Interacts with NHERF

CXCR2 preferentially interacts with NHERF1 in neutrophils. (A), HA-tagged human CXCR2 (overexpressed in HEK293 cells) was pulled down by PDZ scaffold proteins (NHERF1, NHERF2, and PDZK1). The membrane was blotted with anti-HA monoclonal antibody. (B), His-S-tagged murine CXCR2 (overexpressed in HEK293 cells) was pulled down by the indicated PDZ scaffold proteins. The membrane was blotted with anti-mouse CXCR2 monoclonal antibody. (C), NHERF1 and NHERF2 bound to endogenous CXCR2 from human neutrophils. The membrane was immunoblotted with anti-human CXCR2 monoclonal antibody. (D), NHERF1 bound to endogenous CXCR2 from murine bone marrow neutrophils. Cell lysates of HEK293 cells that overexpressed 3HA-murine CXCR2 were loaded as a positive control. The membrane was immunoblotted with anti-murine CXCR2 monoclonal antibody. (E), NHERF1 and NHERF2 bound to endogenous CXCR2 from neutrophil-like cells, dHL-60 cells. The membrane was immunoblotted with anti-human CXCR2 monoclonal antibody. Taken from [1].

We performed a similar experiment on PLC β isoforms, **Figure 3.3**, as they also possess C-terminal PDZ-motifs. The direct downstream effector of CXCR2 G-protein signaling, PLC β 2 (**B**), along with PLC β 1 (**A**) and PLC β 3 (**C**) preferentially bind to NHERF1 and somewhat with NHERF2. This is shown through a GST-tagged pulldown of HEK293 cells overexpressing each PLC β isoform. Further, data showed PLC β 2 from murine bone marrow neutrophils (**D**) and dHL-60 cells (**E**) preferentially interact with NHERF1. Bearing in mind leukocytes have high levels of PLC β 2 and NHERF1, the scaffolding protein NHERF1 was considered to naturally bind both CXCR2 and PLC β 2 in leukocytes.

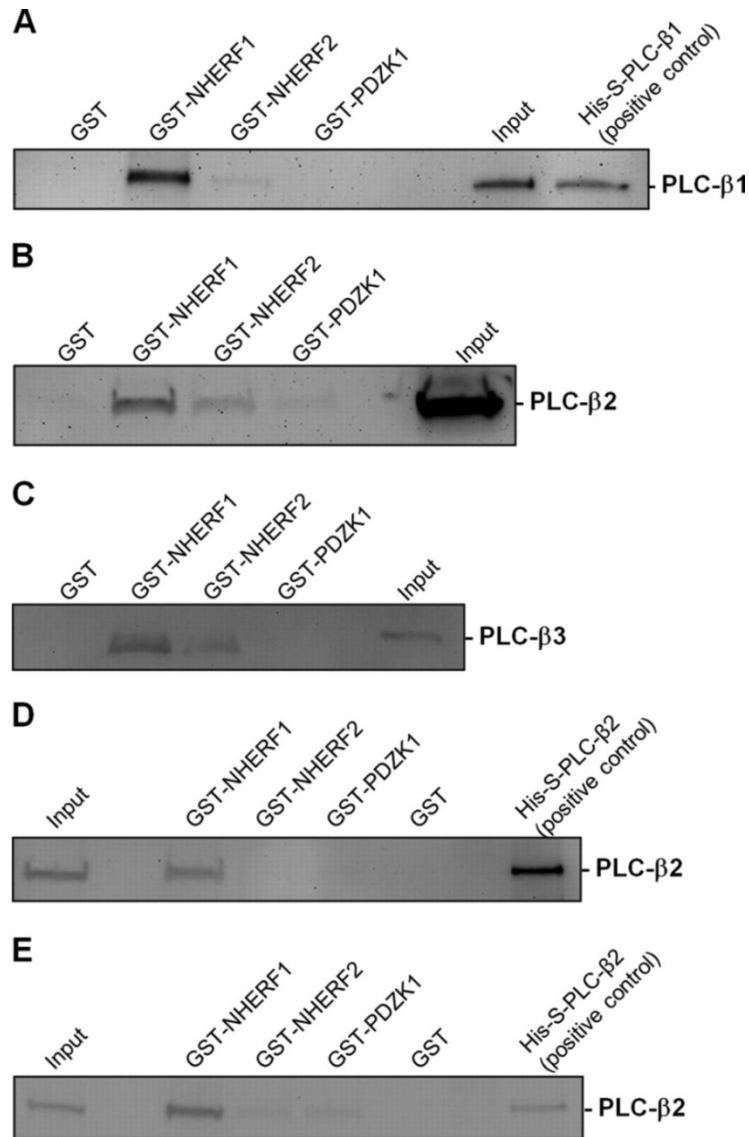


Figure 3.3 PLCβ Isoforms Interact with NHERF

PLC-β isoforms physically interact with PDZ scaffold proteins, whereas PLC-β2 in neutrophils preferentially interacts with NHERF1. A–C, HEK293 cells were overexpressed with FLAG-tagged PLC-β1 (A), PLC-β2 (B), and PLC-β3 (C), and the GST pull-down assays were performed with PDZ scaffold proteins as described under “Experimental Procedures.” The membranes were immunoblotted with anti-PLC-β1 (A), PLC-β2 (B), and PLC-β3 (C) monoclonal antibodies, respectively. Purified His-S-PLC-β1 (20ng) was loaded as positive control for the PLC-β1 antibody (A). D and E, endogenous PLC-β2 from neutrophils freshly isolated from mouse bone marrow (D), or from neutrophil-like cells, dHL-60 cells (E), was pulled down by PDZ scaffold proteins. The membranes were immunoblotted with anti-PLC-β2 monoclonal antibody. Purified His-S-PLC-β2 was loaded as positive control for the PLC-β2 antibody. Image obtained from [1].

We hypothesized the PDZ scaffold proteins, namely NHERF1, would complex CXCR2 and PLC β 2 in a PDZ motif-dependent manner, and we were successfully able to assemble a complex of CXCR2, PDZ scaffold proteins, and PLC β 2 *in vitro*, **Figure 3.4**. His-S-C-tail derivatives of either CXCR2 or PLC β 2 were pulled down by S-protein agarose beads. The complement purified protein (PLC β 2 or CXCR2, respectively) was probed for by Western blot. The pulldown of either His-S-CXCR2 C-tail or His-S-PLC β 2 C-tail can precipitate the entire complex, and NHERF1 seems to be the favored scaffolding protein, and is necessary for complex formation. We also observed complex formation from murine bone marrow neutrophils endogenous CXCR2 and PLC β 2 mediated by NHERF1 *in vivo*. Furthermore we found NHERF1-CXCR2 binding to be dose-dependent.

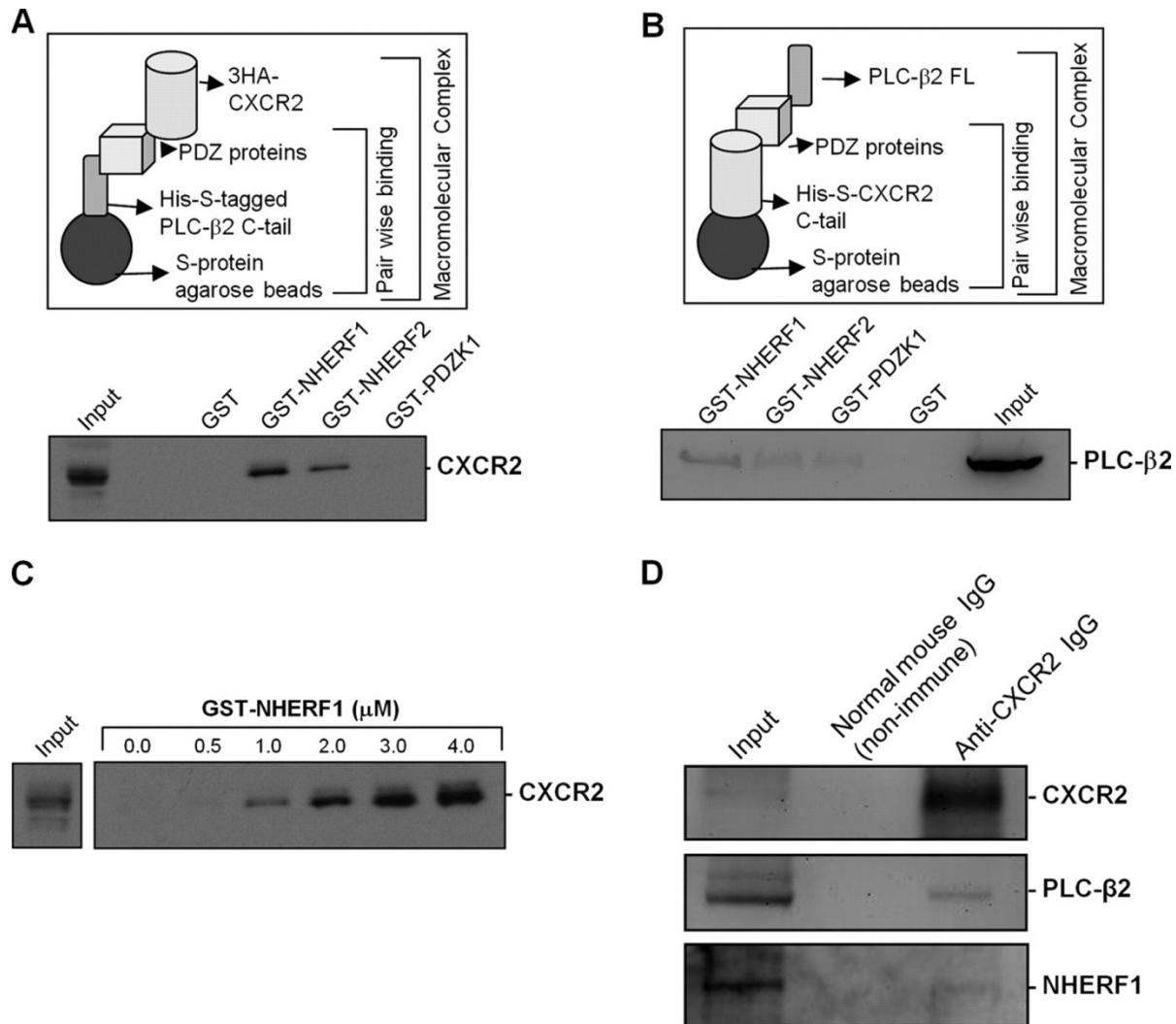


Figure 3.4 Macromolecular Complex Formation

CXCR2, NHERF1, and PLC-β2 form a macromolecular complex *in vitro* and in neutrophils. (A), schematic representation of *in vitro* macromolecular complex assembly (*upper panel*, refer to “Materials & Methods” for details). Macromolecular complex of PLC-β2 C-tail, PDZ scaffold proteins, and human full-length CXCR2 (*lower panel*) are shown. (B), macromolecular complex of PLC-β2 full-length, PDZ scaffold proteins, and mouse CXCR2 C-tail. (C), dose-dependent (GST-NHERF1) macromolecular complex formation of His-S-tagged PLC-β2 C-tail, GST-NHERF1, and HA-tagged human CXCR2. (D), endogenous PLC-β2 and NHERF1 were co-precipitated with CXCR2 from murine bone marrow neutrophils. Image taken from [1].

3.4 CXCR2 C-terminal Synthetic Peptide

Formation of the CXCR2 macromolecular complex can be disrupted by delivery of an exogenous biotin conjugated peptide which mimics the last 13 amino acids on the C-tail of CXCR2 (biotin-FVGSSSGHTSTTL), thus competing with endogenous CXCR2 for PDZ-mediated binding of NHERF1. Our lab demonstrated this by a far Western blot, which shows increasing amounts of CXCR2 binding to NHERF1, and inclusion of the WT CXCR2 C-tail peptide disrupts the interaction, see **Figure 3.5**. Disruption of the CXCR2 macromolecular complex, and CXCR2 dependent downstream activities, was accomplished only by CXCR2 C-tail peptides containing the WT (wild type) PDZ motif. In either mutation (AAA) or deletion (Δ TTL) variants of the CXCR2 C-terminal peptide there was no difference compared to control cells, see [1]. **Figure 3.6** illustrates the nucleation of the CXCR2 macromolecular complex.

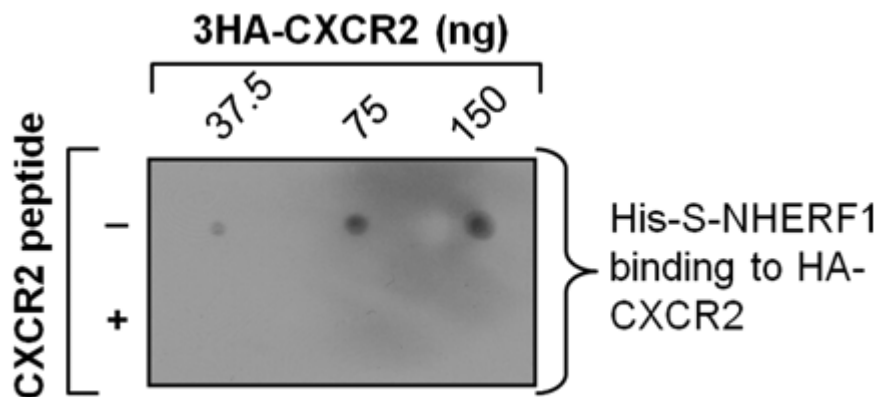


Figure 3.5 CXCR2 C-tail Peptide

A CXCR2 C-tail-specific peptide disrupts the physical interaction between NHERF1 and CXCR2. Binding of His-S-NHERF1 to 3HA-human CXCR2 in the presence of human CXCR2 C-tail WT peptide on a Far Western blot. The membrane was immunoblotted with HRP-conjugated S-protein, which detects S-tag within His-S-NHERF1. Image obtained from [1].

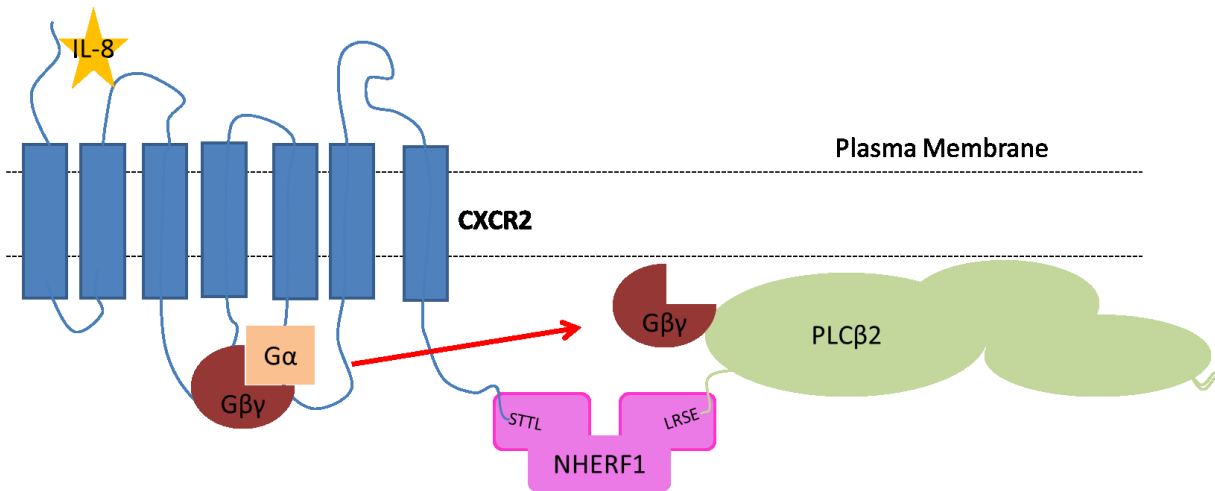


Figure 3.6 NHERF1 Nucleates CXCR2 and PLC β 2
 Diagram depicting PDZ domain interactions of NHERF1 can nucleate CXCR2 and PLC β 2 into a macromolecular complex, localizing receptor and effector together for greater signaling efficiency. C-terminal PDZ-motifs are STTL (CXCR2) and ESRL (PLC β 2).

3.5 CXCR2 Degradation

The NHERF1 scaffolding protein is involved in β 2 adrenergic receptor (β 2AR) internalized sorting between the degradative-endocytotic pathway and receptor recycling to the plasma membrane. A truncation of β 2AR's PDZ motif prevents NHERF1 binding, resulting in increased rates of receptor degradation. Furthermore, the phosphorylation of the P₋₂ serine (β 2AR PDZ-motif is DSSL) inhibits NHERF1 PDZ- β 2AR interaction and affects intracellular sorting [233]. Similarly the C-terminal PDZ domain of CXCR2 is required for efficient internal sorting of CXCR2, as loss of the PDZ-motif affects receptor recycling [85].

I conducted a CXCR2 degradation assay to determine if the CXCR2 C-tail WT peptide would interfere with receptor recycling. If the exogenous peptide affects

receptor recycling, leading to degradation, CXCR2 stimulation could be greatly diminished and could affect functional and migrational data. Degradation was assayed by measurement of the total CXCR2 protein amount over a series of time points. As IL-8 binds to CXCR2 and activates signaling the receptor becomes internalized, see **Figure 3.7**.

Complications arose when trying to assay total cellular membrane protein through a western blotting protocol as Western blots are not sensitive enough to small shifts in protein amount. This is due in part to antibody binding, which is slightly erratic, high levels of background noise, and incomplete transfers of protein to the PVDF membrane. This assay was tested five times, and each gave a different outcome. Three of the five provided quantifiable results and are displayed in the chart below. Also provided is a Western blot image, which demonstrates some of the problems associated with this procedure.

Based on the findings there is no significant change in CXCR2 levels over the course of six hours in CXCR2 C-tail WT treated dHL-60 cells, compared to controls. This indicates no excessive CXCR2 degradation due to the presence of CXCR2 C-tail WT peptide. Further, this assures us that migrational data collected over the two hour time period is due to interruption of PDZ domain binding and not a repressed level of CXCR2. The CXCR2 degradation data shows a trend line average, which decreases slightly as time passes for control and DEL (PDZ-motif truncation) samples, and decreases more abruptly in CXCR2 C-tail WT delivered dHL-60 cells.

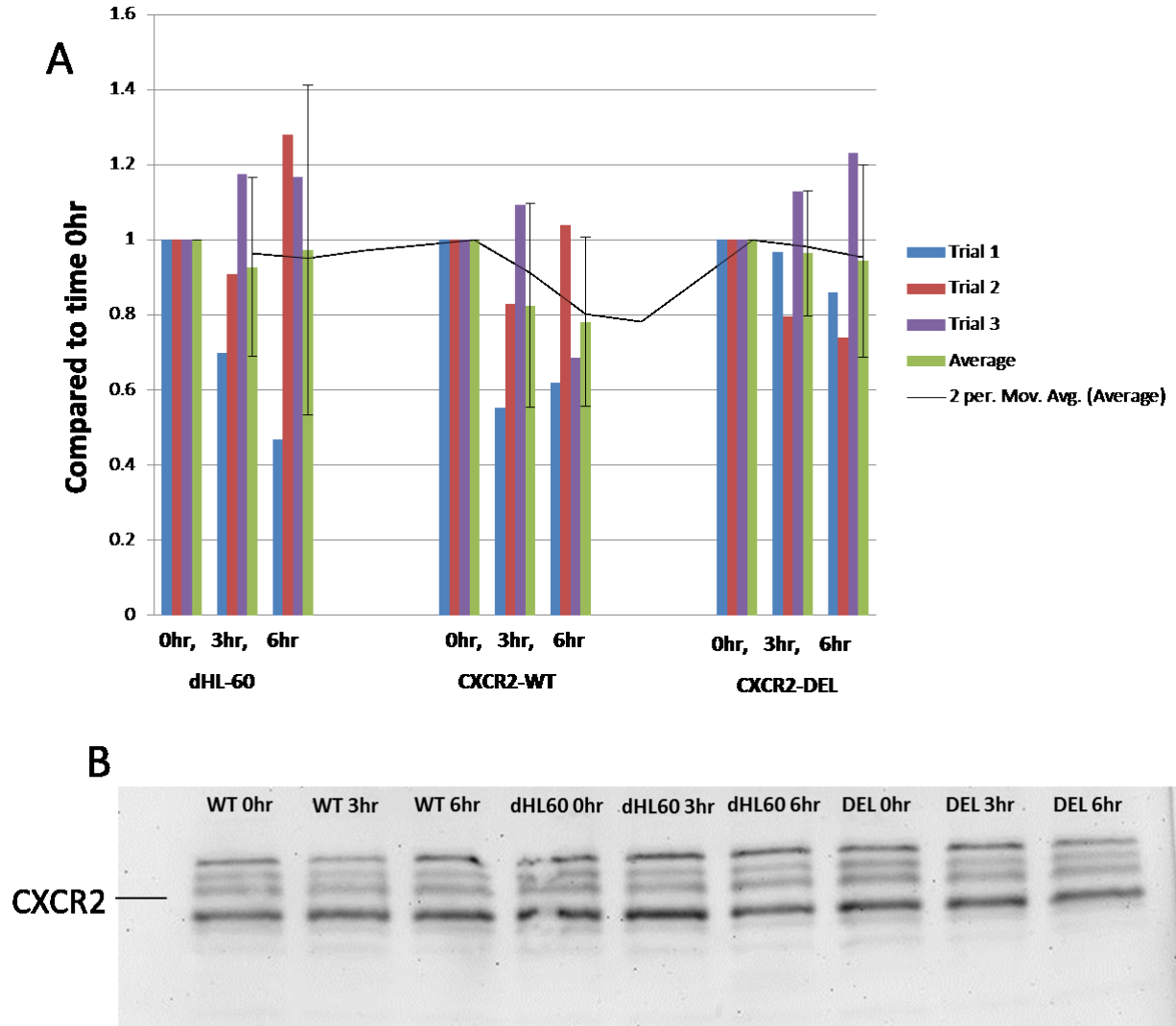


Figure 3.7 CXCR2 Degradation

Cells are treated at various times with 100ng/ml of IL-8, a Western blot is performed, and then probed for CXCR2. (A) Chart depicts trials of three Western blot experiments. Average of all three in a given sample are green bars, average error bars are based on the standard deviation, and moving average is based on the last two average bars. (B) Image of a Western blot depicting some problems associated with the experiment and data acquisition, notice lower band intensity near the edges and incomplete transfer of some bands.

3.6 Migration Introduction

Targeting CXCR2's PDZ domain, which is four residues long, gave a highly specific site to focus on. In functional experiments interruption of the CXCR2 PDZ-domain, through an exogenous CXCR2 C-tail peptide, affects downstream cellular activity, see [1] for functional data. Disruption of complex formation represses CXCR2 calcium mobilization, a hallmark of PLC β 2 signaling [234]. Also, disrupting the NHERF1 PDZ-domain interaction with CXCR2 in dHL-60 cells inhibited GRO α and IL-8 chemotaxis during transwell and thansepithelial monolayer migration. However, fMLP migration was not disrupted in either assay, as bacterial proteins signal through formylated peptide receptors. Following up on our previous paper [1], I further explored dHL-60 cell migration to determine how CXCR2 type I PDZ-motif interactions affect cellular migration and direction. The aim of my experiment was to characterize the phenotypic difference between wild-type control cells and those delivered the CXCR2 C-tail WT peptide, described previously.

CXCR2 is distributed around the cell as a transmembrane protein and is bound to NHERF1 forming a cytosolic signaling complex, which anchors the CXCR2 complex on the cytoskeletal network. Disruption of NHERF1-CXCR2 PDZ-binding could free CXCR2 from the cytoskeleton allowing chemokine signaling to be less stationary as CXCR2 can laterally diffuse along the membrane. CXCR2's resulting activity could be a considerable distance away, and CXCR2 bound adaptor proteins (LASP-1, VASP, IQGAP etc.) could spur actin mobilization in areas separate from the original stimulation site. This would lead to a misrepresentation of the intracellular frontness signaling against the extracellular IL-8 gradient. Also, if CXCR2 were unable to bind the NHERF1-

PLC β 2 complex the receptor associated G-proteins would be further away from downstream target PLC β 2. Therefore, G-protein signaling would be reduced, which could explain the decrease in calcium mobilization observed, and this could further hamper migration activities which are G $\beta\gamma$ dependent.

In the following Zigmond chemotaxis chamber experiment dHL-60 cells were used, along with CXCR2 C-tail peptide derivatives, to assess the effects of CXCR2's PDZ interaction during chemotaxis. Six sample types of dHL-60 cells were used, two control untreated cell types and four cell types treated with Chariot peptide delivery system (with or without CXCR2 C-tail peptides). The two control untreated cell types are dHL-60 cells supplied with (dHL+IL8) or without (dHL-IL8) an IL-8 chemokine gradient. The positive control dHL+IL8 cells are expected to migrate uniformly towards the source of the IL-8 gradient. The negative control dHL-IL8, which are not supplied an IL-8 gradient, are expected to show no directed movement and move at random.

All four Chariot treated sample types are supplied with a gradient of IL-8 and treated with the Chariot peptide delivery system. The positive control group (CHAR) contained no additional CXCR2 C-tail peptide, only the chariot delivery vehicle. Two other experimental sample types were delivered either the CXCR2 C-tail WT peptide (WT), or the CXCR2 C-tail PDZ-deletion peptide which was missing the three terminal PDZ-motif amino acids (DEL). Based on the results of the previous study DEL samples should behave similar to controls, whereas WT cells migration should be disrupted.

The last sample type is identical to the WT samples, delivered with CXCR2 C-tail WT peptide and supplied an IL-8 gradient, but were also exposed to an opposing gradient of fMLP (WT+fMLP). In this sample the intermediate target IL-8, which signals

through CXCR2, should be overlooked for the end target fMLP bacterial derived chemoattractant, which signals through FPR [206]. Therefore the CXCR2 C-tail WT peptide should have no effect on the fMLP directed migration. This was observed, as dHL60 cell function is inhibited by CXCR2 C-tail WT for GRO α and IL8, but not fMLP [1]. In all relevant sample types the IL-8 gradient was supplied from the downward direction and fMLP was supplied from the top. My hypothesis is that the perturbing CXCR2's PDZ-motif binding interaction will disrupt the spatial sensation of a chemokine gradient and impair cellular chemotaxis.

3.7 Distance Traveled

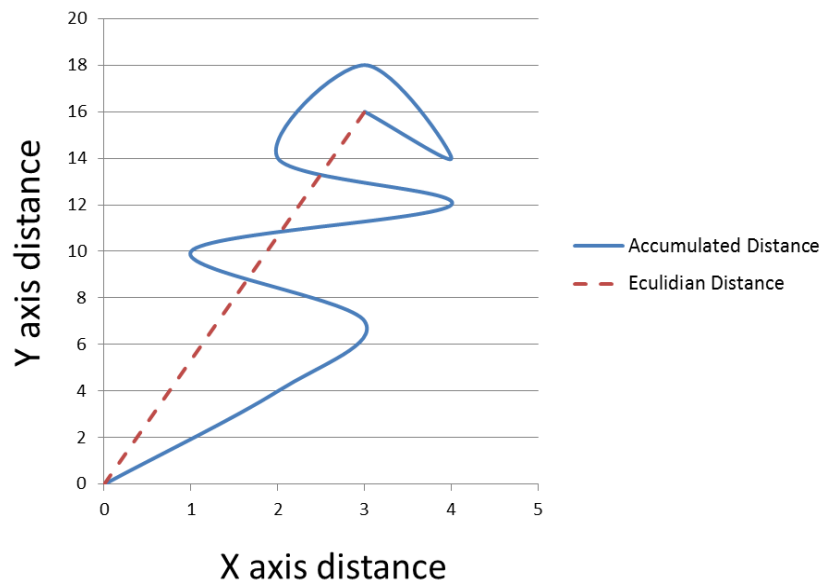


Figure 3.8 Distances Defined

The accumulated distance (Acc) refers to the total length of the path the cell took to arrive at its endpoint. Euclidian distance (Euc) refers to the distance between the endpoint and the origin, as demonstrated in the figure.

The data was divided into two portions, the control non-treated dHL-60 cells and the dHL-60 cells treated with the Chariot peptide delivery system (Note: Samples exposed to fMLP gradients were excluded from either group, as there were too many variables compared to controls). The distance data between the two groups seemed strikingly different at first glance, see **Figure 3.8** and **Table 3.1**. Non-treated control cells moved an average of 126.1um Euclidian distance (Euc) and 883.7um Accumulated distance (Acc), while the peptide treated cells moved an average of 212.4um Euc and 1029.4um Acc. This amounted to only a 16.4% increase in accumulated distance but a 68.4% increase in Euclidian distance. Since the accumulated distance of all peptide delivered cells seems to be constant (20-30% increase compared to dHL+IL8 cells, calculations not shown), the use of the Chariot system might stress the cells, which could increase responsiveness through the inflammatory/chemotactic response. Therefore the two types of conditions were separated to analyze the distance data appropriately.

Table 3.1 Distances Traveled**Distances of non-treated Control samples Vs. Peptide treated samples****This chart portrays the accumulated and Euclidian distances for the two groups, highlighting the differences in distance between treated and non-treated samples.**

	<u>Euclidian Distance</u>			<u>Total</u>	<u>Average</u>	<u>Vs. Control</u>
Control	dHL+IL8	140.6				
	dHL-IL8	111.6		252.2	126.1	
Peptide	CHAR	228.6				
	DEL	247.1				
	WT	161.6		637.3	212.4	68.4%
	WT+fMLP	287.4		287.4	287.4	127.9%
	<u>Accumulated Distance</u>			<u>Total</u>	<u>Average</u>	<u>Vs. Control</u>
Control	dHL+IL8	823.8				
	dHL-IL8	943.7		1767.5	883.7	
Peptide	CHAR	994.8				
	DEL	1086.6				
	WT	1006.9		3088.3	1029.4	16.4%
	WT+fMLP	998.9		998.9	998.9	13.0%

Taking into account the non-peptide delivered control samples, see **Table 3.2**, the accumulated distance is fairly similar with dHL-IL8 cells having ~14.6% more Acc compared to dHL+IL8. But when Euclidian distance is considered, dHL-IL8 cells have 79.4% (20.6% less) Euclidian distance traveled than their counterparts, dHL+IL8 cells. The Euclidian data is what is generally to be expected, as the negative control should move in a less directional manner. Even though the dHL-IL8 Euclidian distance decreased by only 20.6% the accumulated distance travelled by dHL-IL8 is 14.6% greater, which makes it is safe to assume that if both cell types had travelled the same

total accumulated distance the dHL-IL8 Euc deficit would be even greater. This is evident when we take the directness ($D = \text{Euclidian} / \text{Accumulated distance}$) of the two, **Table 3.3.** dHL+IL8 has a $D=17.1\%$ and dHL-IL8 has a $D=11.8\%$. Comparing the two, dHL-IL8 has only 69.3% of dHL+IL8's directness (a 30.7% decrease). Therefore, dHL-IL8 cells would have about ~30% less Euc corrected-distance than dHL+IL8 cells, which is expected, given the dHL-IL8 sample has no chemokine gradient to migrate towards but will still move randomly.

Looking at the group of Chariot-peptide delivered cells we see accumulated distance compared to positive control CHAR is fairly similar, with DEL and WT samples having a slight increase of 9.2% and 1.2% Acc distance, respectively, **Table 3.2.** Euclidian distance shows DEL cells have 8.1% increase compared to CHAR, which correlates closely to their 9.2% increase of Acc distance. Compared to CHAR, WT samples show a 29.3% decrease in Euc distance, and comparing that with their 1.2% increase in Acc gives an account similar to the $D=30\%$ decrease witnessed by dHL-IL8 vs. dHL+IL8. WT+fMLP group Acc is only 0.4% greater than positive control CHAR, yet the Euc distance is increased 25.7%, which is significantly higher than the similarly treated WT sample.

Table 3.2 Distances Traveled Vs. Controls

Table depicts total accumulated and Euclidian distances for each sample type. A comparison of negative control (dHL-IL8) or experimental samples (DEL, WT, WT+fMLP) with their positive controls (dHL+IL8, CHAR) for each group, respectively.

	<u>Accumulated Distance</u>		<u>Vs. dHL+IL8</u>	<u>Vs. dHL+IL8</u>
Control	dHL+IL8	823.8		
	dHL-IL8	943.7	1.146	14.6%
	<u>Accumulated Distance</u>		<u>Vs. CHAR</u>	<u>Vs. CHAR</u>
Peptide	CHAR	994.8		
	DEL	1086.6	1.092	9.2%
	WT	1006.9	1.012	1.2%
	WT+fMLP	998.9	1.004	0.4%
	<u>Euclidian Distance</u>		<u>Vs. dHL+IL8</u>	<u>Vs. dHL+IL8</u>
Control	dHL+IL8	140.6		
	dHL-IL8	111.6	0.794	-20.6%
	<u>Euclidian Distance</u>		<u>Vs. CHAR</u>	<u>Vs. CHAR</u>
Peptide	CHAR	228.6		
	DEL	247.1	1.081	8.1%
	WT	161.6	0.707	-29.3%
	WT+fMLP	287.4	1.257	25.7%

Comparing the directness to positive control CHAR, DEL has a D=98.9%, almost identical, showing CXCR2 C-tail DEL-peptide has no substantial influence on migratory directness, **Table 3.3**. WT has a D=69.8% compared to CHAR (30.2% decrease), which is almost identical to the dHL-IL8 vs. dHL+IL8 data (30.7% decrease). WT+fMLP

displays a high directness, $D= 28.8\%$, and is 24.9% greater than CHAR samples. This is most likely due to fMLP being an end target chemoattractant and stimulating a stronger response in the neutrophil-like cells. This data demonstrates an endogenous CXCR2 PDZ-motif peptide disrupts directness of migration towards IL-8, a host produced chemoattractant which signals through CXCR2, but does not disrupt directness of migration towards bacterial derived chemoattractants.

Table 3.3 Directness

Directness of each experimental sample, based on total distance traveled, compared to its positive control. The greater the directness, the more linear (less random) the motion in a given direction.

	<u>Euc/Acc</u>	<u>Directness</u>	<u>Vs. dHL+IL8</u>	<u>Vs. dHL+IL8</u>
dHL+IL8	0.171	17.1%		
dHL-IL8	0.118	11.8%	0.693	-30.7%
	<u>Euc/Acc</u>	<u>Directness</u>	<u>Vs. CHAR</u>	<u>Vs. CHAR</u>
CHAR	0.230	23.0%		
DEL	0.227	22.7%	0.989	-1.1%
WT	0.160	16.0%	0.698	-30.2%
WT+fMLP	0.288	28.8%	1.249	+24.9%

3.8 Directness

Directness (D) is the quotient of Euclidian distance over the accumulated distance ($D=Euc/Acc$). The samples directness through time is the average directness of each cell in a sample at every time-point. Note: Directness is not a comparison of compass direction; it is a comparison of distances travelled, the more direct ($D=1$) the

straighter the path, the less direct ($D=0$) the more random the path. A cell chemotaxing towards a gradient should display a higher directness than a cell migrating randomly.

Assessing the average directness requires distance data, thus the samples were again divided, due to differences previously mentioned. Disregarding the WT+fMLP sample for a moment, **Figure 3.9** shows the control CHAR and DEL samples have the highest overall directness towards IL-8, and are the two most direct moving sample types with a $D=0.25$ and 0.22 , respectively. The third most direct moving cell type was the control dHL+IL8, $D=0.19$. WT cells started out with a high directness, but gradually decreased, finishing at $D=0.17$, and the dHL-IL8 had the least direct movement, which is expected from the negative control, $D=0.13$.

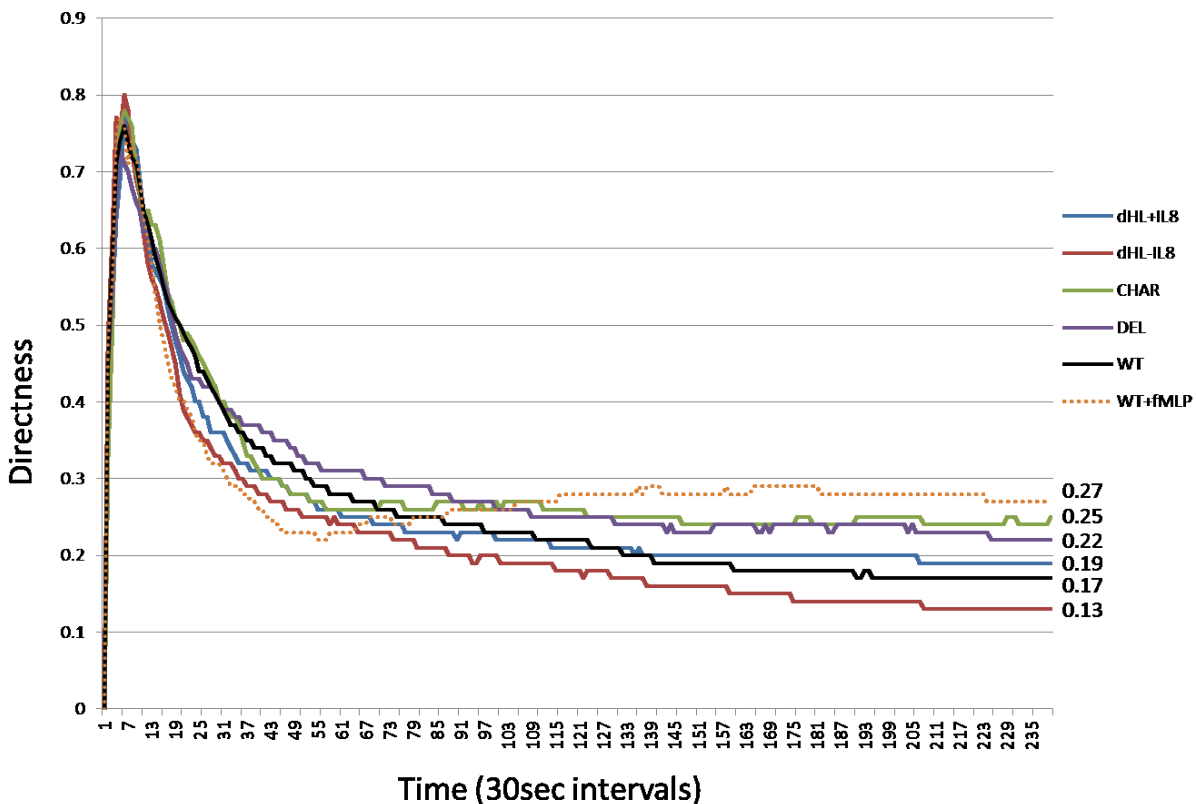


Figure 3.9 Directness Vs. Time

Average directness of each experimental sample throughout the 120 minute experiment. End target fMLP directed samples have the highest overall directness, followed by positive controls, and negative control dHL-IL8 have the lowest overall directness.

Parallels can be drawn between the differences in directness of the two groups of cells. dHL+IL8 has a higher end-value directness than the dHL-IL8 control (difference of 0.06), similarly CHAR has a higher directness than the WT sample (difference of 0.08), while CHAR and DEL samples display more similar values (difference of 0.03). Furthermore, WT+fMLP cells have the highest directed movement, compared to WT there is a difference of 0.10, and only fMLP to account for the difference. An explanation of the extremely high rate of directness in the beginning of the experiment might come from the way in which directness is calculated; as time passes each cell has a greater opportunity to turn, thereby changing the endpoint, and affecting the Euclidian distance, but accumulated distance is always increasing. This is doubly true if the cell makes a U-turn and decreases its Euclidian distance while increasing the accumulated distance. Since only moving cells were counted, and most move relatively straight for short periods of time, their original few motions would have yielded high directness, until turns, random movement, or directed migration patterns take over.

The difference in directed movement is evident when averaging the directness of each group **Table 3.4**. The average percent directness of negative control dHL-IL8 compared to positive control dHL+IL8 is ~68%. Average directness of DEL or WT compared to CHAR is ~89% and ~68% respectively. This is evidence that dHL-60 cells in the presence of an IL-8 chemokine gradient simultaneously treated with a CXCR2 C-tail WT peptide migrate in a directed manner similar to negative control cells in no such IL-8 gradient. Furthermore, the DEL treated cells lacking a competitive exogenous PDZ-motif migrate similar to normal positive controls, and addition of an end target fMLP

gradient restores directional migration in WT samples (WT+fMLP directness is 11.0% greater than CHAR positive control).

Table 3.4 Average Directness

Average directness of all cells in a given sample. The directness is compared to the positive controls, parallels can be drawn between the negative control dHL-IL8 and WT treated samples.

<u>Average Directness</u>		<u>Vs. Positive Control</u>	<u>Vs. Positive Control</u>
dHL+IL8	0.188	1	
dHL-IL8	0.128	0.680	68.0%
CHARIOT	0.245	1	
DEL	0.218	0.889	88.9%
WT	0.166	0.677	67.7%
WT+fMLP	0.272	1.110	111.0%

3.9 Forward Migration Index

Forward migration index (FMI) is the distance travelled in a single plane, either vertical (Y-axis) or horizontal (X-axis), see **Figure 3.10**. Where directness measured the efficiency of migration without direction, FMIs measure the distance travelled either horizontally or vertically from the origin. If a gradient is applied in one plane it's average forward migration towards or away from the source would give an account of the sources attractive or repelling characteristics. An average migration in the other plane, without a gradient, should be near zero because there are no attractive or repulsive influences in said plane. If no gradient is established the average forward migration in

both planes should be around zero, as average migration patterns should even out in an adequate sample size. As you can see from **Figure 3.11** the cells averaged 0.05 units or less in horizontal movement from the origin. Since the IL-8 (or fMLP) gradient was supplied vertically, seeing little horizontal movement is expected.

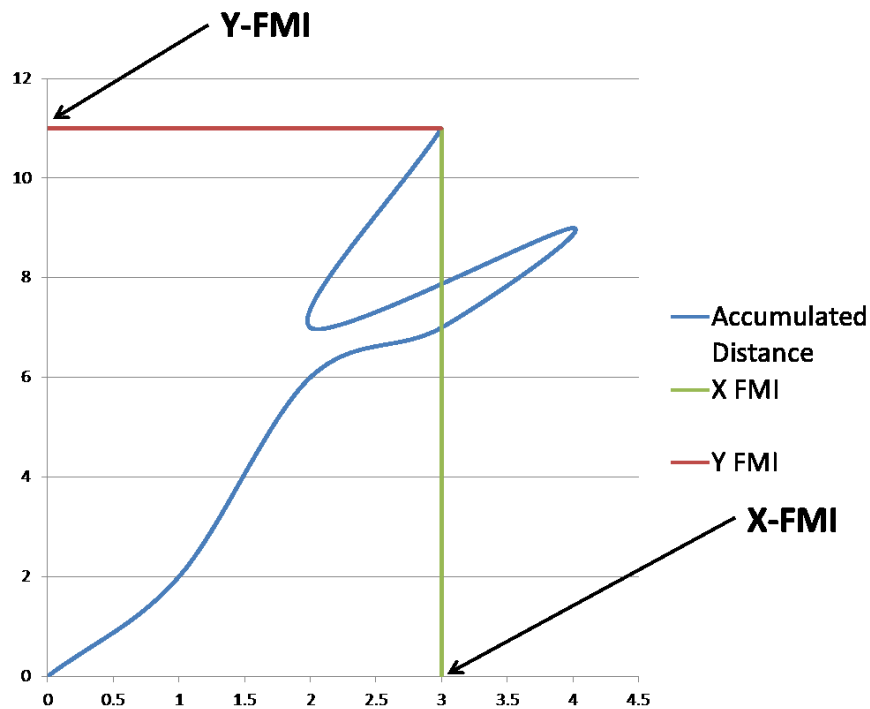


Figure 3.10 Forward Migration Indexes Defined
Schematic diagram showing the Forward Migration Index (FMI). FMI's are only observed on the X or Y axis. It measures how far horizontal or vertical a cell has moved from the origin, as depicted by the green or red lines.

The Y-axis FMI is similar in dHL+IL8 and CHAR positive controls, which moved down (negative Y-value) towards the source of IL-8, as did DEL samples. The only two samples that did not have significant vertical movement were dHL-IL8 and WT cells, see **Table 3.5** and **Figure 3.11**. WT actually moved away from the gradient source, whereas dHL-IL8 cells movement is completely random. Following the hypothesis, if WT chemokine gradient sensation is disrupted then cells should exhibit more “random”

motion compared to a direct one observed by the positive controls. Randomness in WT samples, or absence of gradient in dHL-IL8 samples, is observed by noting that they average almost no horizontal or vertical FMI (less than 0.02UNITS). Though, forward migration was rescued in WT cells exposed to a fMLP gradient, as WT+fMLP samples moved significantly towards the source of bacterial chemoattractant.

Table 3.5 Endpoint FMI's

Endpoint X and Y-FMI of each sample, negative Y-values correlate to IL-8 mediated chemotaxis, positive Y-values correlate to fMLP mediated migration.

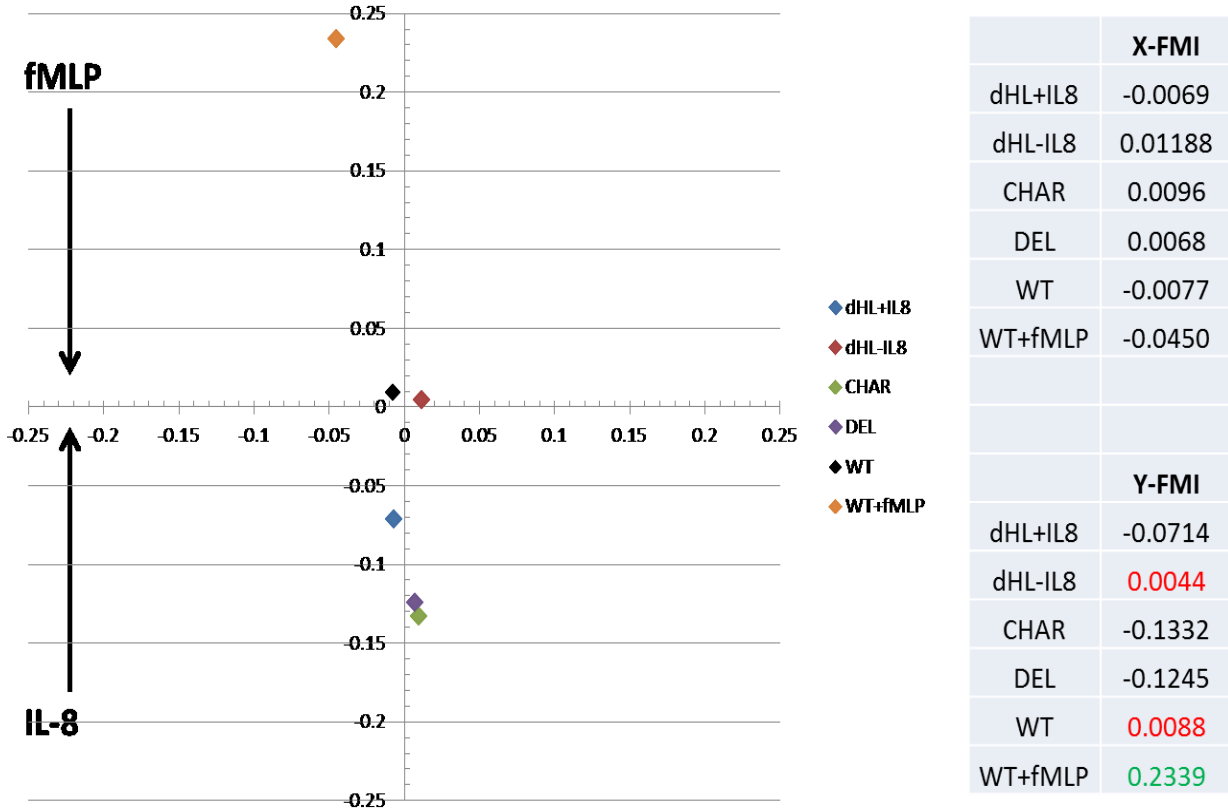


Figure 3.11 Average FMI's

Representation of each samples average FMI's plotted on a graph. Average downward migration correlates to IL-8 mediated chemotaxis, upward migration is towards fMLP. There is no gradient on the X-axis plane, therefore total X-FMI should be minimal.

3.10 FMI Through Time

Looking at an average of each sample we can track the X-axis and Y-axis FMI through time. These are displayed in **Figure 3.12** and **Figure 3.13**. In each case the opposite axis displays the time, each point plotted corresponds to 30sec and all 240 time-points total the two hours the experiment was executed. Considerations should be made for the time it takes to establish a gradient, and the length at which the gradient is effective before homogeneity. As previously stated, a vertical chemoattractant gradient should cause the dHL-60 cells to move downward towards IL-8 (or upwards for fMLP) and have no overall effect on the X-FMI. Likewise dHL-60 cells exposed to no chemokine gradient should have little X or Y-axis FMI.

X-axis FMI, **Figure 3.12**, shows cells migrate to the left (negative X values) early on, this is probably due to the side of the well the chemoattractants were added, when the gradient is being formed. By roughly 20min most samples have tracked back to a zero X-value, which it should theoretically have been from the onset, but does demonstrate their sensitive perception of chemoattractants. Once the gradient is established (roughly 20-30min) the cells do not travel far horizontally for the remainder of the experiment.

The Y-axis FMI, seen in **Figure 3.13**, shows positive controls dHL+IL8 and CHAR moving towards the negative Y-values through time. DEL cells behave similar to the CHAR positive control with regard to an almost identical Y-axis FMI. dHL-IL8 and WT cells stay relatively close to the Y axis ($Y=0$), which stated before, is expected in a population of cells with random migration patterns. Although WT cells were provided an IL-8 gradient they behaved strikingly similar to negative control dHL-IL8 cells. Once

again we see forward migration can be rescued in WT cells by inclusion of a fMLP gradient. This data directly supports the hypothesis, and points to a PDZ-motif dependent disruption of CXCR2 chemokine-directed migration, which is undetected in DEL samples, and rescued by an end target chemoattractant.

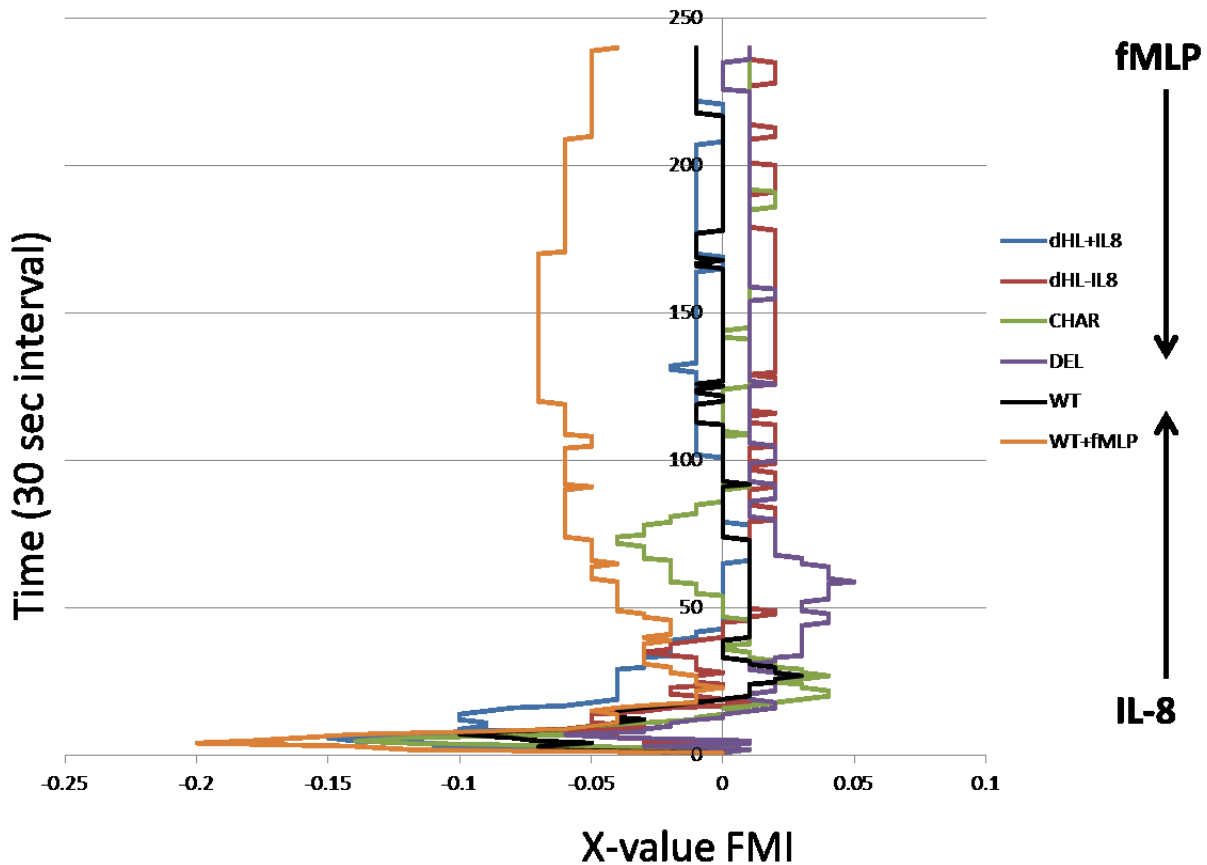


Figure 3.12 X-FMI Vs. Time

Each samples average X-FMI throughout the experiment. A strong pull towards the left is initially observed as the gradient is being formed over the first 20-30min. Gradients are depicted vertically.

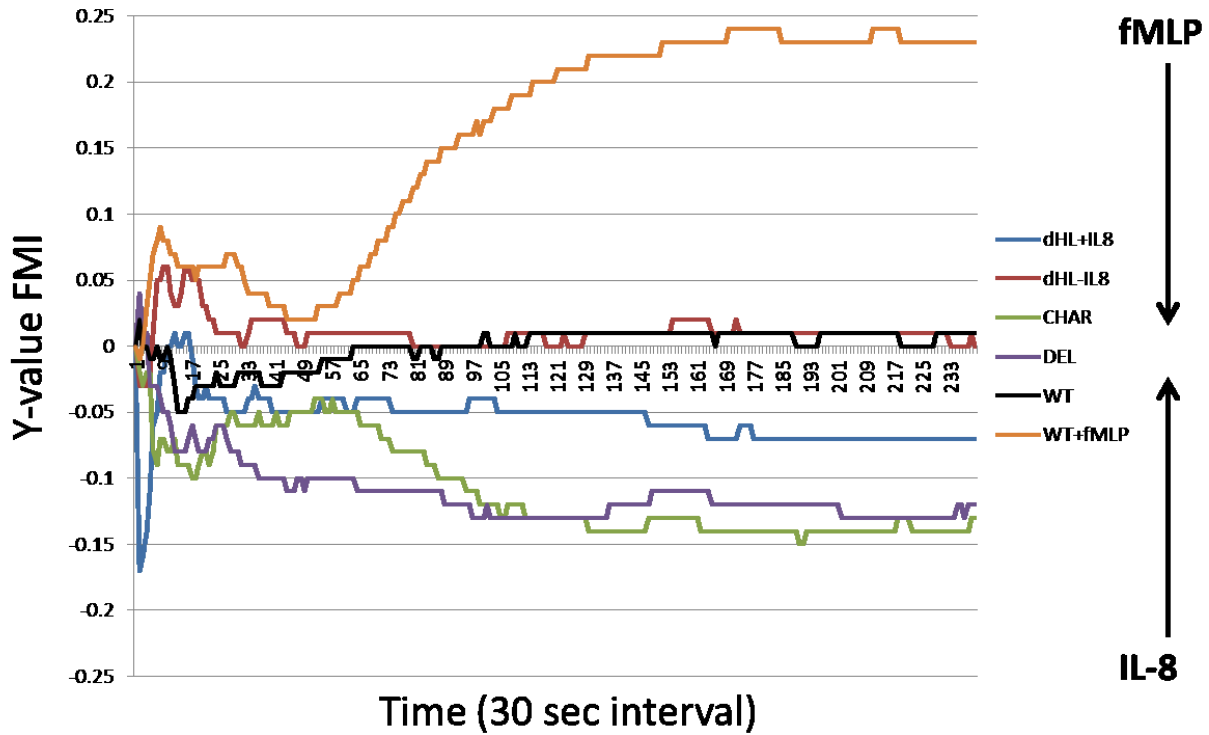


Figure 3.13 Y-FMI Vs. Time

Depicts each samples average Y-FMI throughout the experiment. Samples should move towards their respected targets and random migration of the negative control should be maintained near zero. Origins of the gradients are depicted vertically.

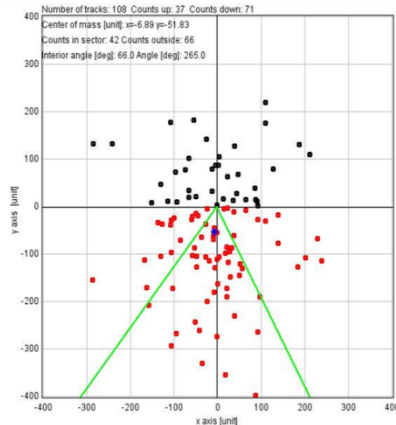
3.11 Sector Maximum

Endpoints of each tracked cell are plotted along the X,Y axis. The sector maximum is the direction (in degrees) in which the maximum number of endpoints falls within a 60° interior angle. For all theoretical purposes any attractant gradient situated along an axis should have a maximum sector at or near the angle value associated with that direction. The counts inside and outside of the given 60° sector are given in the plot along with the angle of greatest value.

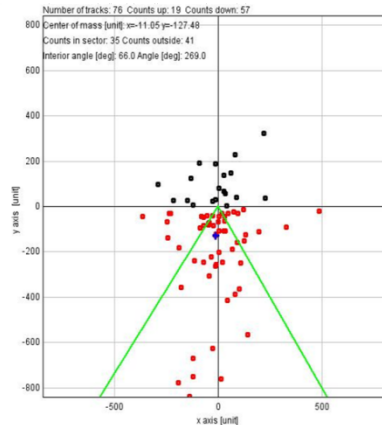
Sector maximum plots are shown in **Figure 3.14**. dHL+IL8 have a maximum sector angle of 265° , which is congruent with expectations of a gradient source situated directly down. That trend is also observed in the CHAR cells which have a maximum sector angle of 269° . DEL samples are similar to the two positive controls with a sector maximum angle of 279° . This alludes to the fact that DEL cells distribute nearly identical to controls when exposed to a chemokine gradient. dHL-IL8 on the other hand shows no such congruence to positive controls, which should be expected in a gradient deficient control group. The dHL-IL8 sector maximum is 44° , which coincides with dHL-IL8 having a high presence of endpoints in the first quadrant.

WT cells also experienced a sector maximum angle in the first quadrant. The WT maximum sector angle is 78° , almost 180° opposite the gradient supplied. Because the WT cells were exposed to the same gradient as the positive controls it must be concluded that the CXCR2 C-tail WT-peptide disrupted the directional sensation of IL-8. CXCR2 signal disruption caused WT samples to move randomly, similar to negative control dHL-IL8. The sector maximum for WT+fMLP samples is 98° , which coincides with their fMLP gradient situated straight up, away from the IL-8 source, demonstrating that CXCR2 C-tail WT peptide does not disrupt fMLP migration in dHL-60 cells.

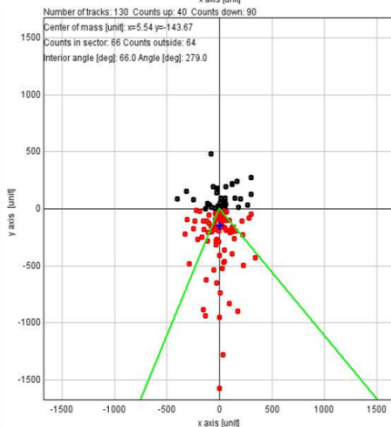
dHL+IL8



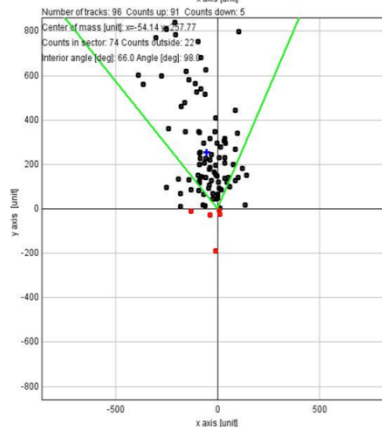
CHAR



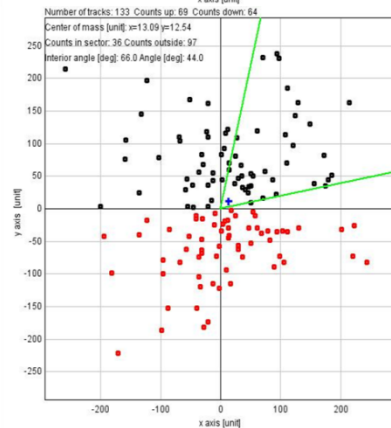
DEL



WT+fMLP



dHL-IL8



WT

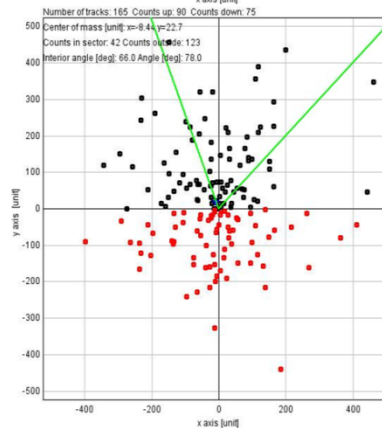


Figure 3.14 Sector Maximum

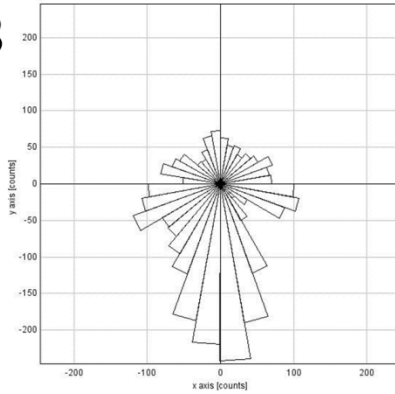
Green vectors identify the sector maximum, a 60° angle. Counts inside and outside of the vector, along with the angular degree are given in each plot. Cells that end in negative Y-values are red, positive Y-values are black, and the center of mass is depicted as a blue (+).

3.12 Rose Diagram

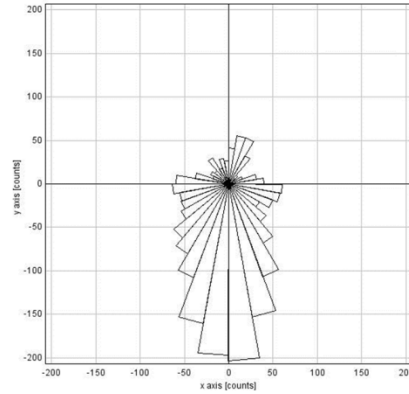
The chemotaxis tool in ImageJ supplies a variety of tools to visualize migration data. One diagram that is easily interpreted is the rose diagram, see **Figure 3.15**. In this assessment the migration endpoints are used in a quantitative manner to analyze overall directional movement in a 360° circle. The diagram is comprised of individual vectors placed every 10°, 36 vectors total. Each vectors size is equal to the quantity of endpoints in that vectors particular range. The total range for each vector is 30°. This means each vector's size comprises of the endpoints within +/- 10° either side of the vector.

Positive control samples dHL+IL8 and CHAR show their biggest vectors pointing downward along the Y-axis, towards the source of IL-8 and higher gradient concentration. The rose diagram for DEL cells looks almost identical to the CHAR cells and also points directly downward. dHL-IL8 has the highest vector values in the first quadrant between 0° and 90°, since there was no gradient or chemokine applied to the dHL-IL8 samples it is assumed they would migrate randomly and form a pseudo circle around the origin, which is roughly represented. The WT samples also move in a similar way, forming a pseudo circle around the origin. The first three quadrants account for a majority but the overall shape is analogous to the negative control (dHL-IL8). The WT+fMLP rose diagram points straight up showing the WT+fMLP sample moved toward fMLP in a directed manner.

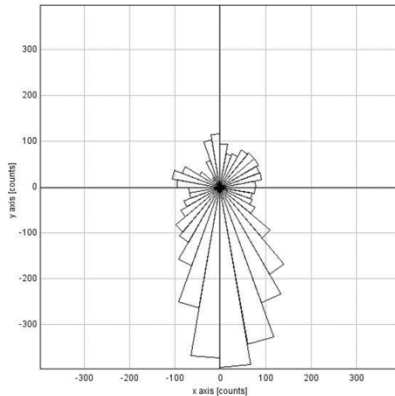
dHL+IL8



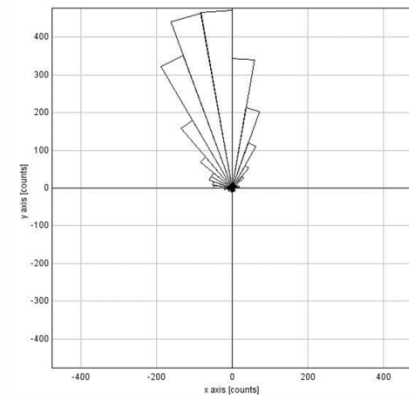
CHAR



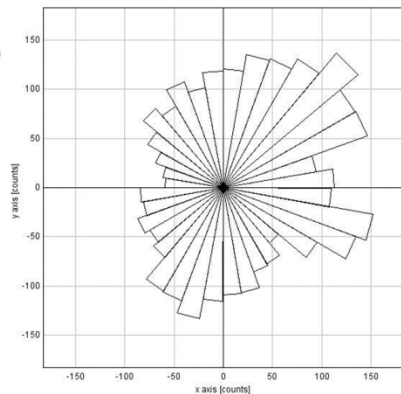
DEL



WT+fMLP



dHL-IL8



WT

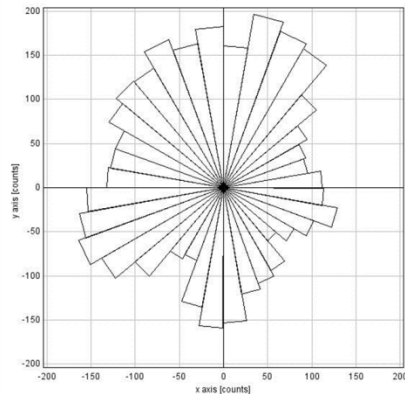


Figure 3.15 Rose Diagrams

An easy to interpret diagram of each samples endpoint distribution. Each vector spans a 10° angle and comprise of endpoints within a 30° angle ($\pm 10^\circ$ on either side). Vector size represents the total number of endpoints within each 30° range.

3.13 Center of Mass

The center of mass (COM) shows an average of the cells positions in a given sample throughout the 120 minute experiment, **Figure 3.16**. Direction and distance have a factor in determining the center of mass. This data provides an excellent account of the average pattern in which samples migrated. The center of mass resembles the average FMI values of each sample and the FMIs observed through time. It also correlates well with the rose diagram and sector maximums.

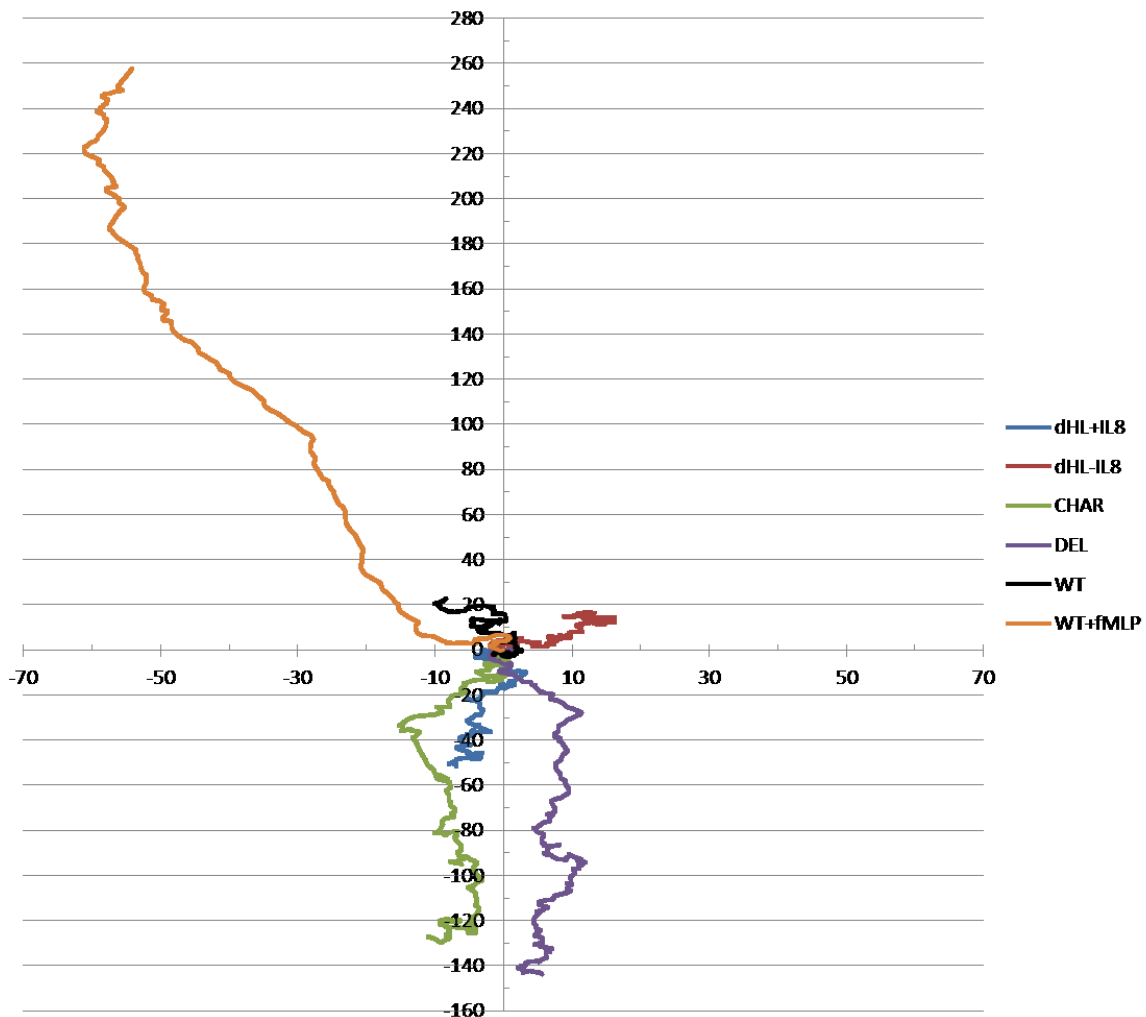


Figure 3.16 Center of Mass Vs. Time

Average center of mass of each sample can be used to determine the majority of cell movement in a given sample. The COM is depicted by a path corresponding to each sample throughout the experiment.

Table 3.6 COM Distance From Origin

Each samples COM distance from the origin and degree deviation from the Y-axis. Angles were calculated using the COM end point and basic trigonometry: $\text{Sin}(\theta) = \text{Opposite} / \text{Hypotenuse}$, $\text{Cos}(\theta) = \text{Adjacent} / \text{Hypotenuse}$, $\text{Tan}(\theta) = \text{Opposite} / \text{Adjacent}$, distances are calculated “as the crow flies” by the same trigonometric equations.

	X value	Y value	Angle from Y-axis	Distance (um)
dHL+ IL8	-6.89	-51.83	7.57	52.29
dHL- IL8	13.09	12.54	46.24	18.12
CHAR	-11.05	-127.48	4.95	127.9
DEL	5.54	-143.67	2.2	143.78
WT	-8.44	22.7	20.4	24.22
WT+fMLP	-54.14	257.77	11.86	263.39

Positive controls moved similarly, dHL+IL8 and CHAR COMs moved toward the higher IL-8 gradient, 51.8um and 127.4um respectively, and strayed little from the Y-axis, 7.57° and 4.95° respectively, **Table 3.6**. DEL sample’s COM moved very similar to the positive control types, 143.67um, and only strayed 2.2° from the Y-axis, which shows a strong COM movement toward IL-8. dHL-IL8 sample COM moved away from the origin at a 46.24° angle, and migrated only 18.12um total. The dHL-IL8 COM data indicates no chemoattractant gradient was formed, as there would be planar movement in a unilateral manner. Instead dHL-IL8 moved a negligible distance in both X and Y planes.

WT cells COM most closely resemble dHL-IL8 negative control, moving a total of 24.22um and 20.4° off the Y-axis. Although the WT sample’s COM moves almost three times further vertically than horizontally, the vertical distance is minor compared to

positive controls. Furthermore, the direction of WT's COM is almost exactly opposite the IL-8 gradient supplied. Lastly, the WT+fMLP samples COM moved significantly upward 263.39um, and only 11.86° off the Y axis, showing the strongest collective movement toward a chemokine of any sample.

3.14 Rayleigh Test

The Rayleigh test is a statistical test for determining if a circular distribution of objects is random or uniform. With p-values >0.05 the null hypothesis (uniformity of direction) is rejected. The Rayleigh test is strongly dependent on the number of samples (n) being analyzed in a group, and the Rayleigh test for vector data also incorporates the distance from the origin, see **Table 3.7**. The Rayleigh test can be used in conjunction with a rose diagram (or the sector maximum for an angular value) to give direction to statistically relevant data of each group.

Rayleigh test for dHL+IL8 positive control samples shows that they migrated in a uniformly directional manner $p=3.72E-04$, coupled with the sector maximum (265°) this data statistically demonstrates that dHL+IL8 uniformly responded to the chemokine gradient. CHAR positive control sampled cells also show a uniform distribution, $p=2.44E-06$. Again, by using the statistical data and an angle measure of the sector maximum (269°), we can come to the conclusion that CHAR cells uniformly responded to the IL-8 gradient. DEL cells have the lowest p-value of the IL-8 treated groups, $p=4.40E-10$, which indicates they distributed in an exceedingly uniform manner. The low DEL p-value is partly due to the higher sample size and congruency of distribution. The

DEL p-value and sector maximum angle (279°) also concludes that DEL samples distribute uniformly to the IL-8 chemokine gradient.

On the other hand dHL-IL8 cells have the highest p-value, $p=0.160$, which assures us that the negative control dHL-60 cells are distributed in a random manner. This is the expected outcome from cells lacking a gradient to chemotax towards and assures the previously stated negative-control data is relevant statistically, i.e., the data is random. WT samples also demonstrate random migration, $p=0.153$. This indicates the sector maximum data, or any other data for that matter, is not relevant in statistically determining which direction the WT sample would migrate. But, when WT treated samples are exposed to fMLP uniform distribution is rescued, $p=1.436E-28$. Taking the sector maximum data into account, WT+fMLP samples moved in a statistically relevant, highly uniform, manner towards their end target chemoattractant.

Table 3.7 Rayleigh Test

Displays each samples number of cells (n), and statistical p-value for the Rayleigh test and Rayleigh test for vector data (from the chemotaxis tool ImageJ plugin). A p-value of >0.05 corresponds to random distribution, whereas a p-value <0.05 corresponds to uniformity.

	<u>n</u>	<u>Rayleigh p-value</u>		<u>Rayleigh Vector p-value</u>	<u>Distribution</u>
dHL+IL8	108	3.72E-04		1.65E-05	Uniform
dHL-IL8	133	0.160173596		7.690E-02	Random
CHAR	76	2.44E-06		6.85E-07	Uniform
DEL	128	4.40E-10		1.66E-10	Uniform
WT	165	0.15365164		0.090780823	Random
WT+fMLP	96	1.4367E-28		1.5684E-26	Uniform

CHAPTER 4

DISCUSSION

4.1 Conclusion of Biochemical Data

The data presented in Figures 3.4 and 3.5 were collected through my advisors laboratory with only partial contribution from me. I added this data into the results section to convey the graduation of experiments and knowledge in a comprehensive format. I do not take credit for their work.

Assessment of protein expression in differentiated HL-60 cells was important, as they can be directly compared to naturally derived neutrophils. Determining NHERF expression in dHL-60 cells is significant since NHERF2 competes with NHERF1 for binding of CXCR2 and PLC β 2's PDZ-motifs. Western blot data shows NHERF1 is the primary isoform expressed in dHL-60 cells and NHERF2, was not detected in dHL-60 cells. This rules out possible binding of CXCR2's or PLC β 2's PDZ-motifs by endogenous NHERF2, which if expressed at exceedingly high rates could compete for PDZ-motif binding sites with NHERF1. Western blotting also found PLC β 1 is absent in dHL-60 cells, PLC β 2 is the main isoform expressed in dHL-60 cells, and PLC β 3 is expressed at a much reduced level. This data is consistent with observations of human neutrophils, which use PLC β 2 as the major isoform in chemokine signaling, and have minor activity from PLC β 3 [229-231]. NHERF2 interacts specifically with PLC β 3 and both of these proteins are expressed at extremely low levels in dHL-60 cells [235]. Therefore it can be postulated that NHERF2 or PLC β 3 do not play a significant role in CXCR2 signaling. This data confirms proteins involved in CXCR2 scaffolding and

signaling, namely NHERF1 and PLC β 2, are similar in dHL-60 cells and human neutrophils, as expected.

Through a GST-tagged scaffolding protein pulldown we demonstrated human and murine CXCR2 and PLC β s all bind to NHERF proteins, though this interaction is mainly facilitated by NHERF1. By using His-S-tagged C-tails of both CXCR2 and PLC β 2 we found a CXCR2 macromolecular complex can be formed consisting of CXCR2, NHERF1 and PLC β 2. Using purified proteins meant the complex formation is independent of other cytosolic factors and we further exemplified this by pairwise binding between CXCR2 and NHERF1. Also CXCR2 macromolecular complex was found *in vivo* from isolated mouse bone marrow neutrophils. Lastly, to interrupt the PDZ-mediated binding of this complex a synthetic peptide, which replicates the last 13 residues of CXCR2, was produced. This PDZ-motif containing peptide inhibits complex formation, as seen in the far Western blot, by competing with endogenous CXCR2. Further studies linked PDZ disruption to suppression in CXCR2 functional activity, such as calcium mobilization and transepithelial migration [1].

The CXCR2 degradation experiment showed no significant data. What can be inferred is the total amount of CXCR2 is not diminished to undetectable levels. This in of itself is somewhat valuable as CXCR2 must be available for signaling activity and migrational data is not corrupted due to an excessive lack of chemokine receptor. Based on the average trend line data, it seems plausible that a CXCR2 C-tail WT peptide could interfere with receptor recycling and increase degradation, however, Western blotting is an inappropriate assay to determine this. If this experiment should be conducted again, FACS (fluorescence activated cell sorting) should be considered.

This method would employ a highly sensitive flow cytometer to measure cell surface CXCR2 levels through a fluorescence conjugated antibody.

In conclusion, dHL-60 cells represent viable alternatives for human neutrophils in the context of CXCR2, NHERF proteins and PLC β isoforms. CXCR2 and PLC β 2 both interact with NHERF1 through a PDZ dependent interaction and together they form a macromolecular complex. This complex links CXCR2 and its downstream effector PLC β 2 through the actin binding scaffolding protein NHERF1. Furthermore, an exogenous CXCR2 C-tail synthetic peptide can disrupt the complex formation and repress CXCR2 functioning [1]. This peptide might also disrupt intracellular sorting of CXCR2, although more clarification is needed.

4.2 Conclusion of Migrational Data

Accumulated distances suggest that both dHL-IL8 and WT samples migrated analogous to positive controls, yet their directness was roughly 30% less. The WT samples were exposed to a 50ng/ml gradient of IL-8, whereas dHL-IL8 experienced no such gradient. The DEL samples directed their migration similar to the positive controls and the only difference between DEL and WT samples is the inclusion of a synthetic CXCR2 type I PDZ-motif. Furthermore, migrational directness was reestablished when WT samples were exposed to a fMLP gradient. Therefore, it can be inferred the exogenous PDZ-motif is responsible for the disruption of IL-8 mediated directness of migration. Disrupting CXCR2 PDZ-domain interactions caused dHL-60 cells exposed to an IL-8 gradient to direct migration similar to dHL-60 cells experiencing no IL-8 gradient.

The forward migration index assays the movement on the X or Y-axis. As expected, the control samples and WT+fMLP all have significant Y-axis FMI's. Negative control dHL-IL8 has little X or Y-axis FMI and this display of random movement is also observed in WT samples. The FMI data supports the hypothesis that the WT sample seems unable to recognize the direction of a gradient. DEL samples enforce the importance of PDZ binding disruption and confirm forward migration is not disrupted with the inclusion of a CXCR2 C-tail peptide lacking the PDZ-motif. Data from the sector max, rose diagram and center of mass further exemplify the contrast between DEL and WT samples. Data shows general distribution of dHL+IL8, CHAR and DEL samples towards the chemokine gradient, with the greatest abundance along the negative Y-axis. Meanwhile dHL-IL8 and WT samples show a high degree of random movement and are evenly dispersed around the origin. Yet, inclusion of a fMLP gradient restored normal distribution in the WT samples, due to fMLP signaling through FPR, not CXCR2.

The Rayleigh test statistically confirms these findings. DEL samples distribute uniformly to the IL-8 gradient, akin to positive controls. WT samples, like negative control dHL-IL8, do not distribute uniformly and exhibit statistically random migration. Importantly, exposure to fMLP rescues directional chemotaxis in WT treated cells. It is worthwhile to note that the WT accumulated distance was comparable to the positive controls and DEL or WT+fMLP directed migration was not disrupted. This establishes that CXCR2's PDZ-motif interaction, however important in chemokine directional sensation, does not play a key role in moving the cell forward. But, whether or not disrupting CXCR2 nucleation into a macromolecular complex affects anchoring of CXCR2/actin modulating proteins (Arp2/3, VASP, LASP-1, IQGAP, etc.), sustaining the

leading edge, or possibly disrupts other PDZ interactions (NHERF2-PTEN), has yet to be determined.

In summary, Zigmond chemotaxis chamber migrational data confirms significant differences between the two experimental samples. dHL-60 cells migrated as expected and delivery of the CXCR2 C-tail peptide containing the PDZ-motif severely repressed IL-8-mediated chemotactic migration. Also, the CXCR2 C-tail peptide lacking the PDZ motif had no effect on overall migration, which rules out residues in the CXCR2 C-tail peptide affecting chemotaxis. Therefore, it can be concluded that PDZ motif-domain interactions play an important role in directing dHL-60 cells during CXCR2/IL-8-mediated chemotaxis, and disruption of PDZ-mediated CXCR2 macromolecular complex formation abolishes spatial sensation in a chemokine gradient. The data collected from the Zigmond chemotaxis chamber verifies the hypothesis, that perturbing CXCR2's PDZ-motif binding interaction will disrupt spatial sensation of the chemokine gradient and impair cellular chemotaxis, is correct.

4.3 Thoughts

Excessive infiltration of neutrophils is the cause of many inflammatory diseases [17]. As neutrophils infiltrate into tissue the surrounding area is subjected to a variety of proteolytic enzymes and reactive oxygen species deployed by neutrophils to combat infection, which causes extensive tissue damage and delays wound healing [236, 237]. Yet their role in bacterial clearance remains imperative to host pathological defense [238]. When searching for a therapeutic approach to combat auto-inflammatory disease

a balance must be reached, in order to provide anti-inflammatory relief, without compromising a legitimate immune response.

Some therapeutic methods (neutralizing antibodies or small organic compounds) utilize an extracellular antagonist of CXCR2 to allosterically or competitively disrupt chemokine binding [239]. In either case, the effect is a complete inhibition of the CXCR2 signaling cascade and buildup of IL-8, which cannot be scavenged by receptors [240]. A systemic shutdown of CXCR2 would suppress the hosts ability to initiate an immune response, induce angiogenesis of endothelial cells, or begin wound healing after injury [241]. The data presented in our recent report [1] and this report target a specific peptide motif in the cytosol and represents a novel strategy to disrupt CXCR2 mediated signaling without complete blockade of the signaling system. Disruption of CXCR2-PDZ domain interaction still allows IL-8 binding, receptor internalization, and a diminished chemokine response [1]. Yet, chemotaxis towards host derived inflammatory chemokines becomes impaired, leaving the cells unable to spatially detect a gradient, while chemotaxis towards bacterial peptides (fMLP) remains normal.

Tissue damage caused by sterile injury exhibits damage associated molecular patterns (DAMPs), derived from human mitochondria, which attract neutrophils through formylated peptide receptors [242]. Additionally, a study of CXCR2^{-/-} mice showed they have no impairment in clearance of bacteria, as mouse neutrophils could utilize other means to reach their targets [243]. This represents evidence for CXCR2-PDZ disruption not interfering in sterile injury or bacterial related inflammatory responses, while providing a therapeutic target for chronic/hyper inflammatory diseases derived from excessive chemokine production.

4.4 Future Directions

The goal of disease associated research is to understand the mechanisms involved, and use this knowledge for therapeutic development. One major facet of developing therapeutics should focus on the consequences of globally or locally disrupting CXCR2's PDZ-motif interaction. This would hinge on the discovery of a drug or soluble molecule to disrupt CXCR2 cytosolic PDZ-motif interactions, replicating the effects of the CXCR2 C-tail WT peptide used. Drug discovery is by no means an easy task and may not become feasible or fruitful but, if such a compound exists, could prove beneficial in research of autoimmune diseases. Although there is no account of the effects PDZ-domain disruption would cause in other areas of the body, as PDZ domains occur frequently and their disruption could pose problems in distal locations.

Therefore, *in vivo* experimentation should be considered an obtainable goal. Murine air-pouch models or those mimicking human inflammatory diseases should be assessed for viability and executed. This would require genetically modified mice (or another animal model), with mutation of the CXCR2 PDZ-motif. Although, truncation of CXCR2 PDZ-motif is not identical to a soluble drug, any *in vivo* results should be more in line with actual biological systems. By cytosolically targeting CXCR2's macromolecular complex formation, new therapies can be developed, opening the door to innovative opportunities in similar systems.

REFERENCES

1. Wu, Y., et al., *A chemokine receptor CXCR2 macromolecular complex regulates neutrophil functions in inflammatory diseases*. J Biol Chem, 2012. **287**(8): p. 5744-55.
2. Karthikeyan, S., et al., *Crystal structure of the PDZ1 domain of human Na(+)/H(+) exchanger regulatory factor provides insights into the mechanism of carboxyl-terminal leucine recognition by class I PDZ domains*. J Mol Biol, 2001. **308**(5): p. 963-73.
3. Alberts, B., *Leukocyte functions and percentage breakdown*, in *Molecular Biology of the Cell* 2005: NCBI Bookshelf
4. Pillay, J., et al., *In vivo labeling with 2H2O reveals a human neutrophil lifespan of 5.4 days*. Blood, 2010. **116**(4): p. 625-7.
5. Massena, S., et al., *A chemotactic gradient sequestered on endothelial heparan sulfate induces directional intraluminal crawling of neutrophils*. Blood, 2010. **116**(11): p. 1924-31.
6. Laudanna, C. and R. Alon, *Right on the spot. Chemokine triggering of integrin-mediated arrest of rolling leukocytes*. Thromb Haemost, 2006. **95**(1): p. 5-11.
7. Baggiolini, M., A. Walz, and S.L. Kunkel, *Neutrophil-activating peptide-1/interleukin 8, a novel cytokine that activates neutrophils*. J Clin Invest, 1989. **84**(4): p. 1045-9.
8. Smith, C.D., C.C. Cox, and R. Snyderman, *Receptor-coupled activation of phosphoinositide-specific phospholipase C by an N protein*. Science, 1986. **232**(4746): p. 97-100.
9. Furie, M.B. and G.J. Randolph, *Chemokines and tissue injury*. Am J Pathol, 1995. **146**(6): p. 1287-301.
10. Nathan, C., *Neutrophils and immunity: challenges and opportunities*. Nat Rev Immunol, 2006. **6**(3): p. 173-82.
11. Hemler, M.E., *VLA proteins in the integrin family: structures, functions, and their role on leukocytes*. Annu Rev Immunol, 1990. **8**: p. 365-400.

12. Witko-Sarsat, V., et al., *Neutrophils: molecules, functions and pathophysiological aspects*. Lab Invest, 2000. **80**(5): p. 617-53.
13. Servant, G., et al., *Polarization of chemoattractant receptor signaling during neutrophil chemotaxis*. Science, 2000. **287**(5455): p. 1037-40.
14. Yoshimura, T., et al., *Purification of a human monocyte-derived neutrophil chemotactic factor that has peptide sequence similarity to other host defense cytokines*. Proc Natl Acad Sci U S A, 1987. **84**(24): p. 9233-7.
15. Baggiolini, M., B. Dewald, and B. Moser, *Human chemokines: an update*. Annu Rev Immunol, 1997. **15**: p. 675-705.
16. Rossi, D. and A. Zlotnik, *The biology of chemokines and their receptors*. Annu Rev Immunol, 2000. **18**: p. 217-42.
17. Strieter, R.M., et al., *The functional role of the ELR motif in CXC chemokine-mediated angiogenesis*. J Biol Chem, 1995. **270**(45): p. 27348-57.
18. Hebert, C.A., R.V. Vitangcol, and J.B. Baker, *Scanning mutagenesis of interleukin-8 identifies a cluster of residues required for receptor binding*. J Biol Chem, 1991. **266**(28): p. 18989-94.
19. Sarmiento, J., et al., *Diverging mechanisms of activation of chemokine receptors revealed by novel chemokine agonists*. PLoS One, 2011. **6**(12): p. e27967.
20. Clark-Lewis, I., et al., *Structure-activity relationships of interleukin-8 determined using chemically synthesized analogs. Critical role of NH₂-terminal residues and evidence for uncoupling of neutrophil chemotaxis, exocytosis, and receptor binding activities*. J Biol Chem, 1991. **266**(34): p. 23128-34.
21. Baggiolini, M., P. Imboden, and P. Detmers, *Neutrophil activation and the effects of interleukin-8/neutrophil-activating peptide 1 (IL-8/NAP-1)*. Cytokines, 1992. **4**: p. 1-17.

22. Baggiolini, M., B. Dewald, and B. Moser, *Interleukin-8 and related chemotactic cytokines--CXC and CC chemokines*. Adv Immunol, 1994. **55**: p. 97-179.
23. Murphy, P.M. and H.L. Tiffany, *Cloning of complementary DNA encoding a functional human interleukin-8 receptor*. Science, 1991. **253**(5025): p. 1280-3.
24. Matsushima, K., et al., *Molecular cloning of a human monocyte-derived neutrophil chemotactic factor (MDNCF) and the induction of MDNCF mRNA by interleukin 1 and tumor necrosis factor*. J Exp Med, 1988. **167**(6): p. 1883-93.
25. Oppenheim, J.J., et al., *Properties of the novel proinflammatory supergene "intercrine" cytokine family*. Annu Rev Immunol, 1991. **9**: p. 617-48.
26. Leonard, E.J. and T. Yoshimura, *Neutrophil attractant/activation protein-1 (NAP-1 [interleukin-8])*. Am J Respir Cell Mol Biol, 1990. **2**(6): p. 479-86.
27. Holmes, W.E., et al., *Structure and functional expression of a human interleukin-8 receptor*. Science, 1991. **253**(5025): p. 1278-80.
28. Lee, J., et al., *Characterization of two high affinity human interleukin-8 receptors*. J Biol Chem, 1992. **267**(23): p. 16283-7.
29. Ahuja, S.K., et al., *Molecular evolution of the human interleukin-8 receptor gene cluster*. Nat Genet, 1992. **2**(1): p. 31-6.
30. Cerretti, D.P., et al., *Molecular characterization of receptors for human interleukin-8, GRO/melanoma growth-stimulatory activity and neutrophil activating peptide-2*. Mol Immunol, 1993. **30**(4): p. 359-67.
31. Jones, S.A., B. Moser, and M. Thelen, *A comparison of post-receptor signal transduction events in Jurkat cells transfected with either IL-8R1 or IL-8R2. Chemokine mediated activation of p42/p44 MAP-kinase (ERK-2)*. FEBS Lett, 1995. **364**(2): p. 211-4.

32. Jones, S.A., et al., *Different functions for the interleukin 8 receptors (IL-8R) of human neutrophil leukocytes: NADPH oxidase and phospholipase D are activated through IL-8R1 but not IL-8R2.* Proc Natl Acad Sci U S A, 1996. **93**(13): p. 6682-6.
33. Addison, C.L., et al., *The CXC chemokine receptor 2, CXCR2, is the putative receptor for ELR+ CXC chemokine-induced angiogenic activity.* J Immunol, 2000. **165**(9): p. 5269-77.
34. Murdoch, C., P.N. Monk, and A. Finn, *Cxc chemokine receptor expression on human endothelial cells.* Cytokine, 1999. **11**(9): p. 704-12.
35. White, J.R., et al., *Identification of a potent, selective non-peptide CXCR2 antagonist that inhibits interleukin-8-induced neutrophil migration.* J Biol Chem, 1998. **273**(17): p. 10095-8.
36. Stillie, R., et al., *The functional significance behind expressing two IL-8 receptor types on PMN.* J Leukoc Biol, 2009. **86**(3): p. 529-43.
37. Hartl, D., et al., *Cleavage of CXCR1 on neutrophils disables bacterial killing in cystic fibrosis lung disease.* Nat Med, 2007. **13**(12): p. 1423-30.
38. Neel, N.F., et al., *IQGAP1 is a novel CXCR2-interacting protein and essential component of the "chemosynapse".* PLoS One, 2011. **6**(8): p. e23813.
39. Boisvert, W.A., et al., *A leukocyte homologue of the IL-8 receptor CXCR-2 mediates the accumulation of macrophages in atherosclerotic lesions of LDL receptor-deficient mice.* J Clin Invest, 1998. **101**(2): p. 353-63.
40. Chapman, R.W., et al., *A novel, orally active CXCR1/2 receptor antagonist, Sch527123, inhibits neutrophil recruitment, mucus production, and goblet cell hyperplasia in animal models of pulmonary inflammation.* J Pharmacol Exp Ther, 2007. **322**(2): p. 486-93.
41. Podolin, P.L., et al., *A potent and selective nonpeptide antagonist of CXCR2 inhibits acute and chronic models of arthritis in the rabbit.* J Immunol, 2002. **169**(11): p. 6435-44.

42. Liu, L., et al., *Myelin repair is accelerated by inactivating CXCR2 on nonhematopoietic cells*. J Neurosci, 2010. **30**(27): p. 9074-83.
43. Robinson, S., et al., *The chemokine growth-regulated oncogene-alpha promotes spinal cord oligodendrocyte precursor proliferation*. J Neurosci, 1998. **18**(24): p. 10457-63.
44. Tsai, H.H., et al., *The chemokine receptor CXCR2 controls positioning of oligodendrocyte precursors in developing spinal cord by arresting their migration*. Cell, 2002. **110**(3): p. 373-83.
45. Ajuebor, M.N., et al., *Contrasting roles for CXCR2 during experimental colitis*. Exp Mol Pathol, 2004. **76**(1): p. 1-8.
46. Buanne, P., et al., *Crucial pathophysiological role of CXCR2 in experimental ulcerative colitis in mice*. J Leukoc Biol, 2007. **82**(5): p. 1239-46.
47. Kulke, R., et al., *The CXC receptor 2 is overexpressed in psoriatic epidermis*. J Invest Dermatol, 1998. **110**(1): p. 90-4.
48. Qiu, Y., et al., *Biopsy neutrophilia, neutrophil chemokine and receptor gene expression in severe exacerbations of chronic obstructive pulmonary disease*. Am J Respir Crit Care Med, 2003. **168**(8): p. 968-75.
49. Murphy, P.M., *The molecular biology of leukocyte chemoattractant receptors*. Annu Rev Immunol, 1994. **12**: p. 593-633.
50. Strader, C.D., et al., *Structure and function of G protein-coupled receptors*. Annu Rev Biochem, 1994. **63**: p. 101-32.
51. Wu, D., G.J. LaRosa, and M.I. Simon, *G protein-coupled signal transduction pathways for interleukin-8*. Science, 1993. **261**(5117): p. 101-3.
52. Allen, S.J., S.E. Crown, and T.M. Handel, *Chemokine: receptor structure, interactions, and antagonism*. Annu Rev Immunol, 2007. **25**: p. 787-820.

53. Rodbell, M., *The complex regulation of receptor-coupled G-proteins*. Adv Enzyme Regul, 1997. **37**: p. 427-35.
54. Gilman, A.G., *G proteins: transducers of receptor-generated signals*. Annu Rev Biochem, 1987. **56**: p. 615-49.
55. Wieland, T., et al., *Role of GDP in formyl-peptide-receptor-induced activation of guanine-nucleotide-binding proteins in membranes of HL 60 cells*. Eur J Biochem, 1992. **205**(3): p. 1201-6.
56. Simon, M.I., M.P. Strathmann, and N. Gautam, *Diversity of G proteins in signal transduction*. Science, 1991. **252**(5007): p. 802-8.
57. Pedersen, S.E. and E.M. Ross, *Functional reconstitution of beta-adrenergic receptors and the stimulatory GTP-binding protein of adenylate cyclase*. Proc Natl Acad Sci U S A, 1982. **79**(23): p. 7228-32.
58. Hekman, M., et al., *Reconstitution of beta-adrenergic receptor with components of adenylate cyclase*. EMBO J, 1984. **3**(13): p. 3339-45.
59. Downes, G.B. and N. Gautam, *The G protein subunit gene families*. Genomics, 1999. **62**(3): p. 544-52.
60. Raymond, J.R., et al., *Adrenergic receptors. Models for regulation of signal transduction processes*. Hypertension, 1990. **15**(2): p. 119-31.
61. Dohlman, H.G., et al., *Model systems for the study of seven-transmembrane-segment receptors*. Annu Rev Biochem, 1991. **60**: p. 653-88.
62. Pfeuffer, T. and E.J. Helmreich, *Structural and functional relationships of guanosine triphosphate binding proteins*. Curr Top Cell Regul, 1988. **29**: p. 129-216.
63. Birnbaumer, L., *G proteins in signal transduction*. Annu Rev Pharmacol Toxicol, 1990. **30**: p. 675-705.

64. Ishii, M. and Y. Kurachi, *Physiological actions of regulators of G-protein signaling (RGS) proteins*. Life Sci, 2003. **74**(2-3): p. 163-71.
65. Baggiolini, M. and I. Clark-Lewis, *Interleukin-8, a chemotactic and inflammatory cytokine*. FEBS Lett, 1992. **307**(1): p. 97-101.
66. Katz, A., D. Wu, and M.I. Simon, *Subunits beta gamma of heterotrimeric G protein activate beta 2 isoform of phospholipase C*. Nature, 1992. **360**(6405): p. 686-9.
67. Camps, M., et al., *Isozyme-selective stimulation of phospholipase C-beta 2 by G protein beta gamma-subunits*. Nature, 1992. **360**(6405): p. 684-6.
68. Lefkowitz, R.J., W.P. Hausdorff, and M.G. Caron, *Role of phosphorylation in desensitization of the beta-adrenoceptor*. Trends Pharmacol Sci, 1990. **11**(5): p. 190-4.
69. Lohse, M.J., *Molecular mechanisms of membrane receptor desensitization*. Biochim Biophys Acta, 1993. **1179**(2): p. 171-88.
70. Inglese, J., et al., *Structure and mechanism of the G protein-coupled receptor kinases*. J Biol Chem, 1993. **268**(32): p. 23735-8.
71. Premont, R.T., J. Inglese, and R.J. Lefkowitz, *Protein kinases that phosphorylate activated G protein-coupled receptors*. FASEB J, 1995. **9**(2): p. 175-82.
72. Seibold, A., et al., *Desensitization of beta2-adrenergic receptors with mutations of the proposed G protein-coupled receptor kinase phosphorylation sites*. J Biol Chem, 1998. **273**(13): p. 7637-42.
73. Zhang, J., et al., *Role for G protein-coupled receptor kinase in agonist-specific regulation of mu-opioid receptor responsiveness*. Proc Natl Acad Sci U S A, 1998. **95**(12): p. 7157-62.
74. Holroyd, E.W., et al., *Effect of G protein-coupled receptor kinase 2 on the sensitivity of M4 muscarinic acetylcholine receptors to agonist-induced internalization and desensitization in NG108-15 cells*. J Neurochem, 1999. **73**(3): p. 1236-45.

75. Iwata, K., et al., *Dynamin and rab5 regulate GRK2-dependent internalization of dopamine D2 receptors*. Eur J Biochem, 1999. **263**(2): p. 596-602.
76. Ben-Baruch, A., et al., *The differential ability of IL-8 and neutrophil-activating peptide-2 to induce attenuation of chemotaxis is mediated by their divergent capabilities to phosphorylate CXCR2 (IL-8 receptor B)*. J Immunol, 1997. **158**(12): p. 5927-33.
77. Feniger-Barish, R., et al., *Differential modes of regulation of cxc chemokine-induced internalization and recycling of human CXCR1 and CXCR2*. Cytokine, 1999. **11**(12): p. 996-1009.
78. von Zastrow, M. and B.K. Kobilka, *Ligand-regulated internalization and recycling of human beta 2-adrenergic receptors between the plasma membrane and endosomes containing transferrin receptors*. J Biol Chem, 1992. **267**(5): p. 3530-8.
79. Zhang, J., et al., *Dynamin and beta-arrestin reveal distinct mechanisms for G protein-coupled receptor internalization*. J Biol Chem, 1996. **271**(31): p. 18302-5.
80. Yang, W., D. Wang, and A. Richmond, *Role of clathrin-mediated endocytosis in CXCR2 sequestration, resensitization, and signal transduction*. J Biol Chem, 1999. **274**(16): p. 11328-33.
81. Nasser, M.W., et al., *CXCR1 and CXCR2 activation and regulation. Role of aspartate 199 of the second extracellular loop of CXCR2 in CXCL8-mediated rapid receptor internalization*. J Biol Chem, 2007. **282**(9): p. 6906-15.
82. Fan, G.H., et al., *Identification of a motif in the carboxyl terminus of CXCR2 that is involved in adaptin 2 binding and receptor internalization*. Biochemistry, 2001. **40**(3): p. 791-800.
83. Sai, J., et al., *The IL sequence in the LLKIL motif in CXCR2 is required for full ligand-induced activation of Erk, Akt, and chemotaxis in HL60 cells*. J Biol Chem, 2006. **281**(47): p. 35931-41.
84. Barlic, J., et al., *beta-arrestins regulate interleukin-8-induced CXCR1 internalization*. J Biol Chem, 1999. **274**(23): p. 16287-94.

85. Baugher, P.J. and A. Richmond, *The carboxyl-terminal PDZ ligand motif of chemokine receptor CXCR2 modulates post-endocytic sorting and cellular chemotaxis*. J Biol Chem, 2008. **283**(45): p. 30868-78.
86. Claperon, A., M. Mergey, and L. Fouassier, *Roles of the scaffolding proteins NHERF in liver biology*. Clin Res Hepatol Gastroenterol, 2011. **35**(3): p. 176-81.
87. Weinman, E.J., et al., *Characterization of a protein cofactor that mediates protein kinase A regulation of the renal brush border membrane Na(+)-H+ exchanger*. J Clin Invest, 1995. **95**(5): p. 2143-9.
88. Harrison, S.C., *Peptide-surface association: the case of PDZ and PTB domains*. Cell, 1996. **86**(3): p. 341-3.
89. Harris, B.Z. and W.A. Lim, *Mechanism and role of PDZ domains in signaling complex assembly*. J Cell Sci, 2001. **114**(Pt 18): p. 3219-31.
90. Fanning, A.S. and J.M. Anderson, *PDZ domains: fundamental building blocks in the organization of protein complexes at the plasma membrane*. J Clin Invest, 1999. **103**(6): p. 767-72.
91. Voltz, J.W., E.J. Weinman, and S. Shenolikar, *Expanding the role of NHERF, a PDZ-domain containing protein adapter, to growth regulation*. Oncogene, 2001. **20**(44): p. 6309-14.
92. Fanning, A.S. and J.M. Anderson, *Protein-protein interactions: PDZ domain networks*. Curr Biol, 1996. **6**(11): p. 1385-8.
93. Kornau, H.C., et al., *Domain interaction between NMDA receptor subunits and the postsynaptic density protein PSD-95*. Science, 1995. **269**(5231): p. 1737-40.
94. Reczek, D., M. Berryman, and A. Bretscher, *Identification of EBP50: A PDZ-containing phosphoprotein that associates with members of the ezrin-radixin-moesin family*. J Cell Biol, 1997. **139**(1): p. 169-79.

95. Hall, R.A., et al., *The beta2-adrenergic receptor interacts with the Na⁺/H⁺-exchanger regulatory factor to control Na⁺/H⁺ exchange*. Nature, 1998. **392**(6676): p. 626-30.
96. Karthikeyan, S., T. Leung, and J.A. Ladas, *Structural basis of the Na⁺/H⁺ exchanger regulatory factor PDZ1 interaction with the carboxyl-terminal region of the cystic fibrosis transmembrane conductance regulator*. J Biol Chem, 2001. **276**(23): p. 19683-6.
97. Karthikeyan, S., T. Leung, and J.A. Ladas, *Structural determinants of the Na⁺/H⁺ exchanger regulatory factor interaction with the beta 2 adrenergic and platelet-derived growth factor receptors*. J Biol Chem, 2002. **277**(21): p. 18973-8.
98. Doyle, D.A., et al., *Crystal structures of a complexed and peptide-free membrane protein-binding domain: molecular basis of peptide recognition by PDZ*. Cell, 1996. **85**(7): p. 1067-76.
99. Hall, R.A., et al., *A C-terminal motif found in the beta2-adrenergic receptor, P2Y1 receptor and cystic fibrosis transmembrane conductance regulator determines binding to the Na⁺/H⁺ exchanger regulatory factor family of PDZ proteins*. Proc Natl Acad Sci U S A, 1998. **95**(15): p. 8496-501.
100. Wang, S., et al., *Peptide binding consensus of the NHE-RF-PDZ1 domain matches the C-terminal sequence of cystic fibrosis transmembrane conductance regulator (CFTR)*. FEBS Lett, 1998. **427**(1): p. 103-8.
101. Raghuram, V., D.O. Mak, and J.K. Foskett, *Regulation of cystic fibrosis transmembrane conductance regulator single-channel gating by bivalent PDZ-domain-mediated interaction*. Proc Natl Acad Sci U S A, 2001. **98**(3): p. 1300-5.
102. Raman, D., et al., *Characterization of chemokine receptor CXCR2 interacting proteins using a proteomics approach to define the CXCR2 "chemosynapse"*. Methods Enzymol, 2009. **460**: p. 315-30.

103. Tang, Y., et al., *Association of mammalian trp4 and phospholipase C isozymes with a PDZ domain-containing protein, NHERF*. J Biol Chem, 2000. **275**(48): p. 37559-64.
104. Fouassier, L., et al., *Evidence for ezrin-radixin-moesin-binding phosphoprotein 50 (EBP50) self-association through PDZ-PDZ interactions*. J Biol Chem, 2000. **275**(32): p. 25039-45.
105. Minkoff, C., S. Shenolikar, and E.J. Weinman, *Assembly of signaling complexes by the sodium-hydrogen exchanger regulatory factor family of PDZ-containing proteins*. Curr Opin Nephrol Hypertens, 1999. **8**(5): p. 603-8.
106. Weinman, E.J., C. Minkoff, and S. Shenolikar, *Signal complex regulation of renal transport proteins: NHERF and regulation of NHE3 by PKA*. Am J Physiol Renal Physiol, 2000. **279**(3): p. F393-9.
107. Rebecchi, M.J. and S.N. Pentylala, *Structure, function, and control of phosphoinositide-specific phospholipase C*. Physiol Rev, 2000. **80**(4): p. 1291-335.
108. Suh, P.G., et al., *Multiple roles of phosphoinositide-specific phospholipase C isozymes*. BMB Rep, 2008. **41**(6): p. 415-34.
109. Harden, T.K., S.N. Hicks, and J. Sondek, *Phospholipase C isozymes as effectors of Ras superfamily GTPases*. J Lipid Res, 2009. **50 Suppl**: p. S243-8.
110. Suh, P.G., et al., *The roles of PDZ-containing proteins in PLC-beta-mediated signaling*. Biochem Biophys Res Commun, 2001. **288**(1): p. 1-7.
111. Rhee, S.G. and Y.S. Bae, *Regulation of phosphoinositide-specific phospholipase C isozymes*. J Biol Chem, 1997. **272**(24): p. 15045-8.
112. Jiang, H., et al., *Phospholipase C beta 4 is involved in modulating the visual response in mice*. Proc Natl Acad Sci U S A, 1996. **93**(25): p. 14598-601.
113. Kano, M., et al., *Phospholipase cbeta4 is specifically involved in climbing fiber synapse elimination in the developing cerebellum*. Proc Natl Acad Sci U S A, 1998. **95**(26): p. 15724-9.

114. Williams, R.L. and M. Katan, *Structural views of phosphoinositide-specific phospholipase C: signalling the way ahead*. Structure, 1996. **4**(12): p. 1387-94.
115. Rebecchi, M.J. and S. Scarlata, *Pleckstrin homology domains: a common fold with diverse functions*. Annu Rev Biophys Biomol Struct, 1998. **27**: p. 503-28.
116. Ferguson, K.M., et al., *Scratching the surface with the PH domain*. Nat Struct Biol, 1995. **2**(9): p. 715-8.
117. Jenco, J.M., K.P. Becker, and A.J. Morris, *Membrane-binding properties of phospholipase C-beta1 and phospholipase C-beta2: role of the C-terminus and effects of polyphosphoinositides, G-proteins and Ca²⁺*. Biochem J, 1997. **327 (Pt 2)**: p. 431-7.
118. Runnels, L.W., et al., *Membrane binding of phospholipases C-beta 1 and C-beta 2 is independent of phosphatidylinositol 4,5-bisphosphate and the alpha and beta gamma subunits of G proteins*. Biochemistry, 1996. **35**(51): p. 16824-32.
119. Wang, T., et al., *Differential association of the pleckstrin homology domains of phospholipases C-beta 1, C-beta 2, and C-delta 1 with lipid bilayers and the beta gamma subunits of heterotrimeric G proteins*. Biochemistry, 1999. **38**(5): p. 1517-24.
120. Wang, T., et al., *The pleckstrin homology domain of phospholipase C-beta(2) links the binding of gbetagamma to activation of the catalytic core*. J Biol Chem, 2000. **275**(11): p. 7466-9.
121. Feng, J., et al., *Dissection of the steps of phospholipase C beta 2 activity that are enhanced by G beta gamma subunits*. Biochemistry, 2005. **44**(7): p. 2577-84.
122. Iijima, M., Y.E. Huang, and P. Devreotes, *Temporal and spatial regulation of chemotaxis*. Dev Cell, 2002. **3**(4): p. 469-78.
123. Liu, M. and M.I. Simon, *Regulation by cAMP-dependent protein kinase of a G-protein-mediated phospholipase C*. Nature, 1996. **382**(6586): p. 83-7.

124. Sunahara, R.K., C.W. Dessauer, and A.G. Gilman, *Complexity and diversity of mammalian adenylyl cyclases*. *Annu Rev Pharmacol Toxicol*, 1996. **36**: p. 461-80.
125. Smrcka, A.V. and P.C. Sternweis, *Regulation of purified subtypes of phosphatidylinositol-specific phospholipase C beta by G protein alpha and beta gamma subunits*. *J Biol Chem*, 1993. **268**(13): p. 9667-74.
126. Affolter, M. and C.J. Weijer, *Signaling to cytoskeletal dynamics during chemotaxis*. *Dev Cell*, 2005. **9**(1): p. 19-34.
127. Cramer, L.P., M. Siebert, and T.J. Mitchison, *Identification of novel graded polarity actin filament bundles in locomoting heart fibroblasts: implications for the generation of motile force*. *J Cell Biol*, 1997. **136**(6): p. 1287-305.
128. Cicchetti, G., P.G. Allen, and M. Glogauer, *Chemotactic signaling pathways in neutrophils: from receptor to actin assembly*. *Crit Rev Oral Biol Med*, 2002. **13**(3): p. 220-8.
129. Charest, P.G. and R.A. Firtel, *Feedback signaling controls leading-edge formation during chemotaxis*. *Curr Opin Genet Dev*, 2006. **16**(4): p. 339-47.
130. Heid, P.J., et al., *The role of myosin heavy chain phosphorylation in Dictyostelium motility, chemotaxis and F-actin localization*. *J Cell Sci*, 2004. **117**(Pt 20): p. 4819-35.
131. Janetopoulos, C. and R.A. Firtel, *Directional sensing during chemotaxis*. *FEBS Lett*, 2008. **582**(14): p. 2075-85.
132. Djafarzadeh, S. and V. Niggli, *Signaling pathways involved in dephosphorylation and localization of the actin-binding protein cofilin in stimulated human neutrophils*. *Exp Cell Res*, 1997. **236**(2): p. 427-35.
133. Dai, Y., et al., *Modulation of the chemotactic responsiveness of guinea pig neutrophils to hrIL-8 and fMLP*. *J Leukoc Biol*, 1994. **56**(6): p. 776-83.

134. Entschladen, F., et al., *T lymphocytes and neutrophil granulocytes differ in regulatory signaling and migratory dynamics with regard to spontaneous locomotion and chemotaxis*. Cell Immunol, 2000. **199**(2): p. 104-14.
135. Niggli, V. and H. Keller, *Inhibition of chemotactic peptide-induced development of cell polarity and locomotion by the protein kinase C inhibitor CGP 41 251 in human neutrophils correlates with inhibition of protein phosphorylation*. Exp Cell Res, 1993. **204**(2): p. 346-55.
136. Vanhaesebroeck, B. and M.D. Waterfield, *Signaling by distinct classes of phosphoinositide 3-kinases*. Exp Cell Res, 1999. **253**(1): p. 239-54.
137. Ferguson, G.J., et al., *PI(3)Kgamma has an important context-dependent role in neutrophil chemokinesis*. Nat Cell Biol, 2007. **9**(1): p. 86-91.
138. Suire, S., et al., *Gbetagammas and the Ras binding domain of p110gamma are both important regulators of PI(3)Kgamma signalling in neutrophils*. Nat Cell Biol, 2006. **8**(11): p. 1303-9.
139. Sasaki, A.T., et al., *Localized Ras signaling at the leading edge regulates PI3K, cell polarity, and directional cell movement*. J Cell Biol, 2004. **167**(3): p. 505-18.
140. Ward, S.G., *Do phosphoinositide 3-kinases direct lymphocyte navigation?* Trends Immunol, 2004. **25**(2): p. 67-74.
141. Funamoto, S., et al., *Spatial and temporal regulation of 3-phosphoinositides by PI 3-kinase and PTEN mediates chemotaxis*. Cell, 2002. **109**(5): p. 611-23.
142. Meili, R. and R.A. Firtel, *Follow the leader*. Dev Cell, 2003. **4**(3): p. 291-3.
143. Campbell, R.B., F. Liu, and A.H. Ross, *Allosteric activation of PTEN phosphatase by phosphatidylinositol 4,5-bisphosphate*. J Biol Chem, 2003. **278**(36): p. 33617-20.
144. Takahashi, Y., et al., *PTEN tumor suppressor associates with NHERF proteins to attenuate PDGF receptor signaling*. EMBO J, 2006. **25**(4): p. 910-20.

145. Nishio, M., et al., *Control of cell polarity and motility by the PtdIns(3,4,5)P3 phosphatase SHIP1*. Nat Cell Biol, 2007. **9**(1): p. 36-44.
146. van Haastert, P.J., I. Keizer-Gunnink, and A. Kortholt, *Essential role of PI3-kinase and phospholipase A2 in Dictyostelium discoideum chemotaxis*. J Cell Biol, 2007. **177**(5): p. 809-16.
147. Keizer-Gunnink, I., A. Kortholt, and P.J. Van Haastert, *Chemoattractants and chemorepellents act by inducing opposite polarity in phospholipase C and PI3-kinase signaling*. J Cell Biol, 2007. **177**(4): p. 579-85.
148. Iijima, M., et al., *Novel mechanism of PTEN regulation by its phosphatidylinositol 4,5-bisphosphate binding motif is critical for chemotaxis*. J Biol Chem, 2004. **279**(16): p. 16606-13.
149. Huang, Y.E., et al., *Receptor-mediated regulation of PI3Ks confines PI(3,4,5)P3 to the leading edge of chemotaxing cells*. Mol Biol Cell, 2003. **14**(5): p. 1913-22.
150. Ridley, A.J., *Rho proteins, PI 3-kinases, and monocyte/macrophage motility*. FEBS Lett, 2001. **498**(2-3): p. 168-71.
151. Wang, F., et al., *Lipid products of PI(3)Ks maintain persistent cell polarity and directed motility in neutrophils*. Nat Cell Biol, 2002. **4**(7): p. 513-8.
152. Srinivasan, S., et al., *Rac and Cdc42 play distinct roles in regulating PI(3,4,5)P3 and polarity during neutrophil chemotaxis*. J Cell Biol, 2003. **160**(3): p. 375-85.
153. Costa, C., et al., *Negative feedback regulation of Rac in leukocytes from mice expressing a constitutively active phosphatidylinositol 3-kinase gamma*. Proc Natl Acad Sci U S A, 2007. **104**(36): p. 14354-9.
154. Welch, H.C., et al., *P-Rex1, a PtdIns(3,4,5)P3- and Gbetagamma-regulated guanine-nucleotide exchange factor for Rac*. Cell, 2002. **108**(6): p. 809-21.
155. Zheng, Y., S. Bagrodia, and R.A. Cerione, *Activation of phosphoinositide 3-kinase activity by Cdc42Hs binding to p85*. J Biol Chem, 1994. **269**(29): p. 18727-30.

156. Bokoch, G.M., et al., *Rac GTPase interacts specifically with phosphatidylinositol 3-kinase*. *Biochem J*, 1996. **315 (Pt 3)**: p. 775-9.
157. Chung, C.Y., et al., *Role of Rac in controlling the actin cytoskeleton and chemotaxis in motile cells*. *Proc Natl Acad Sci U S A*, 2000. **97(10)**: p. 5225-30.
158. Niggli, V., *Signaling to migration in neutrophils: importance of localized pathways*. *Int J Biochem Cell Biol*, 2003. **35(12)**: p. 1619-38.
159. Akasaki, T., H. Koga, and H. Sumimoto, *Phosphoinositide 3-kinase-dependent and -independent activation of the small GTPase Rac2 in human neutrophils*. *J Biol Chem*, 1999. **274(25)**: p. 18055-9.
160. Weiner, O.D., et al., *A PtdInsP(3)- and Rho GTPase-mediated positive feedback loop regulates neutrophil polarity*. *Nat Cell Biol*, 2002. **4(7)**: p. 509-13.
161. Sanui, T., et al., *DOCK2 regulates Rac activation and cytoskeletal reorganization through interaction with ELMO1*. *Blood*, 2003. **102(8)**: p. 2948-50.
162. Allen, W.E., et al., *A role for Cdc42 in macrophage chemotaxis*. *J Cell Biol*, 1998. **141(5)**: p. 1147-57.
163. Nobes, C.D. and A. Hall, *Rho GTPases control polarity, protrusion, and adhesion during cell movement*. *J Cell Biol*, 1999. **144(6)**: p. 1235-44.
164. Johnson, D.I., *Cdc42: An essential Rho-type GTPase controlling eukaryotic cell polarity*. *Microbiol Mol Biol Rev*, 1999. **63(1)**: p. 54-105.
165. Macara, I.G., *Parsing the polarity code*. *Nat Rev Mol Cell Biol*, 2004. **5(3)**: p. 220-31.
166. Wu, D., *Signaling mechanisms for regulation of chemotaxis*. *Cell Res*, 2005. **15(1)**: p. 52-6.
167. Li, Z., et al., *Directional sensing requires G beta gamma-mediated PAK1 and PIX alpha-dependent activation of Cdc42*. *Cell*, 2003. **114(2)**: p. 215-27.

168. Feng, Q., D. Baird, and R.A. Cerione, *Novel regulatory mechanisms for the Dbl family guanine nucleotide exchange factor Cool-2/alpha-Pix*. EMBO J, 2004. **23**(17): p. 3492-504.
169. Van Keymeulen, A., et al., *To stabilize neutrophil polarity, PIP3 and Cdc42 augment RhoA activity at the back as well as signals at the front*. J Cell Biol, 2006. **174**(3): p. 437-45.
170. Suetsugu, S., et al., *Optimization of WAVE2 complex-induced actin polymerization by membrane-bound IRSp53, PIP(3), and Rac*. J Cell Biol, 2006. **173**(4): p. 571-85.
171. Charest, P.G. and R.A. Firtel, *Big roles for small GTPases in the control of directed cell movement*. Biochem J, 2007. **401**(2): p. 377-90.
172. Machesky, L.M., et al., *Scar, a WASp-related protein, activates nucleation of actin filaments by the Arp2/3 complex*. Proc Natl Acad Sci U S A, 1999. **96**(7): p. 3739-44.
173. Castellano, F., et al., *Inducible recruitment of Cdc42 or WASP to a cell-surface receptor triggers actin polymerization and filopodium formation*. Curr Biol, 1999. **9**(7): p. 351-60.
174. Firtel, R.A. and C.Y. Chung, *The molecular genetics of chemotaxis: sensing and responding to chemoattractant gradients*. Bioessays, 2000. **22**(7): p. 603-15.
175. Schmeichel, K.L. and M.C. Beckerle, *The LIM domain is a modular protein-binding interface*. Cell, 1994. **79**(2): p. 211-9.
176. Chew, C.S., et al., *Lasp-1 binds to non-muscle F-actin in vitro and is localized within multiple sites of dynamic actin assembly in vivo*. J Cell Sci, 2002. **115**(Pt 24): p. 4787-99.
177. Raman, D., et al., *LIM and SH3 protein-1 modulates CXCR2-mediated cell migration*. PLoS One, 2010. **5**(4): p. e10050.
178. Lin, Y.H., et al., *Regulation of cell migration and survival by focal adhesion targeting of Lasp-1*. J Cell Biol, 2004. **165**(3): p. 421-32.

179. Spence, H.J., et al., *AP-1 differentially expressed proteins Krp1 and fibronectin cooperatively enhance Rho-ROCK-independent mesenchymal invasion by altering the function, localization, and activity of nondifferentially expressed proteins*. Mol Cell Biol, 2006. **26**(4): p. 1480-95.
180. Krause, M., et al., *Ena/VASP proteins: regulators of the actin cytoskeleton and cell migration*. Annu Rev Cell Dev Biol, 2003. **19**: p. 541-64.
181. Reinhard, M., et al., *The 46/50 kDa phosphoprotein VASP purified from human platelets is a novel protein associated with actin filaments and focal contacts*. EMBO J, 1992. **11**(6): p. 2063-70.
182. Barzik, M., et al., *Ena/VASP proteins enhance actin polymerization in the presence of barbed end capping proteins*. J Biol Chem, 2005. **280**(31): p. 28653-62.
183. Ferron, F., et al., *Structural basis for the recruitment of profilin-actin complexes during filament elongation by Ena/VASP*. EMBO J, 2007. **26**(21): p. 4597-606.
184. Pasic, L., T. Kotova, and D.A. Schafer, *Ena/VASP proteins capture actin filament barbed ends*. J Biol Chem, 2008. **283**(15): p. 9814-9.
185. Neel, N.F., et al., *VASP is a CXCR2-interacting protein that regulates CXCR2-mediated polarization and chemotaxis*. J Cell Sci, 2009. **122**(Pt 11): p. 1882-94.
186. Chitaley, K., et al., *Vasodilator-stimulated phosphoprotein is a substrate for protein kinase C*. FEBS Lett, 2004. **556**(1-3): p. 211-5.
187. Butt, E., et al., *Actin binding of human LIM and SH3 protein is regulated by cGMP- and cAMP-dependent protein kinase phosphorylation on serine 146*. J Biol Chem, 2003. **278**(18): p. 15601-7.
188. Chew, C.S., et al., *Lasp-1 is a regulated phosphoprotein within the cAMP signaling pathway in the gastric parietal cell*. Am J Physiol, 1998. **275**(1 Pt 1): p. C56-67.
189. Briggs, M.W. and D.B. Sacks, *IQGAP1 as signal integrator: Ca²⁺, calmodulin, Cdc42 and the cytoskeleton*. FEBS Lett, 2003. **542**(1-3): p. 7-11.

190. Fukata, M., M. Nakagawa, and K. Kaibuchi, *Roles of Rho-family GTPases in cell polarisation and directional migration*. *Curr Opin Cell Biol*, 2003. **15**(5): p. 590-7.
191. Benzing, T., et al., *14-3-3 interacts with regulator of G protein signaling proteins and modulates their activity*. *J Biol Chem*, 2000. **275**(36): p. 28167-72.
192. Niu, J., et al., *RGS3 interacts with 14-3-3 via the N-terminal region distinct from the RGS (regulator of G-protein signalling) domain*. *Biochem J*, 2002. **365**(Pt 3): p. 677-84.
193. Ross, E.M. and T.M. Wilkie, *GTPase-activating proteins for heterotrimeric G proteins: regulators of G protein signaling (RGS) and RGS-like proteins*. *Annu Rev Biochem*, 2000. **69**: p. 795-827.
194. Snow, B.E., et al., *GTPase activating specificity of RGS12 and binding specificity of an alternatively spliced PDZ (PSD-95/Dlg/ZO-1) domain*. *J Biol Chem*, 1998. **273**(28): p. 17749-55.
195. Xu, J., et al., *Divergent signals and cytoskeletal assemblies regulate self-organizing polarity in neutrophils*. *Cell*, 2003. **114**(2): p. 201-14.
196. Janetopoulos, C., et al., *Temporal and spatial regulation of phosphoinositide signaling mediates cytokinesis*. *Dev Cell*, 2005. **8**(4): p. 467-77.
197. Neujahr, R., et al., *Three-dimensional patterns and redistribution of myosin II and actin in mitotic Dictyostelium cells*. *J Cell Biol*, 1997. **139**(7): p. 1793-804.
198. Rubin, H. and S. Ravid, *Polarization of myosin II heavy chain-protein kinase C in chemotaxing dictyostelium cells*. *J Biol Chem*, 2002. **277**(39): p. 36005-8.
199. Ishizaki, T., et al., *p160ROCK, a Rho-associated coiled-coil forming protein kinase, works downstream of Rho and induces focal adhesions*. *FEBS Lett*, 1997. **404**(2-3): p. 118-24.
200. Eddy, R.J., et al., *Ca²⁺-dependent myosin II activation is required for uropod retraction during neutrophil migration*. *J Cell Sci*, 2000. **113** (Pt 7): p. 1287-98.
201. Szczur, K., et al., *Rho GTPase CDC42 regulates directionality and random movement via distinct MAPK pathways in neutrophils*. *Blood*, 2006. **108**(13): p. 4205-13.

202. Szczur, K., Y. Zheng, and M.D. Filippi, *The small Rho GTPase Cdc42 regulates neutrophil polarity via CD11b integrin signaling*. *Blood*, 2009. **114**(20): p. 4527-37.
203. Pestonjamas, K.N., et al., *Rac1 links leading edge and uropod events through Rho and myosin activation during chemotaxis*. *Blood*, 2006. **108**(8): p. 2814-20.
204. Foxman, E.F., J.J. Campbell, and E.C. Butcher, *Multistep navigation and the combinatorial control of leukocyte chemotaxis*. *J Cell Biol*, 1997. **139**(5): p. 1349-60.
205. Marasco, W.A., et al., *Purification and identification of formyl-methionyl-leucyl-phenylalanine as the major peptide neutrophil chemotactic factor produced by Escherichia coli*. *J Biol Chem*, 1984. **259**(9): p. 5430-9.
206. Le, Y., P.M. Murphy, and J.M. Wang, *Formyl-peptide receptors revisited*. *Trends Immunol*, 2002. **23**(11): p. 541-8.
207. Heit, B., et al., *An intracellular signaling hierarchy determines direction of migration in opposing chemotactic gradients*. *J Cell Biol*, 2002. **159**(1): p. 91-102.
208. Nick, J.A., et al., *Common and distinct intracellular signaling pathways in human neutrophils utilized by platelet activating factor and FMLP*. *J Clin Invest*, 1997. **99**(5): p. 975-86.
209. Heit, B., et al., *PTEN functions to 'prioritize' chemotactic cues and prevent 'distraction' in migrating neutrophils*. *Nat Immunol*, 2008. **9**(7): p. 743-52.
210. Yoo, S.K., et al., *Differential regulation of protrusion and polarity by PI3K during neutrophil motility in live zebrafish*. *Dev Cell*, 2010. **18**(2): p. 226-36.
211. Li, C., et al., *Spatiotemporal coupling of cAMP transporter to CFTR chloride channel function in the gut epithelia*. *Cell*, 2007. **131**(5): p. 940-51.
212. Pizurki, L., et al., *Cystic fibrosis transmembrane conductance regulator does not affect neutrophil migration across cystic fibrosis airway epithelial monolayers*. *Am J Pathol*, 2000. **156**(4): p. 1407-16.

213. Farooq, S.M., et al., *Therapeutic effect of blocking CXCR2 on neutrophil recruitment and dextran sodium sulfate-induced colitis*. J Pharmacol Exp Ther, 2009. **329**(1): p. 123-9.
214. Li, C., et al., *Lysophosphatidic acid inhibits cholera toxin-induced secretory diarrhea through CFTR-dependent protein interactions*. J Exp Med, 2005. **202**(7): p. 975-86.
215. Li, C., et al., *Molecular assembly of cystic fibrosis transmembrane conductance regulator in plasma membrane*. J Biol Chem, 2004. **279**(23): p. 24673-84.
216. Carrigan, S.O., et al., *Neutrophil differentiated HL-60 cells model Mac-1 (CD11b/CD18)-independent neutrophil transepithelial migration*. Immunology, 2005. **115**(1): p. 108-17.
217. Moratz, C. and J.H. Kehrl, *In vitro and in vivo assays of B-lymphocyte migration*. Methods Mol Biol, 2004. **271**: p. 161-71.
218. Sai, J., et al., *Parallel phosphatidylinositol 3-kinase (PI3K)-dependent and Src-dependent pathways lead to CXCL8-mediated Rac2 activation and chemotaxis*. J Biol Chem, 2008. **283**(39): p. 26538-47.
219. Nuzzi, P.A., M.A. Lokuta, and A. Huttenlocher, *Analysis of neutrophil chemotaxis*. Methods Mol Biol, 2007. **370**: p. 23-36.
220. Collins, S.J., *The HL-60 promyelocytic leukemia cell line: proliferation, differentiation, and cellular oncogene expression*. Blood, 1987. **70**(5): p. 1233-44.
221. Gallagher, R., et al., *Characterization of the continuous, differentiating myeloid cell line (HL-60) from a patient with acute promyelocytic leukemia*. Blood, 1979. **54**(3): p. 713-33.
222. Collins, S.J., et al., *Terminal differentiation of human promyelocytic leukemia cells induced by dimethyl sulfoxide and other polar compounds*. Proc Natl Acad Sci U S A, 1978. **75**(5): p. 2458-62.
223. Chaplinski, T.J. and J.E. Niedel, *Cyclic nucleotide-induced maturation of human promyelocytic leukemia cells*. J Clin Invest, 1982. **70**(5): p. 953-64.

224. Perez, H.D., E. Kelly, and R. Holmes, *Regulation of formyl peptide receptor expression and its mRNA levels during differentiation of HL-60 cells*. J Biol Chem, 1992. **267**(1): p. 358-63.
225. Vallari, D.S., R. Austinhirst, and F. Snyder, *Development of specific functionally active receptors for platelet-activating factor in HL-60 cells following granulocytic differentiation*. J Biol Chem, 1990. **265**(8): p. 4261-5.
226. Amatruda, T.T., 3rd, et al., *G alpha 16, a G protein alpha subunit specifically expressed in hematopoietic cells*. Proc Natl Acad Sci U S A, 1991. **88**(13): p. 5587-91.
227. Manes, S., et al., *An isoform-specific PDZ-binding motif targets type I PIP5 kinase beta to the uropod and controls polarization of neutrophil-like HL60 cells*. FASEB J, 2010. **24**(9): p. 3381-92.
228. Bertagnolo, V., et al., *Intranuclear translocation of phospholipase C beta2 during HL-60 myeloid differentiation*. Biochem Biophys Res Commun, 1997. **235**(3): p. 831-7.
229. Jiang, H., et al., *Roles of phospholipase C beta2 in chemoattractant-elicited responses*. Proc Natl Acad Sci U S A, 1997. **94**(15): p. 7971-5.
230. Li, Z., et al., *Roles of PLC-beta2 and -beta3 and PI3Kgamma in chemoattractant-mediated signal transduction*. Science, 2000. **287**(5455): p. 1046-9.
231. Wu, D., C.K. Huang, and H. Jiang, *Roles of phospholipid signaling in chemoattractant-induced responses*. J Cell Sci, 2000. **113 (Pt 17)**: p. 2935-40.
232. Follo, M.Y., et al., *Real-time PCR as a tool for quantitative analysis of PI-PLCbeta1 gene expression in myelodysplastic syndrome*. Int J Mol Med, 2006. **18**(2): p. 267-71.
233. Cao, T.T., et al., *A kinase-regulated PDZ-domain interaction controls endocytic sorting of the beta2-adrenergic receptor*. Nature, 1999. **401**(6750): p. 286-90.
234. Rah, S.Y., et al., *Activation of CD38 by interleukin-8 signaling regulates intracellular Ca²⁺ level and motility of lymphokine-activated killer cells*. J Biol Chem, 2005. **280**(4): p. 2888-95.

235. Hwang, J.I., et al., *Regulation of phospholipase C-beta 3 activity by Na⁺/H⁺ exchanger regulatory factor 2*. J Biol Chem, 2000. **275**(22): p. 16632-7.
236. Ricevuti, G., *Host tissue damage by phagocytes*. Ann N Y Acad Sci, 1997. **832**: p. 426-48.
237. Dovi, J.V., A.M. Szpaderska, and L.A. DiPietro, *Neutrophil function in the healing wound: adding insult to injury?* Thromb Haemost, 2004. **92**(2): p. 275-80.
238. Kumar, V. and A. Sharma, *Neutrophils: Cinderella of innate immune system*. Int Immunopharmacol, 2010. **10**(11): p. 1325-34.
239. Bizzarri, C., et al., *ELR+ CXC chemokines and their receptors (CXC chemokine receptor 1 and CXC chemokine receptor 2) as new therapeutic targets*. Pharmacol Ther, 2006. **112**(1): p. 139-49.
240. Cardona, A.E., et al., *Scavenging roles of chemokine receptors: chemokine receptor deficiency is associated with increased levels of ligand in circulation and tissues*. Blood, 2008. **112**(2): p. 256-63.
241. Rosenkilde, M.M. and T.W. Schwartz, *The chemokine system -- a major regulator of angiogenesis in health and disease*. APMIS, 2004. **112**(7-8): p. 481-95.
242. Zhang, Q., et al., *Circulating mitochondrial DAMPs cause inflammatory responses to injury*. Nature, 2010. **464**(7285): p. 104-7.
243. Cacalano, G., et al., *Neutrophil and B cell expansion in mice that lack the murine IL-8 receptor homolog*. Science, 1994. **265**(5172): p. 682-4.

ABSTRACT**DISRUPTING CXCR2 MACROMOLECULAR COMPLEX PDZ-DOMAIN INTERACTIONS DURING INFLAMMATORY CHEMOTAXIS**

by

MARCELLO P. CASTELVETERE**August 2012****Advisor:** Dr. Chunying Li**Major:** Biochemistry and Molecular Biology**Degree:** Master of Science

Neutrophils are the body's first responders to inflammation, being the most abundant white blood cell type in circulation and they quickly initiate an immune response through chemokine signaling. Inflammatory chemokines signal via their receptor CXCR2, which initiates an inflammatory response, recruiting leukocytes to sites of inflammation. Chemokine signaling is important for proper host protection, yet uncontrolled activity is responsible for a variety of pathological conditions: including rheumatoid arthritis, ischemia-reperfusion injury, arteriosclerosis, multiple sclerosis, psoriasis, inflammatory bowel disease, and allergic reactions.

In this report I show a CXCR2 macromolecular signaling complex exists in neutrophils, containing NHERF1 and PLC β 2. I also demonstrate a novel strategy of cytosolically perturbing the CXCR2 PDZ-domain interaction of the macromolecular complex. This perturbation disrupts spatial sensation of a chemokine gradient, yet still allows cells to mobilize actin and chemotax. Furthermore, I show CXCR2 PDZ-domain perturbation does not disrupt migration through bacterial derived chemoattractant receptors.

AUTOBIOGRAPHICAL STATEMENT

Name: Marcello Pasquale Castelvetero
 Date of Birth: 25 November, 1985
 Father's name: Bruno Castelvetero
 Mother's name: Gabriella Rea-Castelvetero

Education:

Bachelor of Science, Michigan State University, East Lansing (2004-2008)
 Major: Genomics and Molecular Genetics

Masters of Science, Wayne State University School of Medicine, Detroit (2010-2012)
 Major: Biochemistry and Molecular Biology
 Advisor: Dr. Chunying Li

Publications:

- 1). Yanning Wu, Shuo Wang, Shukkur Muhammed Farooq, **Marcello Pasquale Castelvetero**, Yuning Hou, Jiliang Gao, Javier V. Navarro, David Oupicky, Fei, Sun, Chunying Li. A Chemokine Receptor CXCR2 Macromolecular Complex Regulates Neutrophil Functions in Inflammatory Diseases. **Journal of Biological Chemistry**. 287(8): 5744-5755 (2012). Featured/cited in **Faculty of 1000 Biology**.
- 2). **Marcello P. Castelvetero**, Chunying Li. Spatiotemporal regulation of CXCR2 macromolecular signaling complexes in inflammation and cancer. **Molecular Biology** (in press).
- 3). Yuning Hou, Shuo Wang, Yanning Wu, **Marcello P. Castelvetero**, Xiaoqing Guan, George Yoo, Andrew M. Fribley, Chunying Li. Disrupting CXCR2 PDZ-mediated interaction in Head and Neck Squamous Cell Cancer: A potential therapeutic strategy. **2012 KCI Research Retreat** (poster & abstract). WSU-SoM, Detroit, MI; May 9, 2012
- 4). Shuo Wang, Yanning Wu, Yuning Hou, **Marcello Pasquale Castelvetero**, Chunying Li. CXCR2 Macromolecular Complex in Pancreatic Cancer: A Potential Therapeutic Target in Tumor growth. **AACR Special Conference: Pancreatic Cancer: Progress and Challenges**. (Abstract accepted). Lake Tahoe, NV; June 18-21, 2012.
- 5). Shuo Wang, Yanning Wu, Yuning Hou, **Marcello P. Castelvetero**, Xiaoqing Guan, Jacob J. Oblak, Chunying Li. CXCR2 Macromolecular Complex in Pancreatic Cancer: A Potential Therapeutic Target in Tumor growth. **2012 KCI Research Retreat** (poster & abstract). WSU-SoM, Detroit, MI; May 9, 2012.
- 6). Shuo Wang, Yanning Wu, Yuning Hou, **Marcello P. Castelvetero**, Chunying Li. CXCR2 Macromolecular Complex in Pancreatic Cancer: A Potential Therapeutic Target in Tumor growth. **Graduate Student Research Day XV** (poster & abstract). WSU, Detroit, MI; Sept. 29, 2011).
- 7). Shuo Wang, Yanning Wu, Yuning Hou, **Marcello Pasquale Castelvetero**, Annette Stewart, Michael Brennan, Theresa M. Filtz, Chunying Li. Therapeutic Effects of perturbing CXCR2 macromolecular signaling complex on pancreatic cancer tumorigenesis, metastasis, and angiogenesis (Manuscript in preparation, **will submit to Cancer Research**).